

**SOME DYNAMICAL PROBLEMS IN THE MICROPOLAR
THERMOELASTIC MATERIALS WITH VOIDS**

By

R. Lianngenga

(MZU/Ph.D./676 of 16.05.2014)

**In Fulfilment of Requirements for the Degree of Doctor of
Philosophy in Mathematics**

To



**Department of Mathematics & Computer Science
School of Physical Sciences
Mizoram University
Aizawl - 796 004
Mizoram, India
November, 2017**

**DEPARTMENT OF MATHEMATICS & COMPUTER SCIENCE
MIZORAM UNIVERSITY**

**Dr. S. Sarat Singh
Assistant Professor**



**Aizawl – 796 004, Mizoram: INDIA
Fax: 0389 - 2330644
Phone: +919862626776(m)
+919863264645(m)
e-mail: saratcha32@yahoo.co.uk**

CERTIFICATE

This is to certify that the thesis entitled "Some dynamical problems in the micropolar thermoelastic materials with voids" submitted by Mr. R. Liannenga (Registration No: MZU/Ph.D./676 of 16.05.2014) for the degree of Doctor of Philosophy (Ph. D.) of the Mizoram University, embodies the record of original investigation carried out by him under my supervision. He has been duly registered and the thesis presented is worthy of being considered for the award of the Ph. D. degree. This work has not been submitted for any degree of any other university.

**Dr. S. Sarat Singh
(Supervisor)**

MIZORAM UNIVERSITY

TANHRIL

Month: November

Year: 2017

CANDIDATE'S DECLARATION

I, R. Lianggenga, hereby declare that the subject matter of this thesis entitled "Some dynamical problems in the micropolar thermoelastic materials with voids" is the record of work done by me, that the contents of this thesis do not form basis of the award of any previous degree to me or to the best of my knowledge to anybody else, and that the thesis has not been submitted by me for any research degree in other University/Institute.

This is being submitted to the Mizoram University for the fulfilment of the degree of Doctor of Philosophy (Ph. D.) in Mathematics.

R. Lianggenga

(MZU/Ph.D./676 of 16.05.2014)

(Candidate)

Dr. S. Sarat Singh

(Supervisor)

Dept. Maths. & Comp. Sc.

Mizoram University

Prof. Jamal Hussain

(Head of Department)

Dept. Maths. & Comp. Sc.

Mizoram University

ACKNOWLEDGEMENT

I would like express my deepest gratitude to my supervisor, Dr. S. Sarat Singh, for his excellent guidance, encouragement, patience, and providing me an excellent atmosphere for the research work. I also thank for his care and support at every stage for the completion of this work

I am highly obliged to Prof. Jamal Hussain, Head of Department, Mathematics & Computer Science, Mizoram University, for providing all the necessary facilities and his faithful advices during the course of my research work.

I express my gratefulness to Professor R.C. Tiwari, Dean, School of Physical Sciences, Mizoram University for encouraging me to bring the thesis in this form.

I would like to thank Dr. J. P. Singh, Mr. Laltanpuia, Miss. M. Saroja Devi and Mr. Sajal Kanti Das and the staffs of Department of Mathematics & Computer Science, Mizoram University for their support and help during the research work. I also thanks to Mr. J. Lalvohbika, Assistant Professor, Pachhunga University College for his good co-operations and advices.

I am thankful to Mr. Lalawmpuia, Mrs. Lalthakimi Ralte, Mrs. Laldinsangi, Mr. David Rosangliana, Mr. Vanlalruata and all the scholars in the Department of Mathematics & Computer Science for their helps and support throughout my research work.

I also thank to Mr. L. Thangmawia, Dr. L.P. Duhawma, Dr. Denghmingliani Zadeng, Dr. Rajesh Kumar and Mr. H. Vanlalhriata, for their valuable advice, good co-operation and full support during my research work.

I convey my gratitude to Dr. Tawnenga, Principal, Pachhunga University College for his kind support and help in my research work.

I also like to thank Dr. David T. Thawmthanga, National Secretary cum Coordinator, Rastrya Lok Samata Party (RLSP), member of Zonal Railway User Consultative Committee (ZRUCC) under Government of India & consultative member for Mizoram State in Food Corporation of India (FCI) for his kind support in the course of my research work.

I would like to express my deep thanks to my parents for their continuous support and encouragement throughout my research work.

Lastly, a heartiest gratitude goes to the Lord Almighty for blessing me to complete this thesis.

Dated:

Place: Aizawl

R. Lianggenga

PREFACE

The present thesis entitled "Some dynamical problems in the micropolar thermoelastic materials with voids" is an outcome of the research carried out by me under the supervision of Dr. S. Sarat Singh, Department of Mathematics & Computer Science, Mizoram University, Aizawl - 796 004, Mizoram, INDIA.

The thesis studies the phenomena of wave propagation in micropolar thermoelastic materials with voids. It consists of six chapters. The first chapter is the general introduction which consists of microcontinuum theories, linear micropolar theory, Hookes law, elastic waves, helmholtz decomposition theorem, applications of wave propagation and review of literatures.

The second chapter deals with the problem of plane waves in micropolar tharmoelastic materials with voids. The phase velocity and attenuation coefficients of the longitudinal and transverse waves are obtained analytically and numerically. The effects of micro-inertia and thermal relaxation time on the phase velocity and attenuation are discussed.

The third chapter attempts the problem of effect of micro-inertia in the propagation of waves in micropolar thermoelastic materials with voids. We have obtained the amplitude and energy ratios of the reflected waves due to incident longitudinal/shear waves at the plane free surface of micropolar thermoelastic materials with voids. These ratios are numerically computed for a particular model.

Chapter 4 concerns with the problem of effects of thermal and micro-inertia on the refraction of elastic waves in micropolar thermoelastic materials with voids. We have obtained the amplitude and energy ratios corresponding to the reflected and refracted waves separately for the case of incident longitudinal/shear waves at the plane interface between two dissimilar half-spaces of micropolar thermoelastic materials with voids. These ratios are computed numerically to see the effects of thermal and micro-inertia are discussed.

Chapter 5 discusses the problem of effect of micro-inertia on reflection/refraction of plane waves at the orthotropic and thermoelastic micropolar materials with voids. The amplitude

and energy ratios corresponding to the reflected and refracted waves due to incident longitudinal wave are obtained analytically and numerically. The effect of micro-inertia on these ratios are discussed.

Chapter 6 is the last chapter of the thesis and it is the summary and conclusions of the thesis.

In the end of the thesis, a list of references of the books/papers has been given in alphabetical order in the bibliography.

Contents

Certificate	i
Declaration	ii
Acknowledgement	iii
Preface	v
1 General Introduction	1
1.1 Microcontinuum theories	1
1.1.1 Rotation	4
1.1.2 Microstretch and micropolar continua	7
1.2 Linear Micropolar theory	9
1.2.1 Orthotropic micropolar elasticity	9
1.2.2 Micropolar thermoelasticity	11
1.2.3 Micropolar thermoelasticity with voids	12
1.3 Hooke's law	15
1.4 Elastic waves	16
1.5 Helmholtz decomposition theorem	18
1.6 Applications of wave propagation	19
1.7 Review of Literatures	20
2 Plane waves in micropolar thermoelastic materials with voids¹	26
2.1 Introduction	26
2.2 Basic equations	27
2.3 Harmonic waves	28
2.4 Phase velocity & Attenuation	30
2.4.1 For dilatational waves	30
2.4.2 For the shear waves	32

2.5	Special cases	33
2.6	Numerical results and discussion	36
2.7	Conclusions	45
3	Effect of micro-inertia in the propagation of waves in micropolar thermoelastic materials with voids²	46
3.1	Introduction	46
3.2	Basic Equation	47
3.3	Wave Propagation	47
3.4	Amplitude ratio	49
3.5	Energy Partition	50
3.6	Special cases	51
3.7	Numerical results and discussion	54
	3.7.1 For incident coupled longitudinal wave	55
	3.7.2 For incident coupled shear wave	58
3.8	Conclusions	62
4	Effect of thermal and micro-inertia on the refraction of elastic waves in micropolar thermoelastic materials with voids³	63
4.1	Introduction	63
4.2	Basic Equations	64
4.3	Wave propagation	65
4.4	Boundary conditions	68
4.5	Energy partition	70
4.6	Particular cases	71
4.7	Numerical results and discussion	74
	4.7.1 Effect of linear thermal expansion	75
	4.7.2 Effect of micro-inertia	81
4.8	Conclusions	88
5	Effect of micro-inertia on reflection/refraction of plane waves at the orthotropic and thermoelastic micropolar materials with voids⁴	90
5.1	Introduction	90
5.2	Basic Equations	91
5.3	Wave propagation	92
5.4	Boundary conditions	95
5.5	Energy partition	97

5.6	Numerical results and discussion	97
5.6.1	Effect of micro-inertia on amplitude ratios	98
5.6.2	Effect of micro-inertia on energy ratios	101
5.7	Conclusions	104
6	Summary and Conclusions	105
	Bibliography	109
	List of Publications	127

Chapter 1

General Introduction

1.1 Microcontinuum theories

A microcontinuum is a continuous collection of deformable points particles. Physically, these points particles are infinitesimally small in size. They do not violate the continuity of matter and are deformable which leads to microcontinuum theories. A particle, P is identified by its position vector X_K ($K = 1, 2, 3$) in the reference state B and vector attached to P as Ξ_α , $\alpha = 1, 2, \dots, N$ which represent the inner structure of P . They have their own motions as

$$\mathbf{X}(t) \longrightarrow \mathbf{x}, \quad \Xi_\alpha(\mathbf{X}, t) \longrightarrow \boldsymbol{\xi}_\alpha, \quad \alpha = 1, 2, \dots, N. \quad (1.1)$$

Such a material medium is called *microcontinuum of grade N* . We consider Ξ and ξ as the relativistic positions of material points called *microelements* which are contained in the particle P called *macroelements*. The undeformed and deformed states in Figure 1.1 give

$$\mathbf{x}' = \mathbf{x}(\mathbf{X}, t) + \boldsymbol{\xi}(\mathbf{X}, \Xi, t). \quad (1.2)$$

The micromorphic continuum is a special form of Equation (1.2) as

$$\mathbf{x}' = \mathbf{x}(\mathbf{X}, t) + \chi_K(\mathbf{X}, t)\Xi_K, \quad (1.3)$$

where χ_K are deformation vectors.

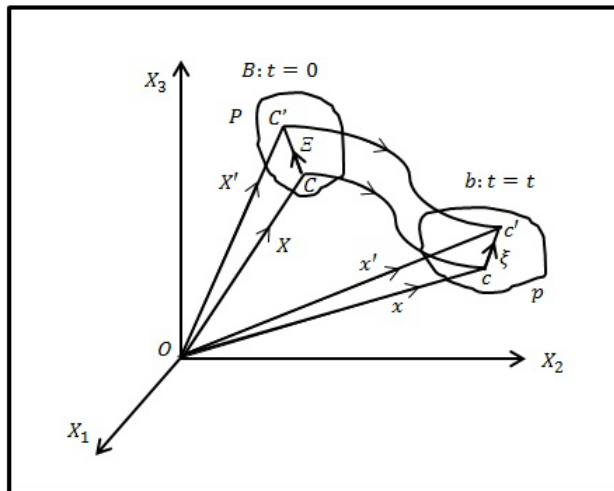


Figure 1.1: Deformation of microelement.

Consider a material point $P(\mathbf{X}, \Xi) \in B$ which is characterized by its centroid C and vector Ξ attached to C . The point C is identified by X_1, X_2, X_3 and vector components Ξ_1, Ξ_2, Ξ_3 in the coordinate frame X_K . The point $P(\mathbf{X}, \Xi)$ is deformed to $p(\mathbf{x}, \xi)$ in a spatial frame of reference b so that $X_K \rightarrow x_k, \Xi_K \rightarrow \xi_k$ ($K = 1, 2, 3; k = 1, 2, 3$). Mathematically, these mappings are defined as

$$\mathbf{X} \rightarrow \mathbf{x} = \hat{\mathbf{x}}(\mathbf{X}, t) \quad \text{or} \quad x_k = \hat{x}_k(X_K, t), \quad (1.4)$$

$$\Xi \rightarrow \xi = \hat{\xi}(\mathbf{X}, t) \quad \text{or} \quad \xi_k = \hat{\xi}_k(X_K, \Xi_K, t), \quad (1.5)$$

which are called *macromotion* and *micromotion* respectively. The material particles are assumed to be very small size as compared to the macroscopic scale of the body. This makes possible for a linear approximation in Ξ as

$$\xi_k = \chi_{kK}(\mathbf{X}, t)\Xi_K, \quad (1.6)$$

where χ_{kK} is microdeformation tensor.

A material body is called a *micromorphic continuum of grade one* if its motions are described

by (1.4) and (1.6) which possess continuous partial derivatives with respect to X_K and t , and they are invertible uniquely as

$$X_K = \hat{X}_k(\mathbf{x}, t), \quad k = 1, 2, 3, \quad (1.7)$$

$$\Xi_K = \mathfrak{X}_{Kk}(\mathbf{x}, t)\xi_k, \quad K = 1, 2, 3; k = 1, 2, 3, \quad (1.8)$$

where \mathfrak{X}_{Kk} is inverse microdeformation tensor.

Theorem 1.1 If, for a fixed t , the function $\hat{x}_k(\mathbf{X}, t)$ is continuous and possesses continuous first-order partial derivatives with respect to X_K in a neighborhood $|\mathbf{X}' - \mathbf{X}| < \varepsilon$ of a point C and if the Jaccobians

$$J \equiv \det\left(\frac{\partial x_k}{\partial X_k}\right), \quad j \equiv \det\chi_{kK}, \quad (1.9)$$

do not vanish there, then unique inverses of (1.4) and (1.6) in the forms (1.7) and (1.8) exist in the neighborhood $|\mathbf{x}' - \mathbf{x}| < \delta$ of a point c , at time t , and (1.7) possess continuous first order partial derivatives with respect to x_k (See Eringen, 1999).

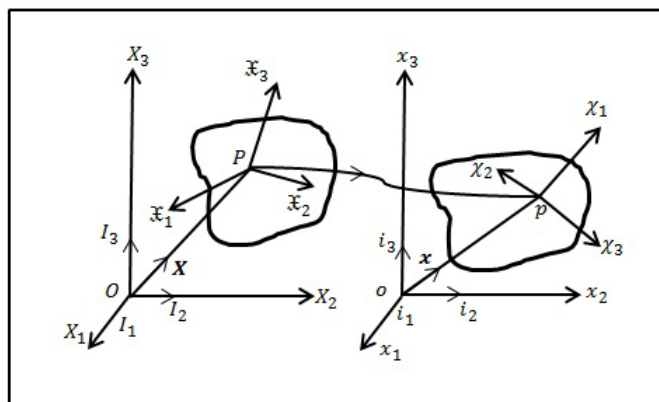


Figure 1.2: Deformation of directors.

The existence of unique inverses (1.4) and (1.6) makes possible for the physical assumption of continuity, indestructibility and impenetrability of matter. No region of positive finite volume is deformed into one of zero or infinite volume. Every region goes into a region,

every surface goes into a surface and every curve into a curve. The three independent directors \mathfrak{X}_K go to the independent directors χ_k as

$$\chi_K = \chi_{kK}(X, t)\iota_k, \quad X_k = \mathfrak{X}_{Kk}(x, t)I_K, \quad (1.10)$$

where I_K and ι_k are Cartesian unit vectors in the material and spatial frames of references B and b . Thus, a material point in the body has three microdeformable directors (χ_K and \mathfrak{X}_k) which represent nine degrees of freedom arising from microdeformation of the physical particle.

1.1.1 Rotation

A matrix F may be decomposed as product of two matrices of an orthogonal and a symmetric matrix due to Cauchy's theorem (Eringen, 1980)

$$\mathbf{F} = \mathbf{R}\mathbf{U} = \mathbf{V}\mathbf{R}, \quad (1.11)$$

with

$$\mathbf{U}^2 = \mathbf{F}'\mathbf{F}, \quad \mathbf{V}^2 = \mathbf{F}\mathbf{F}'$$

where \mathbf{F}' is the transpose of \mathbf{F} , \mathbf{R} is a classical macrorotation tensor (or microrotation tensor) if $F_{kK} = \chi_{kK}$ (or $F_{kK} = \chi_{kK}$), \mathbf{U} and \mathbf{V} are right and left stretch tensor for macrodeformation and microdeformations. In the microdeformation, the above equations may be represented as

$$\boldsymbol{\chi} = \mathbf{r}\mathbf{u} = \mathbf{v}\mathbf{r} \quad (1.12)$$

and

$$\mathbf{u}^2 = \boldsymbol{\chi}'\boldsymbol{\chi}, \quad \mathbf{v}^2 = \boldsymbol{\chi}\boldsymbol{\chi}'$$

There exist microstretch tensors due to the gradients of $\boldsymbol{\chi}$ and Equation (1.12) may be written as

$$\boldsymbol{\chi}_{,K} = \mathbf{r}_{,K}\mathbf{u} + \mathbf{r}\mathbf{u}_{,K} = \mathbf{v}_{,K}\mathbf{r} + \mathbf{v}\mathbf{r}_{,K}. \quad (1.13)$$

In case of micropolar continuum, $\mathbf{u}^2 = \mathbf{v}^2 = \mathbf{1}$ is significant because of $\boldsymbol{\chi}' = \boldsymbol{\mathfrak{X}}$ and $\boldsymbol{\chi}^{\boldsymbol{\mathfrak{X}}} = \mathbf{1}$. Equations (1.13) and (1.12) give

$$\boldsymbol{\chi}_{,K} = \mathbf{r}_{,K} \mathbf{1} = \mathbf{1} \mathbf{r}_{,K}, \quad (1.14)$$

$$\boldsymbol{\chi} = \mathbf{r}, \quad \mathbf{u}^2 = \mathbf{v}^2 = \mathbf{1}. \quad (1.15)$$

We come to know that $\boldsymbol{\chi}$ is the microrotation tensor for the micropolar continua.

The deformation of a particle P in a micromorphic continuum is show in Figure 1.3

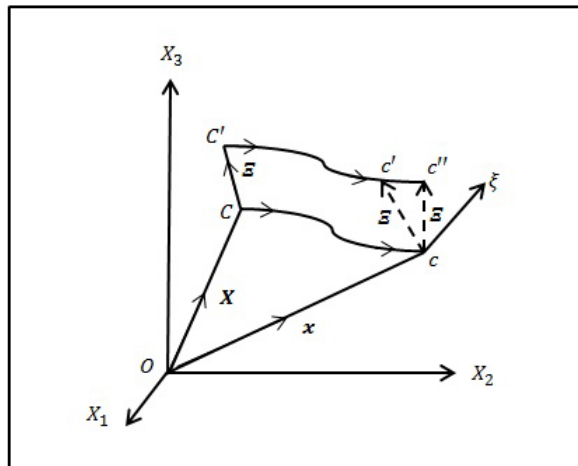


Figure 1.3: Microdeformation of a particle P

This deformation consists of

- (i) a classical macrodeformation with a translation of C to c , a macrorotation at c and macrostretch at c ,
- (ii) microdeformation that carries directors at C with the translation of C to c ,
- (iii) microrotation of directors at c ,
- (iv) microstretch of directors at c which may lead to a further microrotation of directors.

For micropolar continuum, directors are rigid. Here it is possible to represent the motions of directors as a rigid body rotation with respect to an axis.

Theorem 1.2 The finite microrotation tensor, χ_{kl} is characterized by

$$\chi_{kl} = \cos \phi \delta_{kl} - \sin \phi \epsilon_{klm} n_m + (1 + \cos \phi) n_k n_l, \quad (1.16)$$

$$\chi_{kl} = \chi_{kL} \delta_{Ll}, \quad (1.17)$$

where ϕ is the rotation and n_k is unit vector given by

$$\phi = (\phi_k \phi_l)^{1/2}, \quad n_k = \frac{\phi_k}{\phi}.$$

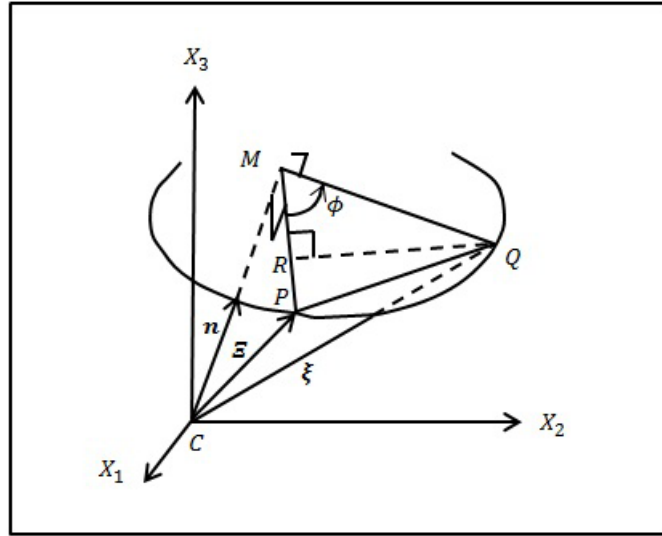


Figure 1.4: Finite microrotation

Proof: Consider a centroidal vector $\overrightarrow{CP} = \Xi$ at the undeformed particle P as shown in Figure 1.4. After ϕ rotation about the axis \overrightarrow{CM} , the point P moves to Q so that

$$\xi = \Xi + \overrightarrow{PQ}, \quad \overrightarrow{PQ} = \overrightarrow{PR} + \overrightarrow{RQ}, \quad (1.18)$$

where \overrightarrow{QR} is perpendicular to \overrightarrow{PM} and

$$\overrightarrow{PR} = -(1 - \cos \phi)(\Xi - \overrightarrow{CM}), \quad \overrightarrow{RQ} = \mathbf{n} \times \Xi \sin \phi, \quad \overrightarrow{CM} = (\mathbf{n} \cdot \Xi) \mathbf{n}. \quad (1.19)$$

With the help of Equations (1.18) and (1.19), we get

$$\boldsymbol{\xi} = \cos \phi \boldsymbol{\Xi} + \mathbf{n} \times \boldsymbol{\Xi} \sin \phi + (1 - \cos \phi)(\mathbf{n} \cdot \boldsymbol{\Xi})\mathbf{n}, \quad (1.20)$$

which follows the proof of (1.16) by the fact of (1.6) and (1.17).

Corollary 1.2.1 The necessary and sufficient conditions that the micropolar directors remain parallel to their original directions, are the vanishing ϕ .

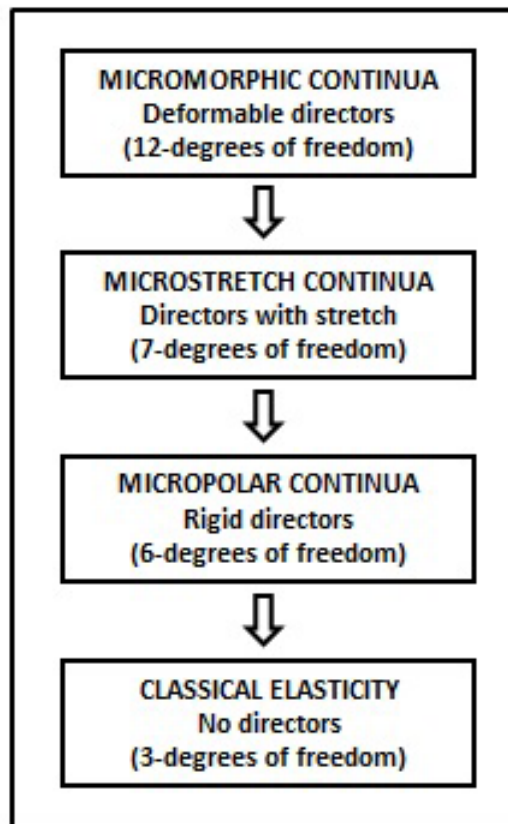


Figure 1.5: Chronological order of continua

1.1.2 Microstretch and micropolar continua

A micromorphic continuum is called *microstretch* if its directors are related by

$$\boldsymbol{x}_{Kk} = \frac{1}{j^2} \chi_{kK}, \quad (k = 1, 2, 3; K = 1, 2, 3). \quad (1.21)$$

We have the orthogonality relations as

$$\chi_{kK} \mathfrak{X}_{Kl} = \delta_{kl}, \quad x_{k,K} X_{L,K} = \delta_{KL}, \quad (1.22)$$

where δ_{kl} and δ_{KL} are shifters defined by

$$I_k \cdot \iota_l = \delta_{kl}, \quad \iota_K \cdot I_L = \delta_{KL}.$$

The relations (1.22) follows

$$j = \det \chi_{kK} = 1 / \det \mathfrak{X}_{Kk}. \quad (1.23)$$

Consequently, χ_{kK} of microstretch continua satisfy

$$\chi_{kK} \chi_{lK} = j^2 \delta_{kl}, \quad \chi_{kK} \chi_{kL} = j^2 \delta_{KL}. \quad (1.24)$$

Theorem 1.3 A microstretch continuum is a micromorphic continuum that is constrained to undergo microrotation and microstretch (expansion and contraction) without microshearing (breathing microrotations).

A micromorphic continuum is called *micropolar* if its directors are orthonormal (Eringen and Suhubi, 1964; Eringen, 1970). The directors of the micropolar continua satisfy

$$\chi_{kK} \chi_{lK} = \delta_{kl}, \quad \mathfrak{X}_{Kk} \mathfrak{X}_{Lk} = \delta_{KL}. \quad (1.25)$$

In this case, $\chi_{kK} = \mathfrak{X}_{Kk}$ and Equation (1.23) reduces to

$$\chi_{kK} \chi_{lK} = \delta_{kl}, \quad \chi_{kK} \chi_{kL} = \delta_{KL}, \quad (1.26)$$

which follows that

$$j = \det \chi_{kK} = 1. \quad (1.27)$$

Equation (1.26) expresses that the directors of micropolar continuum are rigid.

1.2 Linear Micropolar theory

The micropolar continuum is a special case of micromorphic continua in which the directors are rigid and orthonormal. This means that only the microrotation of material particles is allowed in addition to macromotion. The micro-volume does not change with micro-deformation due to rigid directors. In the micropolar theory, the director may be envisaged as an orthogonal tripod circumscribed by a unit sphere, centered within an anisometric particle, i.e. a triaxial ellipsoid. Micropolar media may represent materials that are made up of dipole atoms or dumbbell type molecules subjected to surface and body couples. The theory of micropolar elasticity was developed by Eringen (1966, 1968).

The theory of linear micropolar elasticity is based on the following basic laws:

(a) Conservation of mass, (b) Conservation of micro-inertia, (c) Balance of momentum, (d) Balance of first stress moments, (e) Conservation of energy and (f) Principle of entropy.

The constitutive relations of linear micropolar elasticity are given by (Eringen, 1966)

$$\begin{aligned} T_{kl} &= \lambda u_{r,r} \delta_{kl} + \mu (u_{k,l} + u_{l,k}) + \kappa (u_{l,k} - \epsilon_{klr} \phi_r), \\ M_{kl} &= \alpha \phi_{r,r} \delta_{kl} + \beta \phi_{k,l} + \gamma \phi_{l,k}, \quad (l, k, r = 1, 2, 3) \end{aligned} \quad (1.28)$$

where T_{kl} is stress tensors, and M_{kl} is coupled stress tensors, u_l is components of displacement, ϕ_l is components of microrotation vectors, ϵ_{klr} is alternating symbol, λ , μ are elastic parameters and α , β , γ , κ are micropolar parameters.

1.2.1 Orthotropic micropolar elasticity

The orthotropic material is an anisotropic material. The material that possesses certain physical properties vary along with certain directions is called *anisotropic materials*. Iesan (1973) derived the uniqueness theorem and existence theorem for the homogeneous orthotropic micropolar elastic solid and reduced the boundary value problems to integral equations for which the Fredholm's basic theorems are valid. The linear theory of homogeneous and

anisotropic micropolar elastic solids are based on the following equations (Iesan, 1969)

(a) Kinematic relations:

$$e_{ij} = u_{j,i} - \epsilon_{ijk}\phi_k, \quad \kappa_{ij} = \phi_{j,i}, \quad (i, j = 1, 2, 3) \quad (1.29)$$

(b) The equations of motion:

$$t_{ij} + F_i = \rho \ddot{u}_i, \quad m_{ij,j} + \epsilon_{ijk}t_{jk} + M_i = I_{ij}\ddot{\phi}_j, \quad (i, j, k = 1, 2, 3) \quad (1.30)$$

(c) The constitutive laws:

$$t_{ij} = A_{ijkl}e_{kl} + B_{ijkl}\kappa_{kl}, \quad m_{ij} = B_{klij}e_{kl} + c_{ijkl}\kappa_{kl}, \quad (i, j, k, l = 1, 2, 3) \quad (1.31)$$

or equivalently,

$$e_{ij} = a_{ijkl}t_{kl} + b_{ijkl}m_{kl}, \quad \kappa_{ij} = b_{klij}t_{kl} + c_{ijkl}m_{kl}, \quad (i, j, k, l = 1, 2, 3) \quad (1.32)$$

where ρ is a mass density of the material, t_{ij} and m_{ij} are the stress and couple stress tensor in the orthotropic micropolar elasticity, e_{ij} and κ_{kl} are kinematic characteristics of strain, F_i and M_i are respectively components of body force and body couple, A_{ijkl} , B_{ijkl} , C_{ijkl} and I_{ij} are the characteristic constants so that

$$A_{ijkl} = A_{klij}, \quad C_{ijkl} = C_{klij}, \quad a_{ijkl} = a_{klij}, \quad c_{ijkl} = a_{klij}, \quad I_{ij} = I_{ji}.$$

Orthotropic materials have material properties that differ along three mutually orthogonal two fold axes of rotational symmetry. Such materials have three planes of symmetry. If we restrict our analysis into two dimensional plane deformation parallel to x_1x_2 -plane, we have $\mathbf{u} = (u_1, u_2, 0)$ and $\boldsymbol{\phi} = (0, 0, \phi_3)$ as the displacement vector and microrotation vector respectively. The constitutive equations for orthotropic micropolar are given by (Iesan, 1973)

$$t_{11} = A_{11}u_{1,1} + A_{12}u_{2,2}, \quad t_{12} = A_{78}u_{1,2} + A_{77}u_{2,1} + (A_{78} - A_{77})\phi_3,$$

$$t_{22} = A_{12}u_{1,1} + A_{22}u_{2,2}, \quad t_{21} = A_{78}u_{2,1} + A_{88}u_{1,2} + (A_{88} - A_{78})\phi_3,$$

$$m_{13} = B_{66}\phi_{3,1}, \quad m_{23} = B_{44}\phi_{3,2}, \quad (1.33)$$

where t_{22} , t_{21} , t_{12} , t_{11} , m_{13} and m_{23} are the traction due to normal force stresses, tangential force stresses and tangential couple stresses respectively, and A_{11} , A_{12} , A_{22} , A_{77} , A_{78} , A_{88} , B_{44} , B_{66} are the characteristic constants.

1.2.2 Micropolar thermoelasticity

Thermoelasticity is the study of the relationship between the elastic properties of a material and its temperature, or between thermal conductivity and its stresses. It is a fusion theory of heat conduction and the theory of elasticity. The theory of uncoupled thermoelasticity was introduced by Duhamel (1837) and Neumann (1885). This theory has two major flaws, i.e., the mechanical state of the elastic body has no effect on the temperature and the heat equation being parabolic predicts an infinite speed of propagation for the temperature. Biot (1956) introduced the term strain-rate in the uncoupled uncoupled thermoelasticity which removed the first flaw. Lord and Shulman (1967) introduced the first theory of generalized thermoelasticity with one relaxation time by postulating a new law of heat conduction to replace the classical Fourier's law.

The constitutive relations of linear theory of micropolar thermoelasticity was constructed by Tauchert et al. (1968). They proved the uniqueness theorem in this theory and presented the displacement, micro-rotation and the stresses. They also extended the Duhamel-Neumann analogy of classical thermoelasticity (Sokolnikof, 1946) to micropolar theory. Eringen (1970) also worked on the constitutive relations of different types of micropolar materials including both linear and non-linear thermoelasticity. Boschi and Iesan (1973) incorporated the linear theory of thermoelasticity (Green and Lindsay, 1972) to a homogeneous micropolar continuum with the help of an entropy production inequality proposed by Green and Laws (1972). They derived the basic equations using invariance conditions under superposed rigid body motions. Chanrasekhariah (1986b) introduced the heat-flux among the constitutive variables in the theory of micropolar thermoelasticity. This theory uses the Clausius-Duhem

inequality

$$\rho\dot{\eta} - \frac{\rho q}{\Theta} - \left(\frac{q_k}{\Theta}\right)_{,k} \geq 0, \quad (1.34)$$

where Θ is temperature, q_k is heat flux vector, and q is heat source density.

The constitutive equations of linear micropolar thermoelasticity is given as (Tauchert et al., 1968)

$$\begin{aligned} T_{kl} &= \lambda u_{r,r} \delta_{kl} + \mu(u_{l,k} + u_{k,l}) + \kappa(u_{l,k} - \epsilon_{klr} \phi_r) - (3\lambda + 2\mu + \kappa)\nu\Theta\delta_{kl}, \\ M_{kl} &= \alpha\phi_{r,r} \delta_{kl} + \beta\phi_{k,l} + \gamma\phi_{l,k}, \\ \rho\eta &= (3\lambda + 2\mu + \kappa)\nu u_{k,k} + d\Theta, \quad \tau\dot{q}_r = k_0\Theta_{,r} - q_r, \end{aligned} \quad (1.35)$$

where ν is a linear thermal expansion, and k_0 correspond to thermal conductivity and d is thermal parameter.

1.2.3 Micropolar thermoelasticity with voids

The elastic materials are often found with voids or pores or porous which are uniformly distributed. Voids mean gaps or air or vacuum which contain nothing of mechanical or energetic significant. Goodman and Cowin (1972) introduced the theory of granular materials using an independent kinematical variable called the volume distribution function. The elastic theory with voids generalized the classical theory of elasticity by adding a function which describes the distributions of voids volume fraction within the body (Cowin and Nunziato, 1983). Nunziato and Cowin (1979) developed the linear theory of elastic material with voids as a special case of the non-linear theory. In this theory, the changes in void volume fraction and the strain are taken as independent kinematic variables. Chanrasekhariah (1987b) formulated an initial boundary value problem in terms of stress and volume fraction fields in the context of the linear theory of homogeneous and isotropic elastic materials with voids. Iesan (1985, 1986) studied the linear theory of thermoelastic materials with voids and presented the existence and uniqueness, the reciprocity relations and the variational

characterization in the thermoelastic materials with voids. The constitutive relations of thermoelastic materials with voids are (Iesan, 1986)

$$\begin{aligned} T_{ij} &= \lambda u_{k,k} \delta_{ij} + \mu(u_{i,j} + u_{j,i}) + s\psi \delta_{ij} - m\Theta \delta_{ij}, & g &= -su_{k,k} - \zeta\psi - \xi\Theta, \\ \rho\eta &= m'u_{k,k} - \zeta\psi + d\Theta, & h_i &= a\psi_i, & q_i &= k_0\Theta_{,i} \end{aligned} \quad (1.36)$$

where u_i is components of displacement vector, ψ and Θ are change in volume fraction and temperature change, s , ζ , ξ , a are void's parameters and d , m are thermal parameters, k_0 and ν are thermal conductivity and linear thermal expansion, T_{ij} is a stress tensor, g and h_i are intrinsic equilibrated body force and equilibrated stress vector, q_i and q are heat flux vector and strength of internal heat source, ρ is bulk mass density and η is an entropy change.

Eringen (2003) developed a continuum theory for a mixture of a micropolar elastic solid and a micropolar viscous fluid describe the soil with grains and tortuous rock containing dirty fluids. Passarella (1996) derived the field and constitutive equations of porous micropolar thermoelastic materials using second laws of thermodynamics. The constitutive relations of linear homogeneous micropolar thermoelasticity with voids are (Passarella, 1996)

$$\begin{aligned} T_{ij} &= \mu(u_{i,j} + u_{j,i}) + \lambda u_{k,k} \delta_{ij} + \kappa(u_{i,j} + \epsilon_{ijk} \phi_k) + s\psi \delta_{ij} - m\Theta \delta_{ij}, \\ M_{ij} &= \alpha \phi_{k,k} \delta_{ij} + \beta \phi_{j,i} + \gamma \phi_{i,j}, & h_i &= a\psi_i, \end{aligned} \quad (1.37)$$

$$g = -su_{k,k} - \zeta\psi - \xi\Theta, \quad \dot{q}_i \tau = \Theta_{,i} k_0 - q_i, \quad \rho\eta = mu_{k,k} - \xi\psi + d\Theta, \quad (1.38)$$

where $m = (3\lambda + 2\mu + \kappa)\nu$, M_{ij} is a couple stress tensor, ϕ_i is components of microrotation vector, α , β , γ , κ are micropolar parameters and λ , μ are well known lame's parameters. The field equations in linear homogeneous micropolar thermoelastic materials with voids are (balance of momentum)

$$T_{ij,j} + \rho f_i = \rho \ddot{u}_i, \quad (1.39)$$

(balance of angular momentum)

$$M_{ij,j} - \epsilon_{ijk} T_{jk} + \rho l_i = \rho j_{ij} \ddot{\phi}_i \quad (1.40)$$

(balance of equilibrated stress)

$$h_{i,i} + g + \rho l = \rho \chi \ddot{\psi}. \quad (1.41)$$

(entropy inequality)

$$\rho \dot{\eta} \geq \left(\frac{\rho q}{\Theta} \right) - \left(\frac{q_k}{\Theta} \right)_{,k}, \quad (1.42)$$

where f_i and l_i are body force and body couple, j_{ij} is micro-inertia tensor, l and χ are extrinsic body force and equilibrated inertia.

Using the constitutive relations (1.37)-(1.38) into the field equations (1.39)-(1.42), we get

$$\begin{aligned} (\mu + \kappa) u_{i,kk} + (\lambda + \mu) u_{k,ki} + \kappa \epsilon_{ijk} \phi_{k,j} + s \psi_{,i} - m \Theta \delta_{ij} + \rho f_i &= \rho \ddot{u}_i, \\ \gamma \phi_{i,kk} + (\alpha + \beta) \phi_{k,ki} - \kappa \epsilon_{ijk} u_{j,k} - 2\kappa \phi_i + \rho l_i &= \rho j \ddot{\phi}_i, \\ a \psi_{,kk} - s u_{k,k} - \zeta \psi - \xi \Theta + \rho l &= \rho \chi \ddot{\psi}, \\ k_0 \Theta_{,kk} - \Theta_0 \left(1 + \tau \frac{\delta}{\delta t} \right) \left(m \dot{u}_{k,k} - \xi \dot{\psi} + d \dot{\Theta} - \frac{\rho q}{\Theta_0} \right) &= 0, \end{aligned} \quad (1.43)$$

where τ is thermal relaxation time.

If $d > 0$, $\tau > 0$ and $k_0 > 0$, the hyperbolic type heat equation has a finite speed which is $\sqrt{k_0(\Theta_0 \tau d)^{-1}}$. Eqs. (1.43) can be written in vector form in the absence of body forces and heat sources as

$$(\mu + \kappa) \nabla^2 u + (\lambda + \mu) \nabla \nabla \cdot u + \kappa \nabla \times \phi + s \nabla \psi - m \nabla \Theta = \rho \ddot{u}, \quad (1.44)$$

$$(\gamma \nabla^2 - 2\kappa) \phi + (\alpha + \beta) \nabla \nabla \cdot \phi + \kappa \nabla \times u = \rho_1 \ddot{\phi}, \quad (1.45)$$

$$(a \nabla^2 - \zeta) \psi - s \nabla \cdot u - \xi \Theta = \rho_2 \ddot{\psi}, \quad (1.46)$$

$$k_0 \nabla^2 \Theta - \Theta_0 \left(1 + \tau \frac{\partial}{\partial t} \right) (d \dot{\Theta} + m \nabla \cdot \dot{u} - \xi \dot{\psi}) = 0, \quad (1.47)$$

where $u = (u_1, u_2, u_3)$, $\phi = (\phi_1, \phi_2, \phi_3)$, $\rho_1 = \rho J$ and $\rho_2 = \rho \chi$ are coefficients of inertia.

This field equations correspond to Fourier classical law of micropolar thermoelastic material with voids if $\tau = 0$. If $\tau \geq 0$, the above system of equations correspond to the micropolar thermoelastic material based on Lebon's law of heat conduction. The internal energy density is a positive definite quadratic form (Eringen, 1990a)

$$2\mu + \kappa > 0, \quad \kappa > 0, \quad \zeta > 0, \quad (3\lambda + 2\mu + \kappa)\zeta > 3s^2,$$

$$3\alpha + \beta + \gamma > 0, \quad \alpha \pm \beta > 0, \quad a > 0, \quad k_0 > 0, \quad (1.48)$$

which is the necessary and sufficient conditions for the strain energy density to be non-negative.

1.3 Hooke's law

A continuum body gets deformed when subjected to external loads and returns to its original shape and size after the removal of external forces. The relative position of the constituent particles of a continuous body gets altered when an external force is applied and the continuum body is said to be *strained* and the change in the relative position of the particles is known as *deformation*. At this stage, the particles resist to change their positions but the external force makes them to change their positions up to some extent and when the external forces are withdrawn, these particles at once regain their original shape and size. The elastic property of a continuum body depends on the strength of resistance, so greater the resistance of a body to deform the more is the elasticity. The measure of intensity of internal forces generated in a body is called *Stress* and the deformation of the body due to application of stress is called *strain*. The strain set up in a body in such a way that there is a change in volume but no change in shape is called *dilatation*. Compression (volume reduces) and rarefaction (volume increases) are two kinds of dilatation. The elastic deformation is called *shear* if there is a change in shape and size but not in a volume. Within the elastic

limit, stress is a linear combination of strain. The stress tensor (τ_{ij}) is related with the strain tensor (e_{kl}) as (Achenbach, 1973)

$$\tau_{ij} = C_{ijkl}e_{kl}, \quad (i, j, k, l = 1, 2, 3) \quad (1.49)$$

where $C_{ijkl} = C_{jikl} = C_{klij} = C_{ijlk}$ is the elastic constant which is of fourth order tensor and characterizes the elastic property of the materials. If the elastic constants are functions of the position, then the body is said to be *inhomogeneous* and if they are same for all points of the medium, then the body is called *homogeneous*. A continuum body is said to be *isotropic* if there are no preferred directions so that the elastic constants are same whatever the orientation.

1.4 Elastic waves

The study of wave propagation in elastic continuum has a long and distinguished history. In the 19th century, great Mathematicians such as Cauchy and Poisson exposed that light could be regarded as the propagation of a disturbance in an elastic aether which lead to the development of the theory of elasticity. Poisson, Ostrogradsky, Cauchy, Green, Lamé, Stokes, Clebsch, Christoffel, Rayleigh, Lamb, and Love carried out early investigation on the propagation of waves in elastic solids(Love, 1892).

A wave is an oscillation accompanied by a transfer of energy from one point to another which displace particles of the transmission medium with little or no associated mass transport. There are two main types of waves: (i) Mechanical waves propagate through a medium and (ii) electromagnetic waves which do not require a medium. We will discuss more about elastic waves/acoustic waves which travel through an elastic solid with finite velocity. Elastic waves are examples of mechanical waves. These waves may be divided into two kinds: (i) Body waves and (ii) Surface waves. Body waves travel through the interior of the medium. The density and modulus vary according to temperature, composition and phase. Surface waves travel along the surface of the medium and the strength or amplitude of these waves

decrease exponentially with increasing distance from the boundary surface. There are mainly three types of surface waves: Rayleigh waves, Stoneley waves and Love waves.

Rayleigh waves are the surface waves that travel along the stress free boundary of an elastic half-space such that the disturbance is largely confined to the neighborhood of the free boundary of the half-space. It was introduced by Rayleigh (1877) and hence, called Rayleigh waves. These waves are the result of superposing longitudinal and transverse waves. It is a combination of vibrations due to longitudinal and transverse waves. In the Rayleigh wave propagation, the surface particle motion is found to be counterclockwise elliptical (retrograde), which changes from retrograde at the surface to prograde (clockwise elliptical) at depth, passing through a node at which there is no horizontal motion.

Stoneley waves are those surface waves which can propagate along the interface between liquid-solid or solid-solid half-spaces. They are non-dispersive in nature and can travel along the solid - solid interface when their elastic properties are nearly same. The amplitudes of Stoneley waves have their maximum values at the boundary and decay exponentially towards the depth of each of them.

Love (1911) found that certain type of shear wave can travel in a layer lying over an elastic half-space provided that the phase speed of the wave lies between the phase speed of shear wave in the layer and that of in the half-space. Love waves are horizontally polarized shear waves (SH waves) existing only in the presence of a semi-infinite medium overlain by an upper layer of finite thickness. It is the fastest surface wave and moves the ground side to side in a horizontal plane parallel to the earth's surface but at the right angle to the direction of propagation.

1.5 Helmholtz decomposition theorem

Theorem 1.1 Let $\mathbf{Z}(\mathbf{x})$ be a vector field. Then there exist a scalar potential $V(\mathbf{x})$ and a vector potential $\mathbf{Y}(\mathbf{x})$ such that

$$\mathbf{Z} = \nabla V + \nabla \times \mathbf{Y}, \quad \nabla \cdot \mathbf{Y} = 0. \quad (1.50)$$

This representation is called *Helmholtz decomposition* (Pujol, 2003).

Proof: Let us take a vector Poisson equation of the form

$$\nabla^2 \mathbf{W}(\mathbf{x}) = \mathbf{Z}(\mathbf{x}). \quad (1.51)$$

Using the definition of Laplacian of a vector, we have

$$\nabla^2 \mathbf{W} = \nabla(\nabla \cdot \mathbf{W}) - \nabla \times (\nabla \times \mathbf{W}) \equiv \nabla V + \nabla \times \mathbf{Y} \quad (1.52)$$

with

$$V = \nabla \cdot \mathbf{W}, \quad \mathbf{Y} = -\nabla \times \mathbf{W} \quad (1.53)$$

and

$$\nabla \cdot \mathbf{Y} = -\nabla \cdot (\nabla \times \mathbf{W}) = 0. \quad (1.54)$$

In the Equation (1.51), $\mathbf{Z}(\mathbf{x})$ is a piecewise differentiable vector in a finite open region V' and this vector is associated with

$$\mathbf{W}(\mathbf{x}) = -\frac{1}{4\pi} \int_{V'} \frac{\mathbf{Z}(\boldsymbol{\xi})}{|\mathbf{x} - \boldsymbol{\xi}|} d\mathbf{V}'_{\boldsymbol{\xi}}, \quad (1.55)$$

where $d\mathbf{V}'_{\boldsymbol{\xi}} = d\xi_1 d\xi_2 d\xi_3$, and $|\mathbf{x} - \boldsymbol{\xi}| = \{(x_1 - \xi_1)^2 + (x_2 - \xi_2)^2 + (x_3 - \xi_3)^2\}^{(1/2)}$.

Then, $\mathbf{W}(\mathbf{x})$ satisfies the vector equation (1.51) at interior points where \mathbf{Z} is continuous and $\nabla^2 \mathbf{W} = \mathbf{0}$ at points outside the region V' .

1.6 Applications of wave propagation

The elastic wave propagation has numerous applications in various fields. The subject of elastic wave propagation and their phenomena of reflection and refraction from a boundary surface are very important in the field of Seismology, Earthquake engineering and geophysics. Elastic waves carry lots of information about the characteristics of the medium through which they travel and so it becomes a very reliable tool to the oil exploration and mining sites. They give valuable information about the interior of the material body. The body waves are used in earthquake engineering for predicting earthquake in the dynamic response of soils and man-made structures.

In geophysics, the study of wave propagation and their phenomena of reflection and refraction are helpful not only in exploration of internal structure of the earth but also in exploration of valuable materials buried inside the earth like minerals, metals, hydrocarbons and petroleum. The method of wave propagation used in the exploration of oils, minerals, crystals and others is one of the best suitable method because it is cheap and less time consuming. The wave propagation technique is also used for the estimation of the earth's internal composition. The body waves have been sent from one station and then, the signals are received in another station and examined. These signals give indirect information about the internal structure of the earth. To know about the deep interior of the earth materials, the seismic body waves are very useful. It is proved in the literature that *S*-waves can not travel through the interior of the core (the innermost part of the earth). This had led to the conclusion that the earth core is composed of material which is non-viscous liquid like. Thus, the earth core is believed to be in liquid form at high temperature (which makes the liquid of the core almost a non-viscous) and harder than the solid.

Wave motion is helpful in the production of ceramics or certainly in ceramic behavior. Saggio-Woyansky et al.(1992) have observed that porous ceramics are either reticulate or foam and are made up of a porous network which has relatively low mass, low thermal conductivity and low density. Raiser et al.(1994) have reported experimental results where

microcracking along grain boundaries in ceramics is caused by compressive waves. The study of wave motion in porous ceramics is useful (Straughan, 2008) since they are used for molten metal filters, diesel engine exhaust filters as catalyst supports and industrial hot-gas filters, and both reticulate and foam porous ceramics are used as light-structure plates, in gas combustion burners and in fire protection and thermal insulation materials. Elastic materials with voids is applied in the production of building materials such as bricks and wave propagation in such materials may be helpful.

Acoustic waves comprise a very useful therapeutic modality. Three types of acoustic waves: Extracorporeal Shock Waves(ESWs), Pressure Waves (PWs) and Ultrasound (US) are used in the medical field. Shock waves (Tsaklis, 2010) are characterized by high pressure amplitudes and an abrupt increase in pressure that propagates rapidly through a medium. The energy distribution in the treatment area differs from being wide over a large area or concentrated in a narrow treatment zone and as such influences the therapeutic and biological effect of the shock wave. Pressure waves are usually generated by the collision of solid bodies with an impact speed of a few meters per second, far below the speed the shock wave travels. Ultrasound therapy is one of the modalities of physical medicine used for pain management and for increasing blood flow and mobility.

1.7 Review of Literatures

The subject of wave propagation is an interesting area of research since long. Many problems of waves and vibrations are in open literatures and notable among them are Rayleigh (1885), Voigt (1887), Lamb (1917), Ewing et al. (1957), Brekhoviskikh (1960), Green and Rivlin (1964), Suhubi and Eringen (1964), Green(1965), Acharya and Sengupta (1976), Ben Mena-hem and Singh (1981), Bullen and Bolt (1985), Chanrasekhariah (1991), Graff (1991), Ciarletta and Iesan (1993), Ciarletta and Scalia (1993b), Wang and Dhaliwal (1993), Tomar and Kumar (1995), Sinha and Elsibai (1997), Abd-Alla (1999), Udias (1999), Xia et al. (1999), Sharma (2001), Singh (2002, 2007a), Kumar and Choudhary (2003), Abd-Alla and Ah-

mad (2003), Kumar and Ailawalia (2005), Muller (2007), Ciarletta and Straughan (2007a), Sharma (2007), Das et al. (2008), Chirita and Giba (2010), Singh and Chakraborty (2013), Vinh (2013), Sharma and Kaur (2014) and many others.

Puri and Cowin (1985) analyzed the behavior of plane harmonic waves in linear elastic materials with voids. Chanrasekhariah (1986a) studied surface waves in a homogeneous and isotropic linear elastic half-space containing a distribution of vacuous voids. Singh and Tomar (2006a) obtained the reflection and transmission coefficients of the reflected and transmitted waves due to incident transverse wave between two different porous elastic half-spaces. Dere-siewicz and Rice (1962) derived a general solution of Blot's field equations governing small motions of a porous solid saturated with a viscous liquid. The solution is also employed to study some of the phenomena attendant upon the reflection from a plane, traction-free boundary of each of the three body waves predicted by the equations. Cruz et al.(1992) analyzed the mode conversions which occur during the reflection and transmission of seismic waves at the boundaries of porous media. They have shown the energy partitioned to the various modes depends on the incident angle and on the physical properties of the fluid and solid components on each side of the boundary. Ciarletta and Sumbatyan (2003) studied the reflection of incident plane waves at a free boundary of an elastic solid with voids. Ciarletta and Straughan (2006) investigated the problem of acoustic waves in a porous medium. Ciarletta et al. (2005), Chirita et al. (2006), Straughan (2009), Ciarletta et al.(2014) and Nield and Bejan (2017) also discussed problems of wave propagation in elastic materials with voids.

Chandrasekhariah (1981) investigated the problem of dynamical disturbances in thermoelastic half-spaces with plane boundary due to the application of a step in strain or temperature on the boundary in the context of the linearized Green-Lindsay thermoelasticity theory. Inan and Eringen (1991) discussed the problem of longitudinal wave in thermoelastic plates in the context of non-local thermoelasticity. Green and Naghdi (1993) studied the problem of linear and non-linear theory of thermoelastic materials without energy dissipation. Sinha

and Elsibai (1996) attempted the problem of reflection of thermoelastic waves from the free surface of a generalized thermoelastic materials. Abd-Alla and Al Dawy (2000) discussed the reflection phenomena of SV -waves in a generalized thermoelastic medium and obtained the reflection coefficients. Sharma et al. (2003a) studied the problem of reflection of thermoelastic wave from the insulated and isothermal stress free boundaries of a solid half-space in the context of different theories of generalized thermoelasticity. Singh et al.(2011) applied the theory of generalized thermo-elastic diffusion to study the reflection and transmission of P and SV -waves at an interface of two dissimilar thermo-elastic solids with diffusion. Some problems of wave propagation in thermoelastic materials are Ivanov (1988), Iesan (2004), Singh (2005), Aouadi (2007), Othman and Song (2008), Sharma and Sharma (2009), Singh et al. (2010), Chirita (2011) and Vashishth and Sukhija (2015).

Ciarletta and Scalia (1993a) discussed the problem of non-linear theory of non-simple thermoelastic materials with voids. Dhaliwal and Wang (1995) formulated thermoelasticity theory for elastic materials with voids by including heat-flux among the constitutive variables. Ciarletta and Straughan (2007b) attempted the problem of thermo-poroacoustic acceleration waves in elastic materials with voids. Ciarletta et al. (2007b) introduced thermal displacement wave in a model of wave propagation in a porous material. Singh (2007b) obtained the reflection coefficients of the reflected waves in generalized thermoelastic half-space with voids in context of Lord-Shulman theory. Singh and Tomar (2007) investigated the reflection phenomenon of a set of coupled longitudinal waves from a free plane boundary of a thermo-elastic half-space with voids and obtained amplitude and energy ratios of various reflected waves. Sharma (2008) concluded that the thermal properties of the thermoelastic waves in poroelastic medium have no effect on the transverse wave. The problems of the theory of thermoelastic materials with voids are also analyzed by Ciarletta and Scalia (1990), Pompei and Scalia (1994), Pampolona et al. (2009), Aouadi (2010), Singh and Tomar (2011), Singh (2011) and Boccur et al. (2014).

Cosserat and Cosserat(1909) developed the complete non-linear theory of the asymmetric

elasticity by assuming each of the material's particles can displace and rotate independently during the process of deformation. Mindlin and Tiersten (1962) and Toupin (1962) introduced the couple stress theory. Mindlin (1964) reduced the micromorphic theory into the theory of microstructure by assuming small deformation and slow motion. The Eringen's theories (1964) of micromorphic, microstretch and micropolar continua are the generalization of the classical theory of elasticity. Parfitt and Eringen (1969) investigated the problem of reflection of plane waves from the flat boundary of micropolar half-space and shown the existence of four plane waves. The extensive problems of micropolar and microstretch continua are found in open literatures, i.e., Eringen (1984), Nowacki and Nowacki (1969), Smith (1967), Ariman (1972), Tomar and Gogna (1995), Huang and Liang (1997), Tomar et al. (1998), Pabs (2005), Kumar and Partap (2006), Ramezani and Naghdabadi (2007), Marin (2010) and Kumar and Kaur (2014).

Eringen (1990b) derived the equations of motions, constitutive equations and boundary conditions for the thermomicropolar fluid whose micro-elements could undergo dynamical expansions and contractions. Chanrasekhariah (1987a) obtained the variational principles of Biot and Hamilton-types and a reciprocal principle of Betti Rayleigh-type in the context of a in the context of a linearized anisotropic micropolar thermoelasticity theory. Das and Sengupta (1990) discussed the problem of surface waves in the general theory of micropolar thermoelasticity under the influence of gravity. Boffils and Quintanilla (1995) proved the uniqueness theorem for the solutions in the linear theory of thermo-microstretch elastic solids. Svanadze and De Cicco (2005) constructed the fundamental solution of the system of differential equations in the case of steady oscillations in terms of elementary functions of linear theory of thermomicrostretch elastic solids. Sharma and Marin (2014) attempted the problem of reflection and transmission of plane waves at an imperfect boundary between two thermally conducting micropolar elastic solid half-spaces with two temperatures. The following problems may also be mentioned for the materials of micropolar thermoelasticity, i.e., Kumar and Partab (2007), Othman and Singh (2007), Singh (2001, 2010), Kumar and

Sharma (2008), Aouadi (2009), Passarella and Zampoli (2010), Shaw and Mukhopadhyay (2011), Othman and Atwa (2012) and Kumar et al. (2014).

Scalia (1992) derived a linear grade consistent micropolar theory of thermoelastic materials with voids with the help of an entropy production inequality proposed by Green and Laws (1972). Diabls (1999) derived the deformation tensors and the corresponding deformation velocities based on the motion and micromotion of micropolar materials. Singh (2000) studied the problem of reflection and refraction of plane sound wave at an interface between a liquid half-space and a micropolar generalized thermoelastic solid half-space using the theories of Lord and Shulman (1967) and Green and Lindsay (1972). Mondal and Acharya (2006) investigated the effect of voids and micropolar characters on the propagation of surface waves in a homogeneous micropolar solid medium. Singh and Tomar (2006b) studied the problem of propagation of waves in an infinite porous continuum consisting of a micropolar elastic solid and a micropolar viscous fluid using the theory of Eringen (2003). Tomar (2005) discussed the frequency equations in micropolar elastic plates with voids corresponding to symmetric and antisymmetric modes of vibrations of the plate. Tomar and Singh (2006) attempted the problem of propagation of plane waves and their reflection from a free boundary of a micropolar porous elastic half space. They have found that the presence of the voids in the medium is significant in the the reflection from the free boundary of a half-space for the incident longitudinal wave having low frequency. Ciarletta et al. (2007a) constructed the fundamental solution of the system of differential equations in the case of steady oscillations in terms of elementary functions for micropolar thermoelasticity with voids. Passarella et al.(2011a) studied the problem of heat-flux dependent thermoelasticity for micropolar porous media. Ailawalia and Kumar (2011) discussed the deformation of micropolar generalized thermoelastic medium with voids under the influence of various sources acting on the plane surface. Marin (2016) formulated a heat-flux theory in the context of micropolar porous media by taking into account a new set of state variables, the heat-flux vector and an evolution equation.

Hosten (1991) presented a method of characterizing orthotropic and viscoelastic behavior of some composite materials. He proposed a numerical method for computing the reflection and transmission coefficients of plane waves for any incidence plane through an orthotropic, lossy solid layer. Sharma (2006) derived a mathematical model for the wave propagation in anisotropic generalized thermoelastic medium and showed the existence of four quasi-waves in the medium. Singh (2007c) studied two-dimensional plane wave propagation in an orthotropic micropolar elastic solid and obtained the reflection coefficients of various reflected waves. Kumar and Gupta (2009) solved the problem of plane strain deformation in an orthotropic micropolar generalized thermoelastic half-space subjected to an arbitrary point heat source. Iesan (1974) discussed the torsion problem of homogeneous and orthotropic cylinders in the linear theory of micropolar elasticity and proved the existence theorem. Vinh and Ogden (2004) obtained the formulas for the speed of Rayleigh waves in orthotropic compressible elastic materials in explicit form by using the theory of cubic equations. Passarella et al. (2011b) considered an orthotropic micropolar elastic material subject to a state of plane strain and established the necessary and sufficient conditions for the strong ellipticity of constitutive coefficients. The problems of wave propagation in anisotropic micropolar materials are also studied by Nakamura et al. (1984), Sharma (1988), Singh (2003), Sharma et al. (2003b), Kumar and Choudhary (2004), Zhu and Tsvankin (2006), Aouadi (2008) and Iesan (2010).

Chapter 2

Plane waves in micropolar thermoelastic materials with voids¹

2.1 Introduction

The theory of micropolar continua describes the behavior of complex materials such as bones, blood, cellular solids and polymers. A continuum model is embedded with microstructures which can explain the microscopic motion along with the long range materials interaction. Eringen (1964, 1966, 1968) introduced the linear theory of micropolar elasticity. In this theory, the motion of the particles are expressed in terms of the displacement and micro-rotation vector. Marin (1996) proved the reciprocal theorem, uniqueness results and minimum principle that satisfy the constitutive and field equations of the micropolar materials with voids. Passarella (1996) derived the constitutive and field equations for micropolar porous thermoelasticity.

In this chapter, we study the problem of plane waves in the micropolar thermoelastic materials with voids. There exist six waves in such materials medium, of which, four of them are dilatational waves (micropolar wave and three coupled dilatational waves) and the other two are coupled shear waves. These waves are attenuated. We obtain the phase velocities and attenuations of these waves analytically and numerically. The effects of micro-inertia

¹*Science and Technology Journal*, 4(2), 141-151(2016)

and thermal relaxation time on the phase velocity and attenuation are discussed.

2.2 Basic equations

The equations of motion for the dilatational waves, micropolar wave and shear waves in a homogeneous micropolar thermoelastic materials with voids are given by

(a) Dilatational waves

(i) Coupled dilatational waves:

$$(c_1^2 + c_2^2)\nabla^2 u' + c_3^2\psi - c_4^2\Theta = \ddot{u}', \quad (2.1)$$

$$c_8^2\nabla^2 u' - (c_9^2\nabla^2 - c_{10}^2)\psi + c_{11}^2\Theta = -\ddot{\psi}, \quad (2.2)$$

$$k_0\nabla^2\Theta - \Theta_0(1 + \tau\frac{\partial}{\partial t})(d\dot{\Theta} + m\nabla^2 u' - \xi\dot{\psi}) = 0, \quad (2.3)$$

(ii) Micropolar wave/uncoupled dilatational wave:

$$(c_5^2 + c_6^2)\nabla^2\phi' - c_7^2\phi' = \ddot{\phi}', \quad (2.4)$$

(a) Coupled shear waves

$$c_{12}^2\nabla^2 \mathbf{u}'' + c_2^2\nabla \times \boldsymbol{\phi}'' = \ddot{\mathbf{u}}'', \quad (2.5)$$

$$(c_6^2\nabla^2 - c_7^2)\boldsymbol{\phi}'' + c_{13}^2\nabla \times \mathbf{u}'' = \ddot{\boldsymbol{\phi}}'', \quad (2.6)$$

where λ , μ are Lamé's parameters; k_0 is the thermal conductivity, τ is thermal relaxation time; m , d are thermal parameters; a , ζ , ξ , s are void parameters; α , β , γ , κ are micropolar parameters, ρ is mass density; $\rho_1 = \rho J$, $\rho_2 = \rho \chi$ are coefficients of inertia, Θ is the temperature measure from the reference temperature, ψ is the change of volume fraction, Θ_0 is temperature of the material in a reference state; u' , ϕ' are the scalar potentials corresponding to dilatational waves and \mathbf{u}'' , $\boldsymbol{\phi}''$ are vector potentials corresponding to shear

waves obtained from Helmholtz's decompositions of \mathbf{u} and ϕ as

$$\mathbf{u} = \nabla u' + \nabla \times \mathbf{u}'', \quad \phi = \nabla \phi' + \nabla \times \phi''.$$
 (2.7)

The expressions of $c_1, c_2, c_3, \dots, c_{13}$ are given by

$$\begin{aligned} c_1^2 &= \frac{\lambda + 2\mu}{\rho}, & c_2^2 &= \frac{\kappa}{\rho}, & c_3^2 &= \frac{s}{\rho}, & c_4^2 &= \frac{m}{\rho}, & c_5^2 &= \frac{\alpha + \beta}{\rho_1}, & c_6^2 &= \frac{\gamma}{\rho_1}, & c_7^2 &= \frac{2\kappa}{\rho_1}, \\ c_8^2 &= \frac{s}{\rho_2}, & c_9^2 &= \frac{a}{\rho_2}, & c_{10}^2 &= \frac{\zeta}{\rho_2}, & c_{11}^2 &= \frac{\xi}{\rho_2}, & c_{12}^2 &= \frac{\mu + \kappa}{\rho}, & c_{13}^2 &= \frac{\kappa}{\rho_1}. \end{aligned}$$

2.3 Harmonic waves

The time harmonic waves may be represented by

$$\{u', \phi', \psi, \Theta, \mathbf{u}'', \phi''\} = \{u_0, \phi_0, \psi_0, T_0, \mathbf{A}, \mathbf{B}\} \exp\{ik(\mathbf{n} \cdot \mathbf{r} - ct)\},$$
 (2.8)

where $\omega (= kc)$ is the angular frequency, c is phase velocity, \mathbf{n} is the unit normal vector and \mathbf{r} is position vector.

Using the Equation (2.8) into (2.1)-(2.4), we obtain the system of equations

$$\begin{pmatrix} c_0^2 k^2 - \omega^2 & -c_3^2 & c_4^2 \\ c_8^2 k^2 & \omega^2 - c_{10}^2 - c_9^2 k^2 & -c_{11}^2 \\ c_m^2 k^2 & c_\xi^2 & c_k^2 k^2 - c_d^2 \end{pmatrix} \begin{pmatrix} u_0 \\ \psi_0 \\ T_0 \end{pmatrix} = \begin{pmatrix} 0 \\ 0 \\ 0 \end{pmatrix},$$
 (2.9)

and

$$[\omega^2 - (c_5^2 + c_6^2)k^2 - c_7^2] \phi_0 = 0,$$
 (2.10)

where

$$c_0^2 = c_1^2 + c_2^2, \quad c_m^2 = \frac{m}{\rho_1}, \quad c_\xi^2 = \frac{\xi}{\rho_1}, \quad c_d^2 = \frac{d}{\rho_1}, \quad c_k^2 = \frac{k_0}{\Theta_0 \rho_1 \omega (\omega \tau + i)}.$$

These equations will help to find the phase velocity of the dilatation waves.

Similarly, using the Equation (2.8) into (2.5)-(2.6), we get

$$(\omega^2 - k^2 c_{12}^2) \mathbf{A} + ikc_2^2 (\mathbf{n} \times \mathbf{B}) = 0, \quad (2.11)$$

$$ikc_{13}^2 (\mathbf{n} \times \mathbf{A}) - (c_6^2 k^2 + c_7^2 - \omega^2) \mathbf{B} = 0, \quad (2.12)$$

which correspond to shear waves.

For non-trivial solutions of Equation (2.9), we have

$$Ak^6 + Bk^4\omega^2 + Ck^2\omega^4 + D\omega^6 = 0, \quad (2.13)$$

where

$$\begin{aligned} A &= -c_0^2 c_9^2 c_k^2, \quad B = c_4^2 c_m^2 c_9^2 / \omega^2 + c_8^2 c_k^2 c_3^2 / \omega^2 - c_0^2 c_{10}^2 c_k^2 / \omega^2 + c_0^2 c_9^2 c_d^2 / \omega^2 + c_9^2 c_k^2 + c_0^2 c_k^2, \\ C &= c_0^2 c_{11}^2 c_\xi^2 / \omega^4 + c_4^2 c_m^2 c_{10}^2 / \omega^4 + c_0^2 c_{10}^2 c_d^2 / \omega^4 + c_3^2 c_{11}^2 c_m^2 / \omega^4 + c_4^2 c_\xi^2 c_8^2 / \omega^4 - c_8^2 c_d^2 c_3^2 / \omega^4 \\ &\quad - c_0^2 c_d^2 / \omega^2 - c_9^2 c_d^2 / \omega^2 - c_4^2 c_m^2 / \omega^2 + c_{10}^2 c_k^2 / \omega^2 - c_k^2, \quad D = c_d^2 / \omega^2 - c_{11}^2 c_\xi^2 / \omega^4 - c_{10}^2 c_d^2 / \omega^4. \end{aligned}$$

The above equation may be written as

$$Dc^6 + Cc^4 + Bc^2 + A = 0. \quad (2.14)$$

Eq. (2.14) is cubic in c^2 and by taking $c^2 = V$, we have

$$DV^3 + CV^2 + BV + A = 0. \quad (2.15)$$

The roots of Eq. (2.15) correspond to the phase velocity of coupled dilatational waves.

Similarly, with the help of Equations (2.11)-(2.12), we get

$$Lk^4 + Mk^2\omega^2 + N\omega^4 = 0, \quad (2.16)$$

where

$$L = c_{12}^2 c_6^2, \quad M = -c_6^2 - c_{12}^2 + c_{12}^2 c_7^2 / \omega^2 + c_{13}^2 c_2^2 / \omega^2, \quad N = 1 - c_7^2 / \omega^2.$$

Equation (2.16) can be written as

$$Nc^4 + Mc^2 + L = 0. \quad (2.17)$$

Equation (2.17) is quadratic in c^2 and by taking $c^2 = V$, we have

$$NV^2 + MV + L = 0. \quad (2.18)$$

This equation gives the phase velocity corresponding to the coupled shear waves (Parfitt and Eringen, 1969).

2.4 Phase velocity & Attenuation

We have seen that if the roots are complex and hence the corresponding waves are attenuating in nature. If we take $c_{Ri} = Re(\sqrt{V_i})$ and $c_{Ii} = Im(\sqrt{V_i})$ for $(i = 1, 2, \dots, 6)$, then the phase velocity and attenuation coefficients of the dilatational and shear waves may be defined as

$$v_i = \frac{(c_{Ri}^2 + c_{Ii}^2)}{c_{Ri}}, \quad Att_i = -\frac{2c_{Ii}}{c_{Ri}} \quad (i = 1, 2, \dots, 6), \quad (2.19)$$

where V_i are the solutions of frequency equations corresponding to the dilatational and shear waves.

2.4.1 For dilatational waves

If V_i ($i = 1, 2, 3$) are the roots of Equation (2.15), their analytical expressions are given by

$$V_1 = \left(\sqrt{H^2 + I^3} - H\right)^{1/3} - I \left(\sqrt{H^2 + I^3} - H\right)^{-1/3} - C/3D, \quad (2.20)$$

$$\begin{aligned} V_2 &= \left(\sqrt{H^2 + I^3} - H\right)^{-1/3} I/2 - \left(\sqrt{H^2 + I^3} - H\right)^{1/3} /2 \\ &+ \left(\sqrt{H^2 + I^3} - H\right)^{-1/3} \sqrt{3}I/2 - C/3D + \left(\sqrt{H^2 + I^3} - H\right)^{1/3} \nu/2, \end{aligned} \quad (2.21)$$

$$V_3 = \left(\sqrt{H^2 + I^3} - H\right)^{-1/3} I/2 - \left(\sqrt{H^2 + I^3} - H\right)^{1/3} /2$$

$$-\left(\sqrt{H^2 + I^3} - H\right)^{-1/3} \sqrt{3}I/2 - C/3D + \left(\sqrt{H^2 + I^3} - H\right)^{1/3} \iota/2, \quad (2.22)$$

where

$$H = A/2D + C^3/27D^3 - BC/6D^2, \quad I = B/3D - C^2/9D^2.$$

Equation (2.10) gives the phase velocity corresponding to the fourth dilatational wave as

$$V_4 = \omega^2(c_5^2 + c_6^2)/(\omega^2 - c_7^2). \quad (2.23)$$

This wave is also known as micropolar wave and dispersive. The phase velocity of the fourth dilatational wave depends on the angular momentum and micropolar parameters. We have seen that c_7 is the cutoff frequency for the micropolar wave below which the wavenumber vanishes.

Theorem 2.1. If the condition (1.48) is satisfied, then the roots of Eq. (2.15) satisfy the following properties:

- (a) V_i , ($i = 1, 2, 3$) are complex for $G \neq 0$.
- (b) If $G = 0$, then one of V_i (say V_1) is real and the others are complex.

Also $V_1 > 0$ for $G_0 > 0$, and $V_1 < 0$ for $G_0 < 0$,

where

$$G = (c_4^2\omega^2 - c_4^2c_{10}^2 - c_3^2c_{11}^2)(c_4^2c_8^2 + c_0^2c_{11}^2) - c_4^2c_9^2c_{11}^2\omega^2, \quad G_0 = c_0^2 + c_4^2c_8^2/c_{11}^2.$$

Proof: Let us take V_0 be a real root of Eq. (2.15). The real and imaginary parts of this equation gives

$$(DV_0^2 + B_1V_0 + B_2)V_0\omega\tau + (B_3V_0^2 + B_0V_0 - c_0^2c_9^2)k_0/(\rho_1\omega\Theta_0) = 0,$$

$$DV_0^2 + B_1V_0 + B_2 = 0, \quad (2.24)$$

where

$$B_0 = c_8^2c_3^2/\omega^2 - c_0^2c_{10}^2/\omega^2 + c_9^2 + c_0^2, \quad B_1 = c_0^2c_{11}^2c_\xi^2/\omega^4 + c_4^2c_m^2c_{10}^2/\omega^4 + c_0c_{10}^2c_d^2/\omega^4 + c_4^2c_\xi^2c_8^2/\omega^4$$

$$-c_8^2 c_3^2 / \omega^4 c_0^2 c_d^2 / \omega^2 - c_9^2 c_d^2 / \omega^2 - c_4^2 c_m^2, \quad B_2 = c_4^2 c_m^2 c_9^2 / \omega^2 + c_0^2 c_9^2 c_d^2 / \omega^2, \quad B_3 = c_{10}^2 / \omega^2 - 1.$$

This equation may be written as

$$(c_9^2 + c_{10}^2 / \omega^2 - V_0)(c_0^2 - V_0) = c_8^2 c_3^2 / \omega^2,$$

$$(c_4^2 c_{10}^2 / \omega^2 + c_3^2 c_{11}^2 / \omega^2 - c_4^2) c_m^2 / \omega^2 - (c_4^2 V_0 / \omega^2 - c_4^2 c_8^2 / \omega^2 - c_4^2 c_9^2 / \omega^2) c_\xi^2 V_0 / \omega^2 = 0, \quad (2.25)$$

which again reduces to

$$c_9^2 c_4^2 \omega^2 = (c_4^2 \omega^2 - c_4^2 c_{10}^2 - c_3^2 c_{11}^2) V_0, \quad c_{11}^2 V_0 = c_4^2 c_8^2 + c_0^2 c_{11}^2. \quad (2.26)$$

Hence, from Eq. (2.26), we get

$$GV_0 = 0. \quad (2.27)$$

If $G \neq 0$, it follows that V_i ($i = 1, 2, 3$) are complex.

If $G = 0$, then $G_0 \neq 0$ and from Eq. (2.26), we have $V_0 = G_0$. Hence the theorem.

Theorem 2.2. If the condition (1.48) are satisfied, then V_4 has the following properties:

- (i) $V_4 > 0$ for $\omega > c_7 > 0$,
- (ii) $V_4 \rightarrow \infty$ when $\omega \rightarrow c_7$,
- (iii) $V_4 < 0$ for $0 < \omega < c_7$.

Proof: The proof is trivial and is the consequence of Equation (2.23).

2.4.2 For the shear waves

The phase velocities corresponding to the coupled shear waves are obtained by solving Equation (2.18) and their expressions are given by

$$V_{5,6} = -\frac{M}{2N} \pm \frac{R}{2N}, \quad (2.28)$$

where

$$R^2 = M^2 - 4NL.$$

We come to know that the phase velocities corresponding to the coupled shear waves in micropolar thermoelastic materials with voids depend on the angular frequency, micropolar parameters and elastic constants .

Theorem 2.3. If the condition (1.48) are satisfied, then V_5 and V_6 has the following properties:

- (i) $V_6 > 0$, $V_5 > 0$ for $\omega > c_7$,
- (ii) $V_6 > 0$, and $V_5 \rightarrow \infty$ when $\omega \rightarrow c_7$,
- (iii) $V_6 > 0$, and $V_5 < 0$ for $0 < \omega < c_7$.

Proof: The proof is clear from Equation (2.28). We have seen that the phase velocity corresponding to fourth dilatation wave (*FDW*)/micropolar wave and first coupled shear waves (*FCSW*) are undefined if $\omega \rightarrow c_7$. Therefore, this value c_7 is the cut off frequency for *FDW* and *FCSW*. In this case, the Eq. (2.18) becomes $MV + L = 0$ and the corresponding phase velocity is given by

$$\sqrt{\frac{2\gamma(\mu + \kappa)}{2\gamma - J\kappa}}.$$

If $\omega < c_7$, in this case, the *FDW* and *FCSW* will degenerate into distance decaying vibration (See Parfitt and Eringen, 1969) and $\sqrt{V_4}$, $\sqrt{V_5}$ are purely imaginary satisfying the theorems 2.2 and 2.3.

2.5 Special cases

Case (i): In the absence of thermal effect, the materials reduces to the micropolar elastic materials with voids with

$$m = k_0 = \tau = 0$$

and consequently, $c_m = c_4 = c_k = 0$. Therefore, Equation (2.15) in this condition reduces to

$$DV^2 + CV + B = 0, \tag{2.29}$$

where

$$D = c_d^2 - c_{11}^2 c_\xi^2 / \omega^2 - c_{10}^2 c_d^2 / \omega^2; \quad C = c_0^2 c_{11}^2 c_\xi^2 / \omega^2 + c_0^2 c_{10}^2 c_d^2 / \omega^2 - c_8^2 c_d^2 c_3^2 / \omega^2 - c_0^2 c_d^2 - c_9^2 c_d^2; \quad B = c_0^2 c_d^2 c_9^2.$$

Solving Equation (2.29), we get the phase velocities of coupled dilatational waves as

$$V_{1,2} = \left(-C \pm \sqrt{C^2 - 4BD} \right) / 2D. \quad (2.30)$$

We have seen that there is no change in the phase velocities corresponding to fourth dilatation and the two coupled shear waves. Their values are given by Equations (2.23) and (2.28). So, there are five waves in which three are dilatational and two are coupled shear waves.

Case (ii): In the absence of voids, the material reduces to the micropolar thermoelastic materials with

$$a = \zeta = s = \xi = 0$$

and consequently, $c_3 = c_8 = c_9 = c_{10} = c_\xi = c_{11} = 0$. Equation (2.15) in this condition becomes

$$DV^2 + CV + B = 0, \quad (2.31)$$

where

$$D = c_d^2 / \omega^2, \quad C = -c_4^2 c_m^2 / \omega^2 - c_0^2 c_d^2 / \omega^2 - c_k^2; \quad B = c_0^2 c_k^2.$$

This equation gives the phase velocities of coupled dilatational waves

$$V_{1,2} = \left(-C \pm \sqrt{C^2 - 4BD} \right) / 2D. \quad (2.32)$$

There is no effect on the fourth dilatational wave and the coupled shear waves. So, we come to know there are five waves in the micropolar thermoelastic materials.

Case (iii): If we neglect thermal and voids effect simultaneously, the material reduces to micropolar elastic material with

$$m = k_0 = a = \zeta = \xi = \tau = s = 0.$$

Consequently, $c_m = c_4 = c_k = c_3 = c_8 = c_9 = c_{10} = c_{11} = c_\xi = 0$. Inserting all these values in Eq. (2.15), we get

$$V = (\lambda + 2\mu + \kappa)/\rho. \quad (2.33)$$

This is the phase velocity of dilatational wave so call longitudinal displacement wave. There are no changes in the phase velocities of micropolar dilatational wave and two coupled shear waves. These are the results of Ariman (1972).

Case (iv): If the micropolar effect is neglected, the medium becomes thermo-elastic materials with voids with

$$\alpha = \beta = \gamma = \kappa = 0.$$

Consequently, we get $c_0^2 = c_1^2 = (\lambda + 2\mu)/\rho$, $c_{12}^2 = \mu/\rho$ and $c_2 = c_5 = c_6 = c_7 = c_{13} = 0$.

In such materials, there are three coupled dilatational waves and their phase velocities are given by Equation (2.15) (see Singh, 2011). The phase velocity of shear wave is obtained from Equation (2.18) as

$$V = c_{12}^2 = \mu/\rho. \quad (2.34)$$

Case (v): If we neglect thermal, voids and micropolar effect, the medium reduces to isotropic elastic material with

$$\alpha = \beta = \gamma = \kappa = s = a = \zeta = \tau = k_0 = \xi = m = k_0 = \tau = 0.$$

Consequently,

$$c_2 = c_3 = c_4 = c_5 = c_6 = c_7 = c_8 = c_9 = c_{10} = c_{11} = c_{13} = c_\xi = c_k = c_m = 0,$$

$$c_0 = c_1, c_{12}^2 = \mu/\rho.$$

Inserting all these values into Equations (2.15) and (2.18), we get the phase velocities of dilatational and shear waves, respectively as

$$V = c_1^2 = (\lambda + 2\mu)/\rho \quad \text{and} \quad V = \mu/\rho. \quad (2.35)$$

These results are the results of the classical elasticity (see Achenbach, 1976).

2.6 Numerical results and discussion

In order to compute the phase velocities and attenuation coefficients, the following parameters of the modified aluminium-epoxy composite material are considered (Sharma and Kumar, 2009) and void parameters are taken arbitrarily:

$$\lambda = 7.59 \times 10^{10} \text{ N/m}^2, \mu = 1.89 \times 10^{10} \text{ N/m}^2, \kappa = 0.0149 \times 10^{10} \text{ N/m}^2, \rho = 2.19 \times 10^3 \text{ Kg/m}^3,$$

$$\alpha = 3.688 \times 10^{10} \text{ N}, \beta = 2.68 \times 10^{10} \text{ N}, \gamma = 2.68 \times 10^5 \text{ N}, k_0 = 1.7 \text{ Jm}^{-1}\text{s}^{-1}\text{K}^{-1},$$

$$\Theta_0 = 293 \text{ K}, \nu = 0.02 \times 10^{-5} \text{ K}^{-1}, \chi = 0.00753 \text{ m}^2, d = 2.16 \times 10^{10} \text{ N/m}^2$$

and

$$s = 1.05 \times 10^{10} \text{ N/m}^2, \zeta = 1.49 \times 10^{10} \text{ N/m}^2, \xi = 1.475 \times 10^{10} \text{ N/m}^2, a = 0.668 \times 10^{10} \text{ N}$$

with $\tau = 0.5 \text{ s}$, $J = 0.3 \text{ m}^2$ whenever not mention.

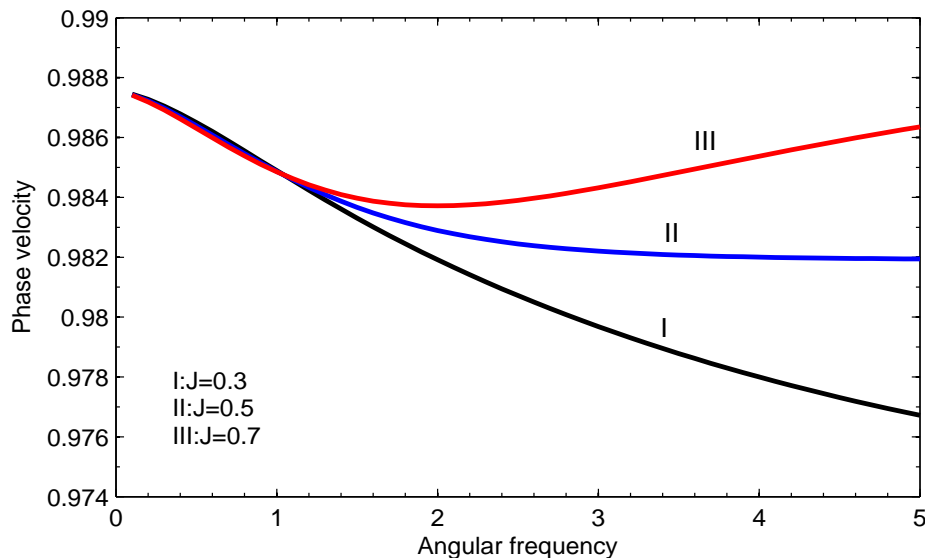


Figure 2.1: Variation of Phase Velocity of *FCDW* with ω for different values of J

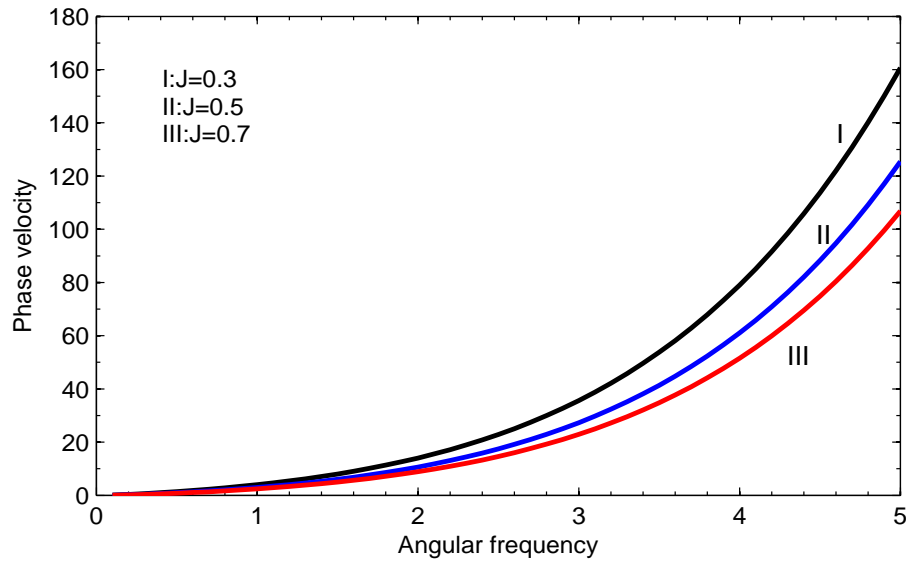


Figure 2.2: Variation of Phase Velocity of *SCDW* with ω for different values of J

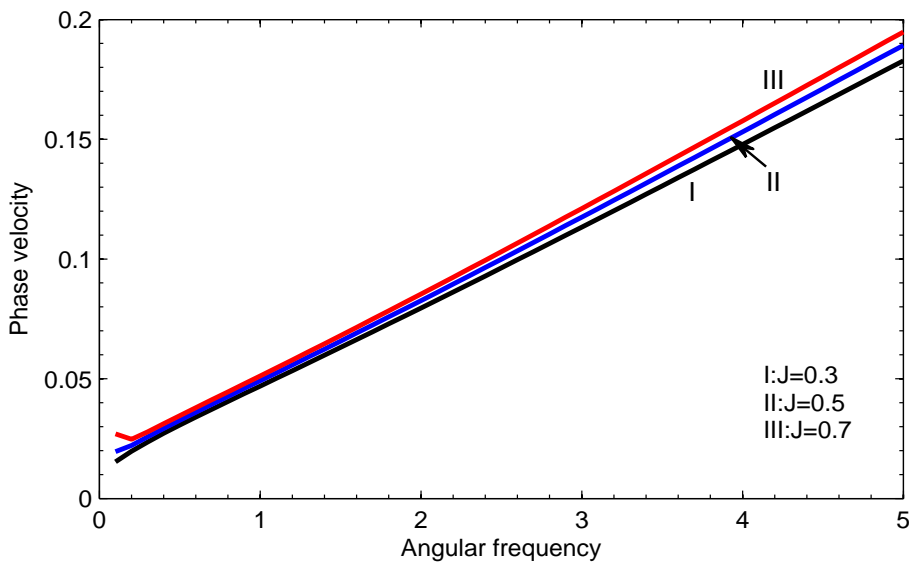


Figure 2.3: Variation of Phase Velocity of *TCDW* with ω for different values of J

The variation of phase velocities and attenuation coefficients with angular frequency at different values of micro-inertia parameter, $J = \{0.3, 0.5, 0.7\}m^2$ are depicted in Figures 2.1-2.9, while at different values of thermal relaxation time, $\tau = \{0, 0.5\}s$ are depicted in

Figures 2.10-2.15. The later is a comparison between the Fourier classical law and Lebon's law of heat conduction. It may be noted that Figures 2.1-2.3 correspond to the phase velocities of coupled dilatational waves ($FCDW, SCDW, TCDW$), Figure 2.4 corresponds to the phase velocity of fourth dilatation wave (FDW), Figures 2.5 & 2.6 correspond to the phase velocities of the coupled shear waves ($FCSW, SCSW$) and Figures 2.7-2.9 correspond to the attenuation coefficients of the coupled dilatational waves. We come to know that fourth dilatational wave (FDW) and first coupled shear wave ($FCSW$) are attenuated only when $\omega < c_7$; and second coupled shear wave ($SCSW$) is non attenuated. In Figure 2.1, Curves I and II show that the phase velocity of first couple dilatational wave ($FCDW$) starts from certain value which decreases with the increase of angular frequency (ω), while curve III starts decreasing from certain point up to the minimum value and then increases with increasing angular frequency. It may be noted that the values of phase velocity increase with the increase of J . It is shown that the phase velocities of second coupled dilatational wave ($SCDW$) and third coupled dilatational wave ($TCDW$) increase with the increase

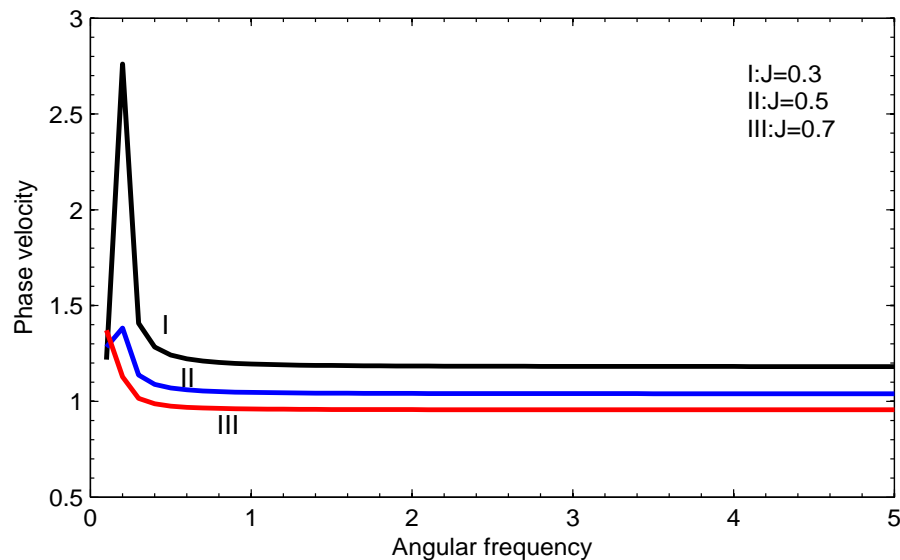


Figure 2.4: Variation of Phase Velocity of FDW with ω for different values of J

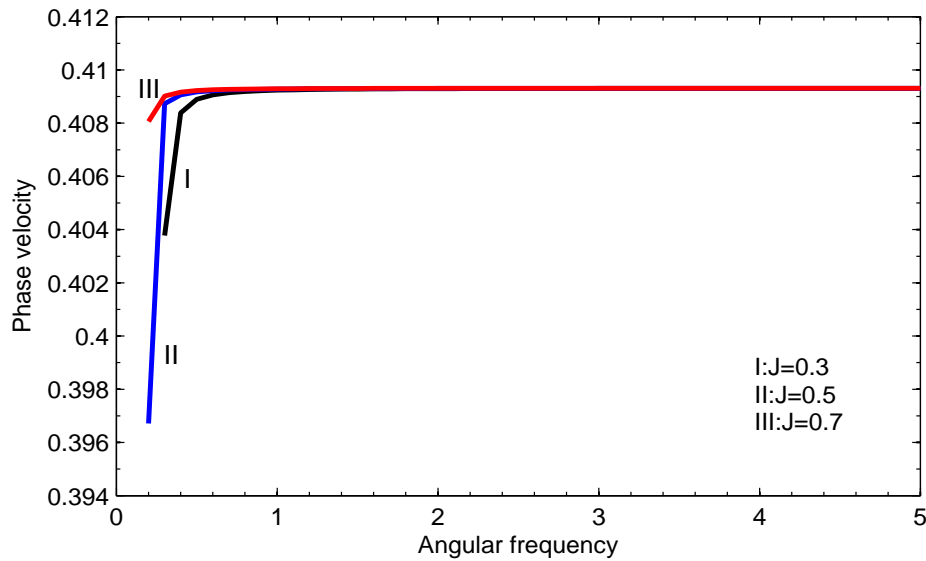


Figure 2.5: Variation of Phase Velocity of *FCSW* with ω for different values of J

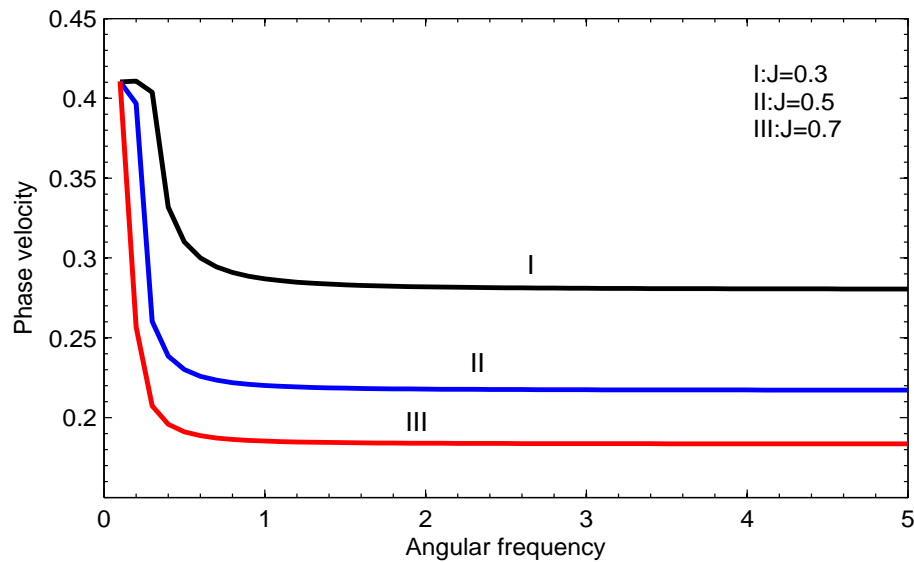


Figure 2.6: Variation of Phase Velocity of *SCSW* with ω for different values of J

of the angular frequency in Figures 2.2 & 2.3. We have observed that the values of phase velocity of *SCDW* and *TCDW* decrease and increase respectively with the increase of J . In Figure 2.4, Curves I & II show that the phase velocity of the *FDW* increase initially upto

the maximum value and then, they decrease to the minimum value near $\omega = 0.5$ thereby making a constant value with the increase of ω , while Curve III show that it is decreasing initially and makes a constant value with the increase of ω . We have observed that with

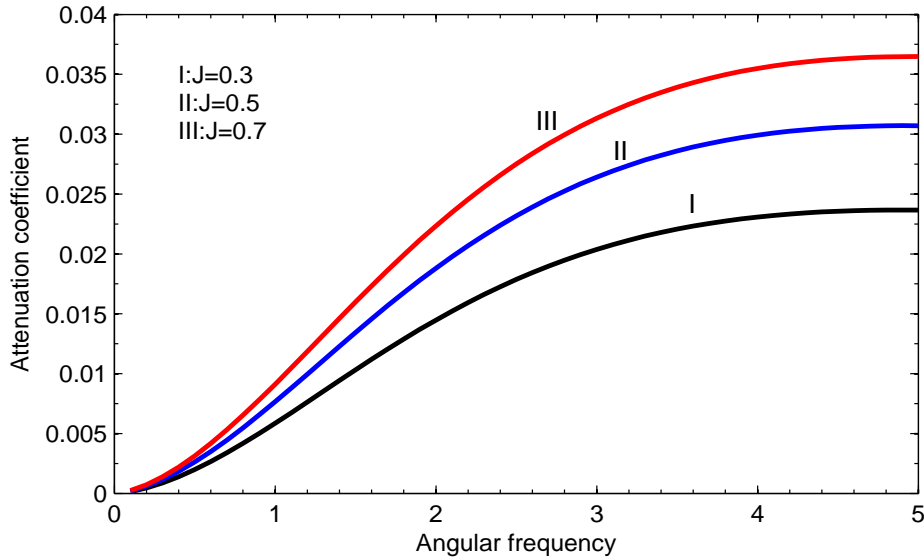


Figure 2.7: Attenuation coefficient of *FCDW* with ω for different values of J

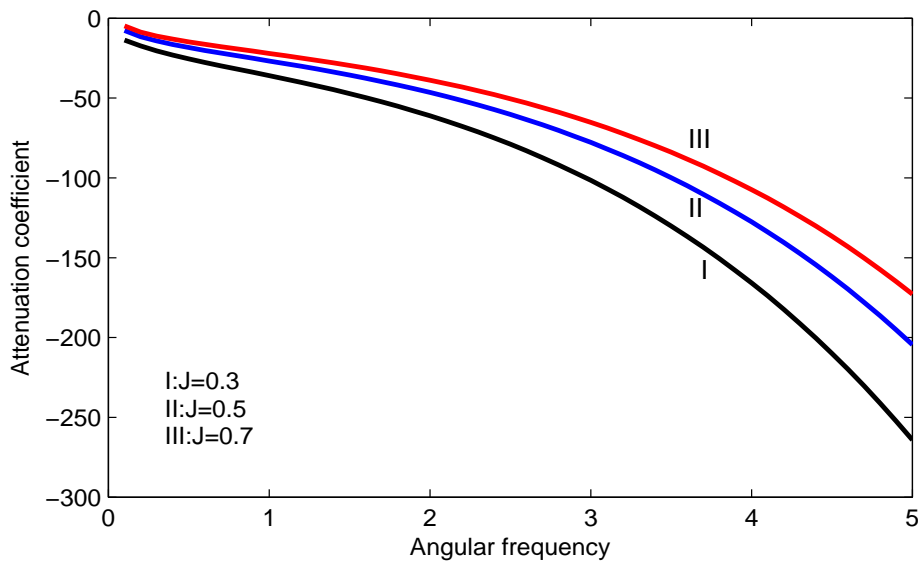


Figure 2.8: Attenuation coefficient of *SCDW* with ω for different values of J

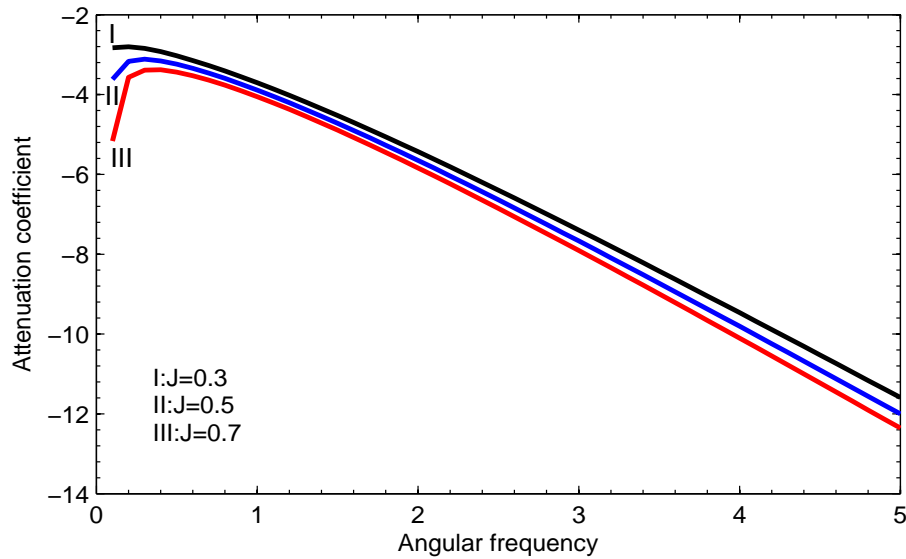


Figure 2.9: Attenuation coefficient of $TCDW$ with ω for different values of J

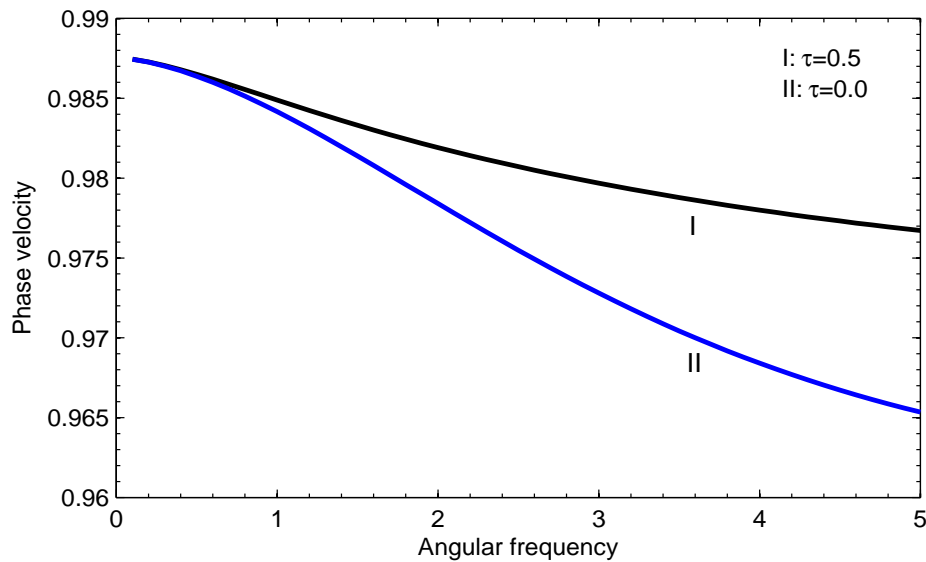


Figure 2.10: Variation of Phase Velocity of $FCDW$ with ω for different values of τ

the increase of J , the values of phase velocity of FDW decrease. Figure 2.5 shows that the phase velocity of $FCSW$ increases initially and then makes a constant value with the increase of ω . We have seen in Figure 2.6 that the nature of phase velocity of $SCSW$ is

similar to that of *FDW*. In Figure 2.7 & 2.8, the attenuation coefficient corresponding to *FCDW* increases with the increase of ω , while that of *TCDW* decreases with the increase of ω . The values of the attenuation coefficients of *FCDW* and *SCDW* increases and decreases

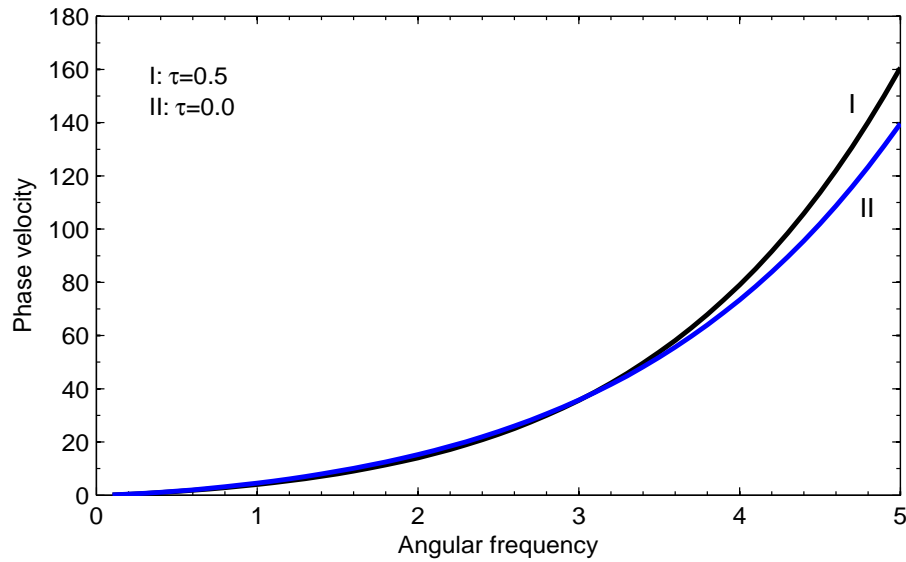


Figure 2.11: Variation of Phase Velocity of *SCDW* with ω for different values of τ

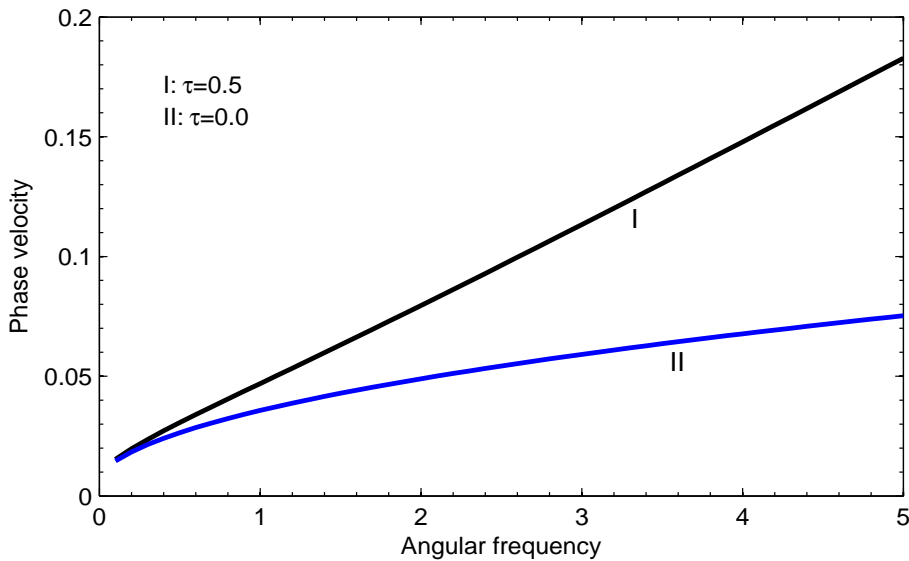


Figure 2.12: Variation of Phase Velocity of *TCDW* with ω for different values of τ

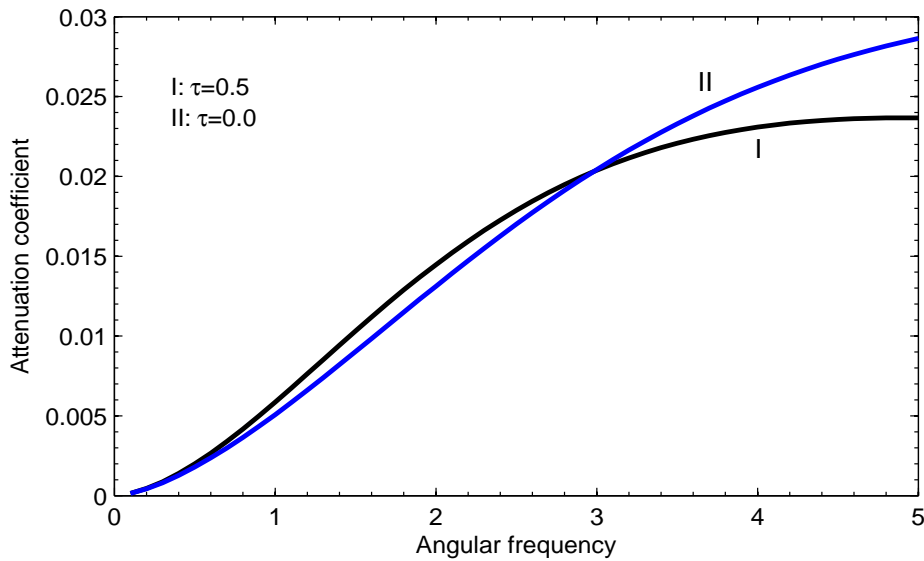


Figure 2.13: Attenuation coefficient of *FCDW* with ω for different values of τ

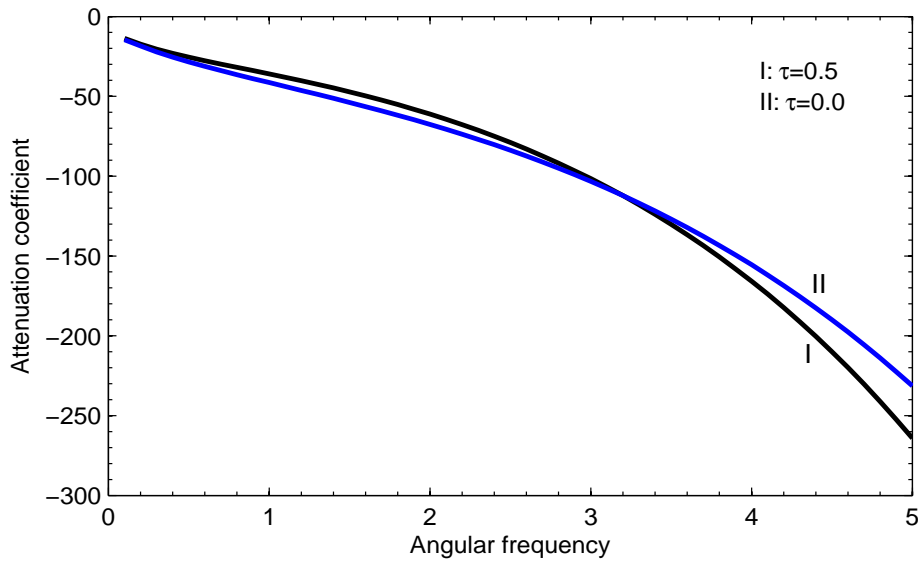


Figure 2.14: Attenuation coefficient of *SCDW* with ω for different values of τ

respectively with the increase of J . The attenuation coefficient of *TCDW* in Figure 2.9 increases initially and then decreases with the increase of ω . We have observed that the values of attenuation coefficient corresponding to *FCSW* increases with the increase of J ,

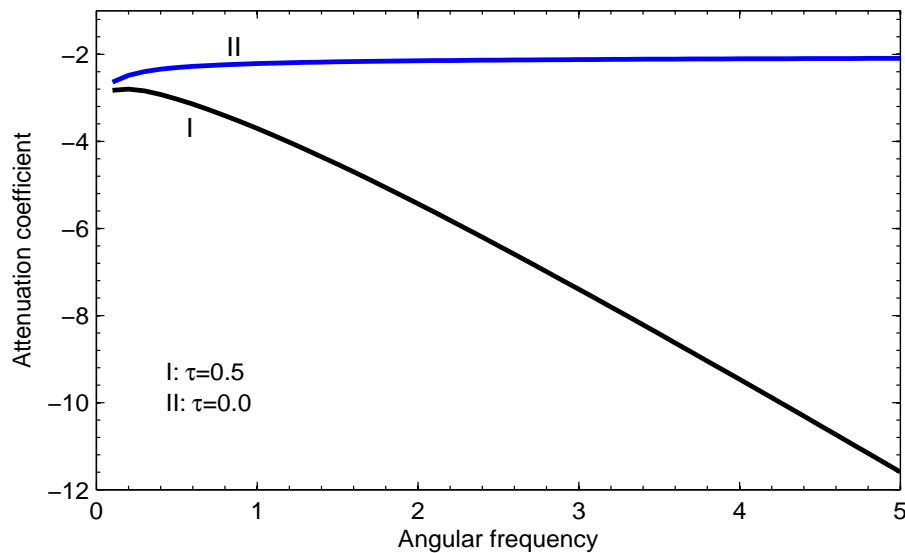


Figure 2.15: Attenuation coefficient of *TCDW* with ω for different values of τ

while that of *SCDW* and *TCDW* decrease with the increase of J . Thus, phase velocities of the dilatational and shear waves are affected by the micro-inertia parameter (J) and angular frequency (ω). In Figures 2.10-2.15, we have compared the two theories, i.e., Fourier classical law ($\tau = 0$) and Lebon's laws of heat conduction ($\tau \geq 0$). It may be noted that the variation of phase velocities corresponding to coupled dilatational waves with ω at different values of thermal relaxation time (τ) are seen in Figures 2.10-2.12, while that of the attenuation coefficients are seen in Figures 2.13-2.15. In Figure 2.10-2.12, the values of phase velocity of *FCDW*, *SCDW* and *TCDW* are greater in Fourier classical law than that of Lebon's laws of heat conduction. We have seen that the values of the attenuation coefficients of *FCDW* in Figure 2.13 and *SCDW* in Figure 2.14 have same values for the two theory at $\omega = \{0.1, 3\} s^{-1}$ and $\omega = \{0.1, 3.2\} s^{-1}$ respectively. In Figure 2.15, we have seen that the values of attenuation coefficient of *TCDW* are greater in Lebon's laws of heat conduction than that of Fourier classical law.

2.7 Conclusions

The problem of propagation of plane harmonic waves in micropolar thermoelastic materials with voids has been investigated. We have obtained the phase velocities of the dilatational and shear waves using the linear theory of micropolar thermoelastic materials with voids. There exists four dilatational waves, which three of them are coupled ($FCDW$, $SCDW$, $TCDW$) and an uncoupled micropolar dilatational waves (FDW); and two shear waves ($FCSW$, $SCSW$) which are coupled together. These phase velocities and their attenuation coefficients are computed numerically and presented graphically. We may conclude the following remarks:

- (i) The phase velocity of micropolar wave (FDW) is a function of micropolar parameters.
- (ii) The shear waves ($FCSW$, $SCSW$) are independent of thermal and void parameters.
- (iii) The phase velocity of dilatational waves depend on the Lamé's constants, micropolar, thermal and void parameters.
- (iv) All the coupled dilatational waves are attenuated only when $G \neq 0$.
- (v) One of the coupled dilatational waves is non attenuated and others are attenuated when $G = 0$.
- (vi) The phase velocities corresponding to $SCDW$, $TCDW$ and attenuation coefficient of $FCDW$ increase with the increase of angular frequency (ω).
- (vii) The attenuation coefficient of $SCDW$ decreases with the increase of ω .
- (viii) The values of phase velocity of $FCDW$ increase with the increase of J .
- (ix) The values of phase velocity of $SCDW$ and $TCDW$ decrease and increase respectively with the increase of J .
- (x) The values of the attenuation coefficients of $FCDW$ and $SCDW$, $TCDW$ increases and decrease respectively with the increase of J .

Chapter 3

Effect of micro-inertia in the propagation of waves in micropolar thermoelastic materials with voids²

3.1 Introduction

The theory of micropolar elasticity is concerned with material media whose constituents are dumbbell molecules. These elements are allowed to rotate independently without stretch. The theory is expected to find applications in the treatment of mechanics of granular materials with elongated rigid grains and composite fibrous materials. Ciarletta et al. (2009) studied the problem of plane waves and vibrations in the theory of micropolar thermoelasticity for materials with voids. They proved the existence theorems of non-trivial solutions and eigenfrequencies of the interior homogeneous boundary value problems of steady vibrations. In this work, we will investigate the effect of micro-inertia on the wave propagation in micropolar thermoelastic materials with voids. We have obtained the amplitude and energy ratios of the reflected coupled longitudinal and shear waves from a plane free boundary of micropolar thermoelastic materials with voids. These ratios are computed separately for the incident longitudinal wave and shear wave. The effect of micro-inertia on these ratios are discussed and presented graphically.

²*Applied Mathematical Modelling*, **49**, 478-497(2017)

3.2 Basic Equation

The equations of motion in homogeneous and isotropic micropolar thermoelastic materials with voids are given as

$$(\lambda + 2\mu + \kappa)\nabla^2 u' + s\psi - m\Theta = \rho\ddot{u}', \quad (3.1)$$

$$s\nabla^2 u' - (a\nabla^2 - \zeta)\psi + \xi\Theta = -\rho_2\ddot{\psi}, \quad (3.2)$$

$$k_0\nabla^2\Theta - \Theta_0(1 + \tau\frac{\partial}{\partial t})(d\dot{\Theta} + m\nabla^2\dot{u}' - \xi\dot{\psi}) = 0, \quad (3.3)$$

$$(\alpha + \beta + \gamma)\nabla^2\phi' - 2\kappa\phi' = \rho_1\ddot{\phi}', \quad (3.4)$$

$$(\mu + \kappa)\nabla^2\mathbf{u}'' + \kappa\nabla \times \phi'' = \rho\ddot{\mathbf{u}}'', \quad (3.5)$$

$$(\gamma\nabla^2 - 2\kappa)\phi'' + \kappa\nabla \times \mathbf{u}'' = \rho_1\ddot{\phi}'', \quad (3.6)$$

where u' , ϕ' are the scalar potentials and \mathbf{u}'' , ϕ'' are vector potentials of displacement and micro-rotation vectors respectively given by Eq. (2.7), λ , μ are Lamé's parameters, k_0 is the thermal conductivity, τ is thermal relaxation time, m , d are thermal parameters, a , ζ , ξ , s are void parameters, α , β , γ , κ are micropolar parameters, ρ is mass density, ρ_1 , ρ_2 are coefficients of inertia, Θ is the temperature measure from the reference temperature, ψ is the change of volume fraction, Θ_0 is temperature of the material in a reference state. It is cleared that u' , ψ and Θ are coupled dilatational waves and \mathbf{u}'' and ϕ'' are coupled shear waves.

3.3 Wave Propagation

Consider the Cartesian co-ordinates with x and y -axis lying horizontally and z axis as vertically pointing downward. Let us take two dimensional problem of wave propagation in the half-space, $M = \{(x, z); -\infty < x < \infty, z \geq 0\}$ which is of micropolar thermoelastic material with voids. We know that the displacement (\mathbf{u}), microrotation vector (ϕ), change in volume

fraction (ψ) and temperature measured (Θ) may be expressed as

$$\mathbf{u} = (u_1, 0, u_3), \quad \phi = (0, \phi_2, 0), \quad \psi = \psi(x, z), \quad \Theta = \Theta(x, z), \quad (3.7)$$

in which

$$u_1 = \frac{\partial u'}{\partial x} - \frac{\partial U_2}{\partial z} \quad \& \quad u_3 = \frac{\partial u'}{\partial z} + \frac{\partial U_2}{\partial x},$$

where U_2 is the y -component of \mathbf{u}'' .

The boundary of the half-space, M at $z = 0$ is thermally insulated so that there is no variations of temperature and is free from all traction. Mathematically, these conditions may be written as

$$T_{33} = 0, \quad T_{31} = 0, \quad M_{32} = 0, \quad h_3 = 0, \quad \Theta_{,3} = 0 \quad \text{at } z = 0,$$

which may be represented as

$$\lambda \frac{\partial^2 u'}{\partial x^2} + (\lambda + 2\mu + \kappa) \frac{\partial^2 u'}{\partial z^2} + (2\mu + \kappa) \frac{\partial^2 U_2}{\partial x \partial z} + s\psi - m\Theta = 0, \quad (3.8)$$

$$(2\mu + \kappa) \frac{\partial^2 u'}{\partial x \partial z} - (\mu + \kappa) \frac{\partial^2 U_2}{\partial z^2} + \mu \frac{\partial^2 U_2}{\partial x^2} - \kappa \phi_2 = 0, \quad (3.9)$$

$$\frac{\partial \phi_2}{\partial z} = 0, \quad \frac{\partial \psi}{\partial z} = 0, \quad \frac{\partial \Theta}{\partial z} = 0. \quad (3.10)$$

The potentials form of u' , ψ , Θ , U_2 and ϕ_2 in the half-space, M may be written as

$$\{u', \psi, \Theta\} = A_0 \{1, \eta_0, \eta'_0\} \exp(P_0) + \sum_{r=1}^3 A_r \{1, \eta_r, \eta'_r\} \exp(P_r), \quad (3.11)$$

$$\{U_2, \phi_2\} = A_{00} \{1, \eta_{00}\} \exp(P_0) + \sum_{r=4}^5 A_r \{1, \eta_r\} \exp(P_r), \quad (3.12)$$

where

$$P_0 = ik_0(x \sin \theta_0 - z \cos \theta_0 - V_0 t), \quad P_r = ik_r(x \sin \theta_r + z \cos \theta_r - V_r t),$$

A_0 and A_{00} are the amplitudes for the incident coupled longitudinal and coupled shear waves respectively at an angle of incidence θ_0 with phase velocity V_0 , A_r ($r = 1, 2, 3$) are

the amplitudes of the reflected coupled longitudinal waves with angles $\theta_r (r = 1, 2, 3)$ and $A_r (r = 4, 5)$ are amplitudes of reflected coupled shear waves with angles $\theta_r (r = 4, 5)$, k_r is the wavenumber and V_r is the phase velocity given by Eqs (2.15), (2.18) and (2.23). We know that the fourth longitudinal wave/micropolar wave is not reflected for the incident wave is coupled longitudinal wave and coupled shear waves (Parfitt and Eringen, 1969). The expressions of the coupling parameters η_r and η'_r are given by

$$\eta_r = \begin{cases} \frac{c_8^2 c_k^2 k_r^4 - (c_8^2 c_d^2 - c_{11}^2 c_m^2) k_r^2}{c_9^2 c_k^2 k_r^4 - (\omega^2 c_k^2 - c_{10}^2 c_k^2 + c_9^2 c_d^2) k_r^2 - c_{11}^2 c_\xi^2 - c_{10}^2 c_d^2 + \omega^2 c_d^2}, & r = 1, 2, 3 \\ c_{13}^2 / \{c_6^2 + c_7^2 / k_r^2 - V_r^2\}, & r = 4, 5 \end{cases}$$

$$\eta'_r = \begin{cases} \frac{c_m^2 c_9^2 k_r^4 + (c_m^2 c_{10}^2 + c_8^2 c_\xi^2 - c_m^2 \omega^2) k_r^2}{-c_9^2 c_k^2 k_r^4 + (\omega^2 c_k^2 - c_{10}^2 c_k^2 + c_9^2 c_d^2) k_r^2 + c_{11}^2 c_\xi^2 + c_{10}^2 c_d^2 - \omega^2 c_d^2}, & r = 1, 2, 3 \\ 0, & r = 4, 5. \end{cases}$$

The expressions of $c_1, c_2, c_3, \dots, c_{13}$ are given by

$$c_1^2 = \frac{\lambda + 2\mu}{\rho}, \quad c_2^2 = \frac{\kappa}{\rho}, \quad c_3^2 = \frac{s}{\rho}, \quad c_4^2 = \frac{m}{\rho}, \quad c_5^2 = \frac{\alpha + \beta}{\rho_1}, \quad c_6^2 = \frac{\gamma}{\rho_1}, \quad c_7^2 = \frac{2\kappa}{\rho_1},$$

$$c_8^2 = \frac{s}{\rho_2}, \quad c_9^2 = \frac{a}{\rho_2}, \quad c_{10}^2 = \frac{\zeta}{\rho_2}, \quad c_{11}^2 = \frac{\xi}{\rho_2}, \quad c_{12}^2 = \frac{\mu + \kappa}{\rho}, \quad c_{13}^2 = \frac{\kappa}{\rho_1}.$$

The Snell's law, for this problem, may be written as

$$k_0 \sin \theta_0 = k_1 \sin \theta_1 = k_2 \sin \theta_2 = k_3 \sin \theta_3 = k_4 \sin \theta_4 = k_5 \sin \theta_5. \quad (3.13)$$

It may be noted that the angle of incidence is equal to the angle of reflected wave.

3.4 Amplitude ratio

Using Eqs. (3.11)-(3.13) into (3.8)-(3.10), we get a system of equations

$$\sum_{r=1}^5 a_{ir} Z_r = b_i, \quad i = 1, 2, 3, 4, 5 \quad (3.14)$$

where non-zero a_{ir} are given by

$$a_{1r} = \{\lambda + (2\mu + \kappa) \cos^2 \theta_r - (s\eta_r - m\eta'_r)/k_r^2\}k_r^2, \quad (r = 1, 2, 3),$$

$$a_{1r} = (2\mu + \kappa)k_r^2 \sin \theta_r \cos \theta_r, \quad (r = 4, 5), \quad a_{2r} = -(2\mu + \kappa)k_r^2 \sin \theta_r \cos \theta_r, \quad (r = 1, 2, 3),$$

$$a_{2r} = \{\mu(\cos^2 \theta_r - \sin^2 \theta_r) + \kappa \cos^2 \theta_4 - \kappa\eta_r/k_r^2\}k_r^2, \quad (r = 4, 5),$$

$$a_{3r} = \eta_r k_r \cos \theta_r, \quad (r = 4, 5), \quad a_{4r} = \eta_r k_r \cos \theta_r, \quad (r = 1, 2, 3), \quad a_{5r} = \eta'_r k_r \cos \theta_r, \quad (r = 1, 2, 3).$$

For the incident coupled longitudinal wave, we have

$$\theta_0 = \theta_1, \quad V_0 = V_1, \quad b_1 = -a_{11}, \quad b_2 = a_{21}, \quad b_3 = 0, \quad b_4 = a_{41}, \quad b_5 = a_{51}.$$

In the case when incident wave is coupled shear wave, we get

$$\theta_0 = \theta_4, \quad V_0 = V_4, \quad b_1 = a_{14}, \quad b_2 = -a_{24}, \quad b_3 = a_{34}, \quad b_4 = 0, \quad b_5 = 0.$$

The amplitude ratios $Z_i = \{\frac{A_i}{A_0}, \frac{A_i}{A_{00}}\}$, $i = 1, 2, 3$ correspond to the reflected coupled longitudinal waves and $Z_i = \{\frac{A_i}{A_0}, \frac{A_i}{A_{00}}\}$, $i = 4, 5$ correspond to the reflected coupled shear waves. It may be noted that the ratios A_i/A_0 represents for the incident coupled longitudinal wave, while A_i/A_{00} represents for the incident coupled shear wave.

3.5 Energy Partition

Let us consider the energy partition among the various reflected waves at the free surface. The rate of energy transmission at the surface ($z = 0$) per unit area is given by (Achenbach, 1976 & Singh and Tomar, 2007)

$$P^* = \langle T_{33}, \dot{u}_3 \rangle + \langle T_{31}, \dot{u}_1 \rangle + \langle M_{32}, \dot{\phi}_2 \rangle + \langle h_3, \dot{\psi} \rangle. \quad (3.15)$$

The rate of energy transmission for the incident coupled longitudinal and coupled shear waves are respectively written as

$$E_{inc} = \left(\lambda + 2\mu + \kappa - \frac{(s + a\eta_1)\eta_1 - m\eta_1'}{k_1^2} \right) \omega k_1^3 \cos \theta_1 A_1^2 \exp\{\Lambda_1\}, \quad (3.16)$$

$$E_{inc} = \left(\mu + \kappa - \frac{\eta_4}{k_4^2}(\gamma\eta_4 + \kappa) \right) \omega k_4^3 \cos \theta_4 A_4^2 \exp\{\Lambda_4\}, \quad (3.17)$$

where $\Lambda_1 = 2ik_1(x \sin \theta_1 - z \cos \theta_1 - V_1 t)$, $\Lambda_4 = 2ik_4(x \sin \theta_4 - z \cos \theta_4) - V_4 t$.

The energy ratios of the various reflected waves for the incident coupled longitudinal and coupled shear waves are given below.

For incident coupled longitudinal wave:

$$\begin{aligned} E_i &= \frac{\{\lambda + 2\mu + \kappa - (s\eta_i + a\eta_i^2 - m\eta_i')/k_i^2\}k_i^3 \cos \theta_i}{\{\lambda + 2\mu + \kappa - (s\eta_1 + a\eta_1^2 - m\eta_1')/k_1^2\}k_1^3 \cos \theta_1} Z_i^2, \quad i = 1, 2, 3 \\ E_i &= \frac{\{\mu + \kappa - \eta_i(\kappa + \gamma\eta_i)/k_i^2\}k_i^3 \cos \theta_i}{\{\lambda + 2\mu + \kappa - (s\eta_1 + a\eta_1^2 - m\eta_1')/k_1^2\}k_1^3 \cos \theta_1} Z_i^2, \quad i = 4, 5. \end{aligned} \quad (3.18)$$

For incident coupled shear wave:

$$\begin{aligned} E_i &= \frac{\{\lambda + 2\mu + \kappa - (s\eta_i + a\eta_i^2 - m\eta_i')/k_i^2\}k_i^3 \cos \theta_i}{\{\mu + \kappa - \eta_4(\kappa + \gamma\eta_4)/k_4^2\}k_4^3 \cos \theta_4} Z_i^2, \quad i = 1, 2, 3 \\ E_i &= \frac{\{\mu + \kappa - \eta_i(\kappa + \gamma\eta_i)/k_i^2\}k_i^3 \cos \theta_i}{\{\mu + \kappa - \eta_4(\kappa + \gamma\eta_4)/k_4^2\}k_4^3 \cos \theta_4} Z_i^2, \quad i = 4, 5. \end{aligned} \quad (3.19)$$

It may be noted that E_i ($i = 1, 2, 3$) represent for the energy ratios of the reflected coupled longitudinal waves and E_i ($i = 4, 5$) represent for the reflected coupled shear waves. We come to know that the energy ratios are the functions of angle of propagation, amplitude ratios, elastic, micropolar, thermal and void parameters.

3.6 Special cases

Case 1: In the absence of thermal effect, the materials reduces to the micropolar elastic materials with voids, in this case, $m = k_0 = \tau = 0$. Consequently, the thermal wave does

not exist and Equation (3.14) is reduced with the following non-zero modified values of a_{ir}

$$a_{1r} = \{\lambda + (2\mu + \kappa) \cos^2 \theta_r - s\eta_r/k_r^2\}k_r^2, \quad a_{2r} = -(2\mu + \kappa) \sin \theta_r \cos \theta_r k_r^2,$$

$$a_{4r} = \eta_r \cos \theta_r k_r, \quad r = 1, 2.$$

It gives the amplitude ratios of the corresponding reflected waves. In this case, the energy ratios, E_4 and E_5 for the incident coupled shear wave are given by Equation (3.19)₂ and the expression of the rest of the energy ratios are reduced as:

(for the incident coupled longitudinal wave)

$$\begin{aligned} E_1 &= Z_1^2; \quad E_2 = \frac{\{\lambda + 2\mu + \kappa - (s\eta_2 + a\eta_2^2)/k_2^2\}k_2^3 \cos \theta_2}{\{\lambda + 2\mu + \kappa - (s\eta_1 + a\eta_1^2)/k_1^2\}k_1^3 \cos \theta_1} Z_2^2, \\ E_i &= \frac{\{\mu + \kappa - \eta_i(\kappa + \gamma\eta_i)/k_i^2\}k_i^3 \cos \theta_i}{\{\lambda + 2\mu + \kappa - (s\eta_1 + a\eta_1^2)/k_1^2\}k_1^3 \cos \theta_1} Z_i^2, \quad i = 4, 5. \end{aligned} \quad (3.20)$$

(for the incident coupled shear wave)

$$E_i = \frac{\{\lambda + 2\mu + \kappa - (s\eta_i + a\eta_i^2)/k_i^2\}k_i^3 \cos \theta_i}{\{\mu + \kappa - \eta_4(\kappa + \gamma\eta_4)/k_4^2\}k_4^3 \cos \theta_4} Z_i^2, \quad i = 1, 2. \quad (3.21)$$

Case 2: In the absence of voids, the material reduces to the micropolar thermoelastic materials, in this case $a = \zeta = s = \xi = 0$. Consequently, one of the couple longitudinal waves does not exist and Eq. (3.14) is changed with the following non-zero modified values of a_{ir}

$$a_{1r} = \{\lambda + (2\mu + \kappa) \cos^2 \theta_r + m\eta'_r/k_r^2\}k_r^2, \quad a_{2r} = -(2\mu + \kappa) \sin \theta_r \cos \theta_r k_r^2,$$

$$a_{5r} = \eta'_r \cos \theta_r k_r, \quad r = 1, 2.$$

This will help to find the corresponding amplitude ratios of the reflected waves. Here, the expression of energy ratios, E_4 and E_5 for incident coupled shear wave are given by Eq. (3.19)₂ and rest of the ratios are given as

(for incident coupled longitudinal wave)

$$\begin{aligned} E_1 &= Z_1^2, & E_2 &= \frac{(\lambda + 2\mu + \kappa + m\eta'_2/k_2^2) k_2^3 \cos \theta_2}{(\lambda + 2\mu + \kappa + m\eta'_1/k_1^2) k_1^3 \cos \theta_1} Z_2^2, \\ E_i &= \frac{(\mu + \kappa - \eta_i(\kappa + \gamma\eta_i)/k_i^2) k_i^3 \cos \theta_i}{(\lambda + 2\mu + \kappa + m\eta'_1/k_1^2) k_1^3 \cos \theta_1} Z_i^2, & i &= 4, 5. \end{aligned} \quad (3.22)$$

(for incident coupled shear wave)

$$E_i = \frac{(\lambda + 2\mu + \kappa + m\eta'_i/k_i^2) k_i^3 \cos \theta_i}{(\mu + \kappa - \eta_4(\kappa + \gamma\eta_4)/k_4^2) k_4^3 \cos \theta_4} Z_i^2, \quad i = 1, 2. \quad (3.23)$$

This result is perfectly matched with Singh (2007a).

Case 3: If we neglect thermal and voids effect simultaneously, the material reduces to micropolar elastic material and in this case, $m = k_0 = a = \zeta = \xi = \tau = s = 0$. Consequently, only one longitudinal wave is reflected and Eq. (3.14) is modified with non-zero, a_{11} :

$$a_{11} = \{\lambda + (2\mu + \kappa) \cos^2 \theta_1\} k_1^2.$$

It helps to find the amplitude ratios of the reflected waves. These results are similar with Parfitt and Eringen (1969). The energy ratios, E_4 and E_5 for the incident coupled shear wave are given by Eq. (3.19)₂ and others are reduced as

(for incident coupled longitudinal wave)

$$E_1 = Z_1^2, \quad E_i = \frac{(\mu + \kappa - \eta_i(\kappa + \gamma\eta_i)/k_i^2) k_i^3 \cos \theta_i}{(\lambda + 2\mu + \kappa) k_1^3 \cos \theta_1} Z_i^2, \quad i = 4, 5. \quad (3.24)$$

(for incident coupled shear wave)

$$E_1 = \frac{(\lambda + 2\mu + \kappa) k_1^3 \cos \theta_1}{(\mu + \kappa - \eta_4(\kappa + \gamma\eta_4)/k_4^2) k_4^3 \cos \theta_4} Z_1^2. \quad (3.25)$$

Case 4: If the micropolar effect is neglected, the medium becomes thermo-elastic materials with voids with $\alpha = \beta = \gamma = \kappa = 0$ and $c_1^2 = (\lambda + 2\mu)/\rho$, $c_{12}^2 = \mu/\rho$. Consequently, one of the couple shear wave does not exist and Eq. (3.14) changes with the following non-zero

modified values of a_{ir}

$$a_{1r} = \{\lambda + 2\mu \cos^2 \theta_r - (s\eta_r - m\eta'_r)/k_r^2\}k_r^2, \quad a_{2r} = -2\mu \sin \theta_r \cos \theta_r k_r^2, \quad (r = 1, 2, 3),$$

$$a_{14} = 2\mu \sin \theta_4 \cos \theta_4 k_4^2, \quad a_{24} = \mu(\cos^2 \theta_4 - \sin^2 \theta_4)k_4^2.$$

It helps to find the amplitude ratios of the reflected waves. Also, the energy ratios of the reflected waves are given below

(for incident coupled longitudinal wave)

$$E_1 = Z_1^2, \quad E_i = \frac{\{\lambda + 2\mu - (s\eta_i + a\eta_i^2 - m\eta'_i)/k_i^2\}k_i^3 \cos \theta_i}{\{\lambda + 2\mu - (s\eta_1 + a\eta_1^2 - m\eta'_1)/k_1^2\}k_1^3 \cos \theta_1} Z_i^2, \quad (i = 2, 3)$$

$$E_4 = \frac{\mu k_4^3 \cos \theta_4}{\{\lambda + 2\mu - (s\eta_1 + a\eta_1^2 - m\eta'_1)/k_1^2\}k_1^3 \cos \theta_1} Z_4^2. \quad (3.26)$$

(for incident coupled shear wave)

$$E_i = \frac{\{\lambda + 2\mu - (s\eta_i + a\eta_i^2 - m\eta'_i)/k_i^2\}k_i^3 \cos \theta_i}{\mu k_4^3 \cos \theta_4} Z_i^2, \quad i = 1, 2, 3, \quad E_4 = Z_4^2. \quad (3.27)$$

These results are exactly match with Singh and Tomar (2007).

3.7 Numerical results and discussion

In this section, the numerical values of the amplitude and energy ratios of the reflected waves are computed and the results are represented graphically for a particular model. The physical constants for micropolar thermoelastic solid are taken from Gauthier (1982) and the values corresponding to the voids are taken arbitrarily as

$$\lambda = 7.59 \times 10^{10} \text{ N/m}^2, \quad \mu = 1.89 \times 10^{10} \text{ N/m}^2, \quad \kappa = 0.0149 \times 10^{10} \text{ N/m}^2, \quad \rho = 2190 \text{ Kg/m}^3,$$

$$\gamma = 0.268 \times 10^6 \text{ N}, \quad \Theta_0 = 293 \text{ K}, \quad \tau = 0.13s, \quad k_0 = 1.7 \times 10^2 \text{ Jm}^{-1}\text{s}^{-1}\text{K}^{-1}, \quad \nu = 2 \times 10^{-7} \text{ K}^{-1},$$

$$\chi = 0.00753 \text{ m}^2, \quad d = 2.16 \times 10^6 \text{ N/m}^2, \quad s = 1.02 \times 10^{10} \text{ N/m}^2, \quad \zeta = 1.49 \times 10^{10} \text{ N/m}^2,$$

$$\xi = 1.475 \times 10^6 \text{ N/m}^2, \quad a = 0.668 \times 10^{-9} \text{ N}.$$

In these figures, we use $J = \{\text{Curves I \& IV: } 0.10, \text{ Curves II \& V: } 0.13, \text{ Curves III \& VI: } 0.16\} \times 10^{-4} \text{ m}^2$. The variation of amplitude ($|Z_i|$, $i = 1, 2, 3, 4, 5$) and energy ratios

($|E_i|$, $i = 1, 2, 3, 4, 5$) of reflected waves for incident coupled longitudinal wave with angle of incidence are depicted in Figures 3.1-3.3 and Figures 3.4-3.6 respectively for different values of J , while those of reflected waves for the incident coupled shear wave are depicted respectively in Figures 3.7-3.9 and 3.10-3.12 for different values of J .

3.7.1 For incident coupled longitudinal wave

In Figure 3.1, the amplitude ratio $|Z_1|$ starts from certain values which decreases to the minimum value at $\theta_0 = 62^\circ$ and then increases with the increase of angle of incidence. We have observed that the values of $|Z_1|$ increase with the increase of J . The amplitude ratios, $|Z_2|$ (Curves I, II, III) & $|Z_3|$ (Curves IV, V, VI) in Figure 3.2 of the reflected coupled longitudinal waves decrease with the increase of angle of incidence. In Figure 3.3, Curves I and II are magnified with 10^4 and 10^3 respectively and it is clear that $|Z_4|$ (Curves I, II, III) of the coupled reflected wave increases to the maximum value near $\theta_0 = 50^\circ$ which decreases thereafter with the increase of the angle of incidence. Here, we see that $|Z_4|$ increases with

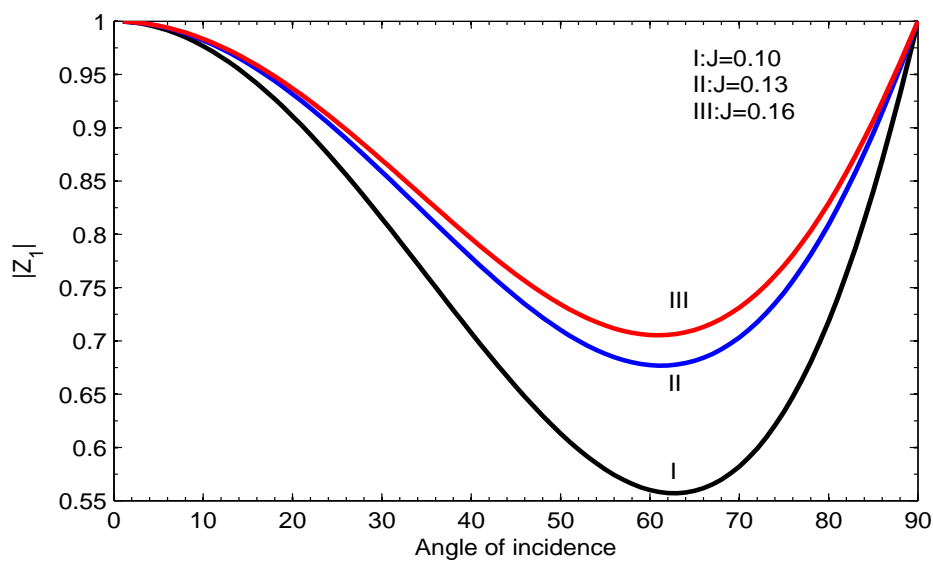


Figure 3.1: Variation of $|Z_1|$ with θ_0 for incident coupled longitudinal wave

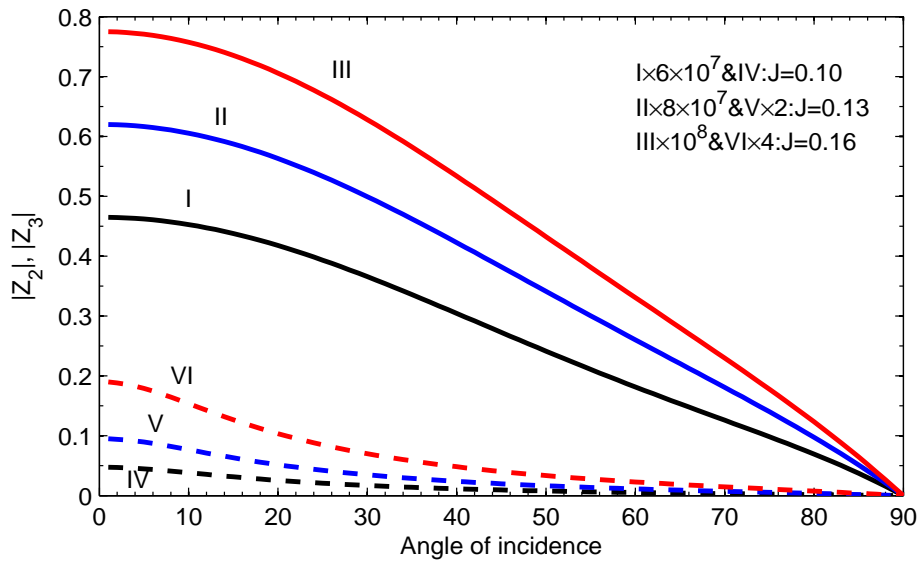


Figure 3.2: Variation of $|Z_2|$ and $|Z_3|$ with θ_0 for incident coupled longitudinal wave

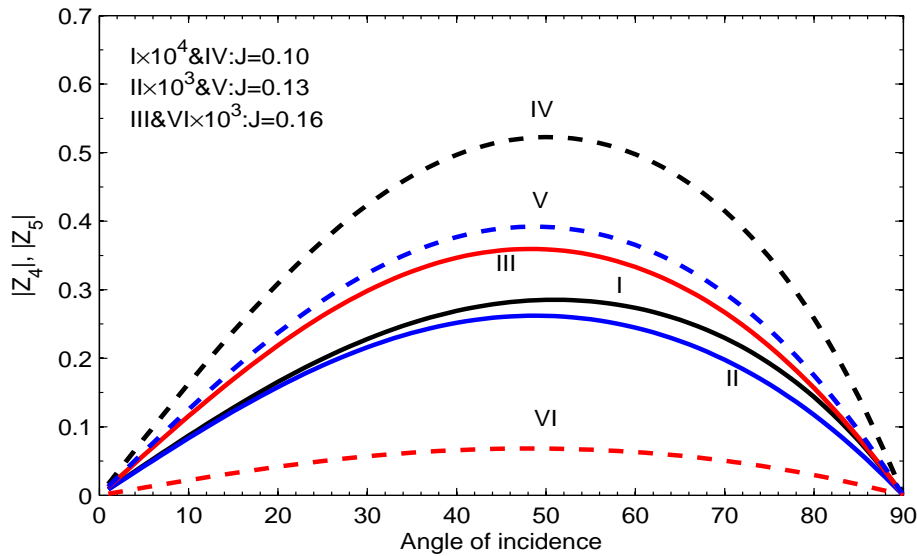


Figure 3.3: Variation of $|Z_4|$ and $|Z_5|$ with θ_0 for incident coupled longitudinal wave

the increase of J . Similar nature of $|Z_5|$ (Curves IV, V, VI) with that of $|Z_4|$ is seen in the same figure, where Curve VI is magnified with 10^3 but their values decrease with the increase of J . In Figure 3.4, the energy ratio, $|E_1|$ for the reflected coupled wave starts from

certain value which decreases to the minimum value near $\theta_0 = 64^\circ$ and then increases with the increase of the angle of incidence. The values of $|E_1|$ increase with the increase of J . The energy ratios, $|E_2|$ (Curves I, II, III) and $|E_3|$ (Curves IV, V, VI) in Figure 3.5 of the

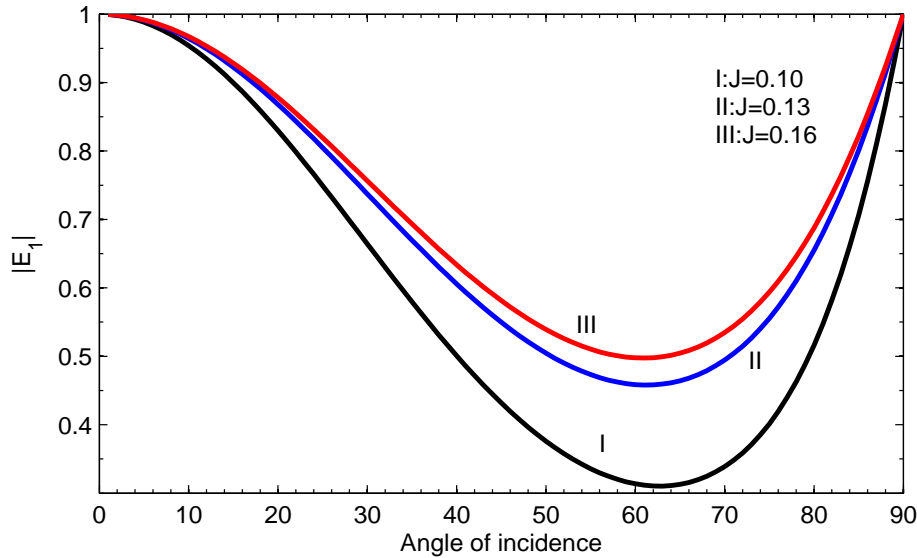


Figure 3.4: Variation of $|E_1|$ with θ_0 for incident coupled longitudinal wave

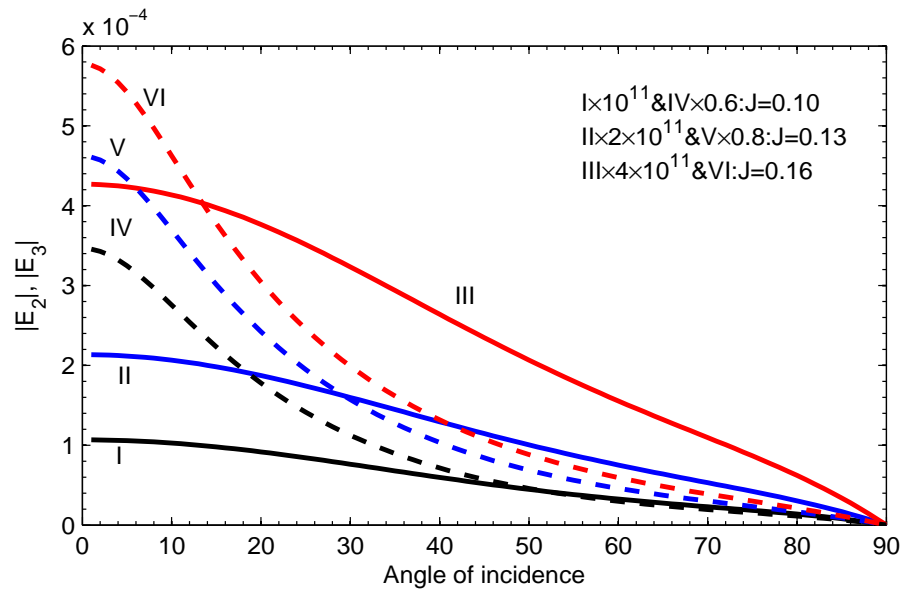


Figure 3.5: Variation of $|E_2|$ and $|E_3|$ with θ_0 for incident coupled longitudinal wave

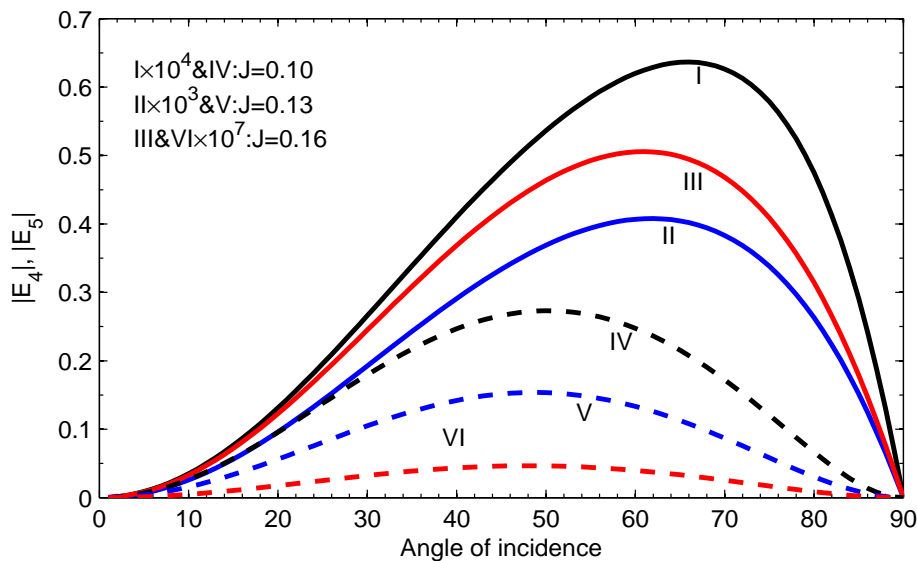


Figure 3.6: Variation of $|E_4|$ and $|E_5|$ with θ_0 for incident coupled longitudinal wave

reflected coupled longitudinal waves decrease with the increase of θ_0 . Figure 3.6 shows that $|E_4|$ (Curves I, II, III) and $|E_5|$ (Curves IV, V, VI) increase to their maximum values and then decrease with the increase of θ_0 . We have observed that the values of $|E_4|$ and $|E_5|$ increase and decrease respectively with the increase of J . The sum of energy ratios is close to unity.

3.7.2 For incident coupled shear wave

In Figure 3.7, the amplitude ratio, $|Z_1|$ (Curves I, II, III) increases initially upto $\theta_0 = 22^\circ$ for Curve I and 29° for Curves II and III which decreases to the minimum value at $\theta_0 = 33^\circ$ for Curve I, 43° for Curve II and 45° for Curve III. Thereafter, all the curves increase with the increase of the angle of incidence. We have observed that the values of $|Z_1|$ increase with the increase of J and there are critical angles for different values of J . The natures of $|Z_2|$ (Curves IV, V, VI) in Figure 3.7 and $|Z_3|$ in Figure 3.8 of the reflected coupled longitudinal waves are interesting in the fact that different parabolic regions can be seen for different values of J and their values are very small. In the Figure 3.9, Curves I and II show that $|Z_4|$

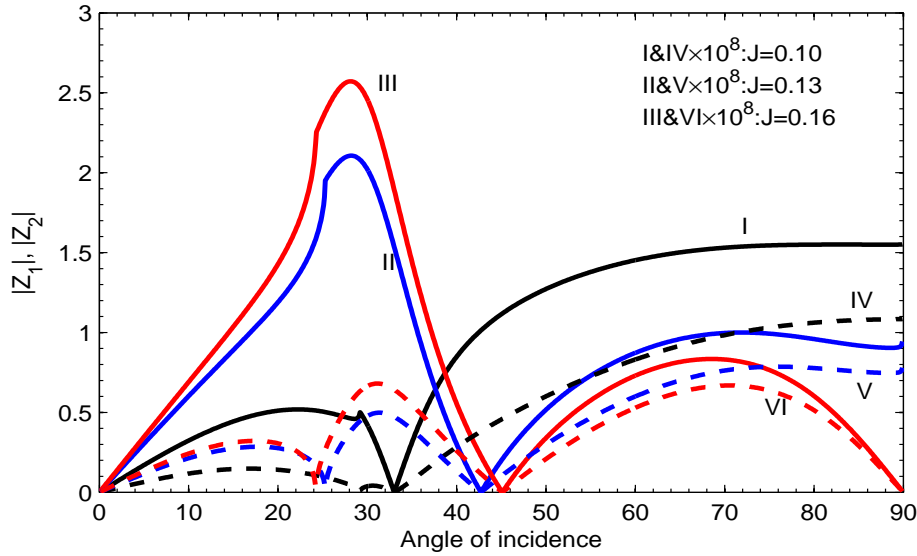


Figure 3.7: Variation of $|Z_1|$ and $|Z_2|$ with θ_0 for incident coupled shear wave

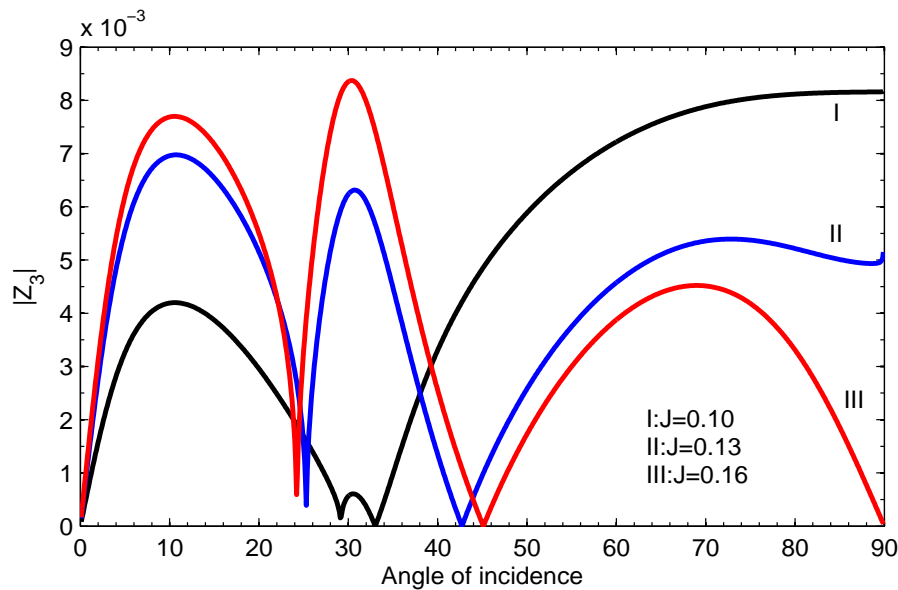


Figure 3.8: Variation of $|Z_3|$ with θ_0 for incident coupled shear wave

almost constant, while Curve III shows that $|Z_4|$ is parabolic in the region $0^\circ \leq \theta_0 \leq 27^\circ$ and then takes a constant value with the increase of θ_0 . Curve IV in the same figure shows that

$|Z_5|$ starts from certain value which decreases upto $\theta_0 = 33^\circ$ and then makes a parabolic region which increases with the increase of angle of incidence. The value of $|Z_5|$ decreases in Curve V upto $\theta_0 = 22^\circ$ and increases upto certain value of θ_0 and then it decreases to the minimum value at $\theta_0 = 45^\circ$ which increases again thereafter. Curve VI is magnified

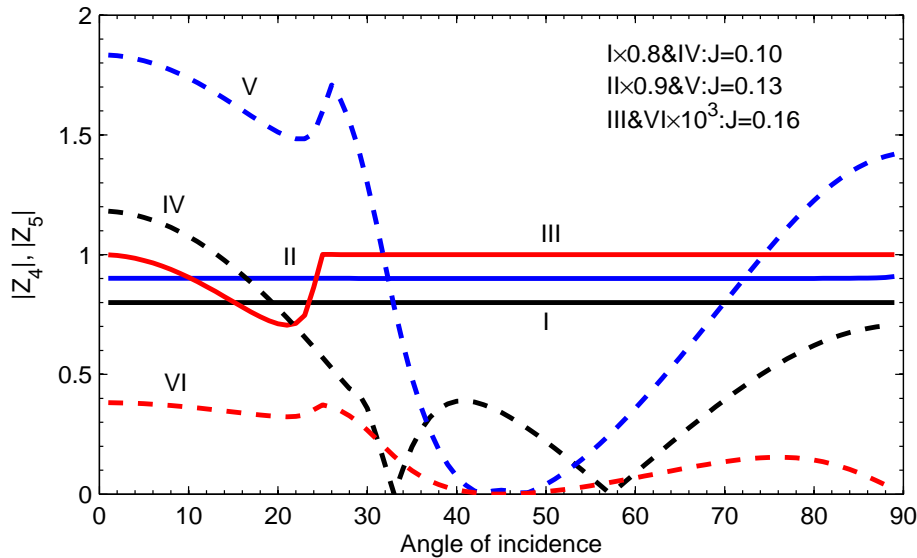


Figure 3.9: Variation of $|Z_4|$ and $|Z_5|$ with θ_0 for incident coupled shear wave

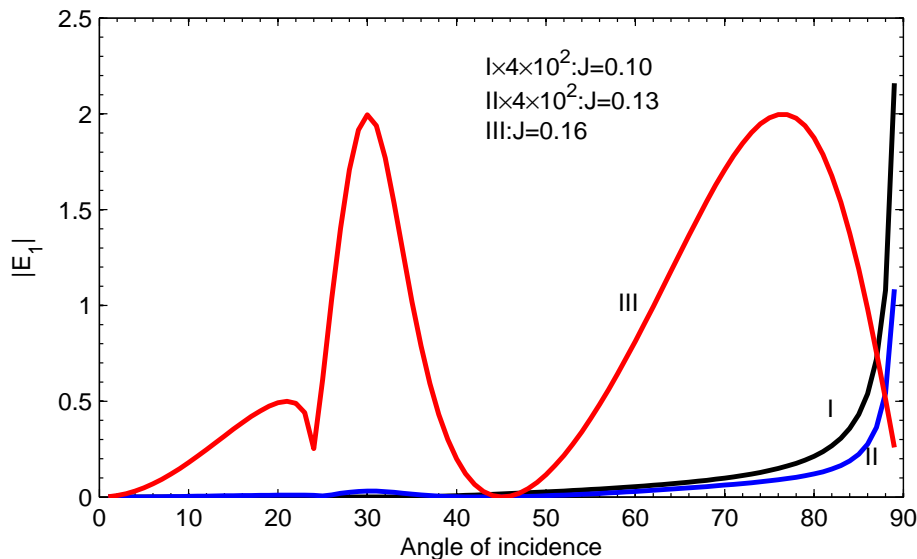


Figure 3.10: Variation of $|E_1|$ with θ_0 for incident coupled shear wave

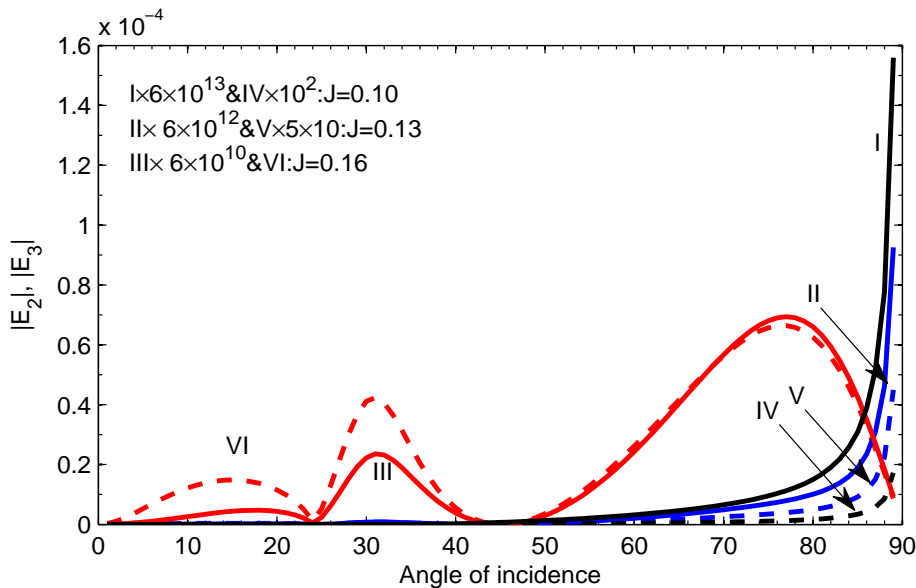


Figure 3.11: Variation of $|E_2|$ and $|E_3|$ with θ_0 for incident coupled shear wave

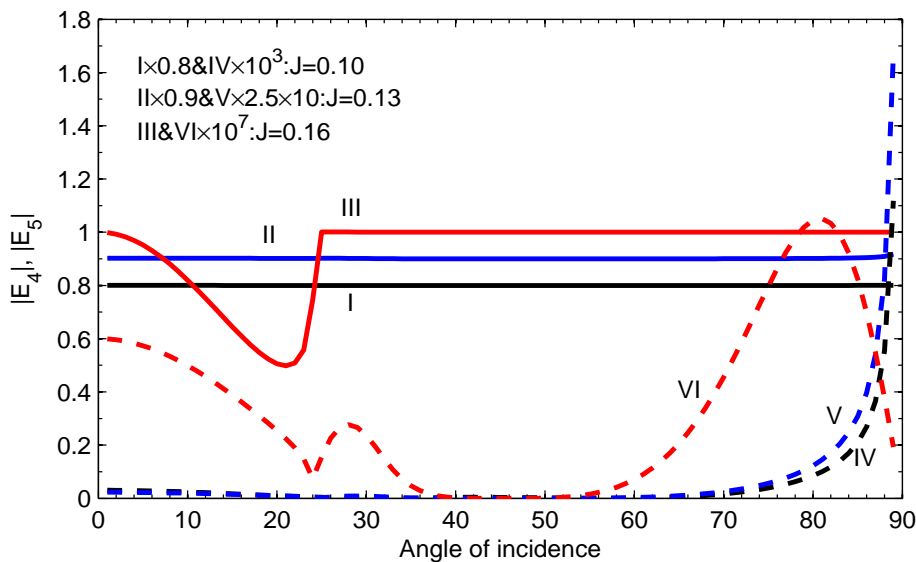


Figure 3.12: Variation of $|E_4|$ and $|E_5|$ with θ_0 for incident coupled shear wave

with 10^3 and it shows the decreasing nature of $|Z_5|$ thereby making a parabolic region in $45^\circ \leq \theta_0 \leq 90^\circ$. We have observed similar nature of $|E_1|$ in Figure 3.10 and $|E_2|$ (Curves I, II, III) and $|E_3|$ (Curves IV, V, VI) in Figure 3.11. Curves I, II, IV & V show that they

increase with the increase of angle of incidence, while Curve III & VI show three parabolic regions with the increase of angle of incidence. In Figure 3.12, $|E_4|$ (Curves I, II, III) of the reflected coupled shear wave makes a constant value in Curves I and II, while Curve III is parabolic in the region $0 \leq \theta_0 \leq 28^\circ$ and then it makes a constant value with the increase of θ_0 . The energy ratio, $|E_5|$ (Curves IV, V, VI) increases with the increase of θ_0 in Curves IV and V. In case of Curve VI, $|E_5|$ decreases initially and then it increases with the increase of θ_0 . In this case also, the sum of energy ratios is close to unity. We have seen that both the amplitude and energy ratios depend on the J and angle of incidence.

3.8 Conclusions

The effect of micro-inertia in the wave propagation in plane half-space of micropolar thermoelastic materials with voids has been investigated. Using the appropriate boundary conditions, the expressions of the amplitude and energy ratios of the reflected waves are obtained analytically and numerically. We come to know that there exist six plane waves of three coupled longitudinal waves, one uncoupled longitudinal wave and two coupled shear waves. The following remarks may be mentioned:

- (i) Amplitude and energy ratios are the functions of elastic, micropolar, thermal and void parameters and angle of incidence.
- (ii) The micropolar wave is not reflected for the incident coupled longitudinal/shear wave.
- (iii) Amplitude ratios, $|Z_1|$, $|Z_2|$, $|Z_3|$, $|Z_4|$ for the incident coupled longitudinal wave increase with the increase of J , while $|Z_5|$ decrease with the increase of J .
- (iv) Energy ratios of the reflected coupled longitudinal waves for incident coupled waves increase with the increase of J .
- (v) We have observed that the effect of J on the amplitude and energy ratios for the incident shear wave are more than that of incident longitudinal wave.
- (vi) The sum of energy ratios of reflected waves for the incident coupled longitudinal and coupled shear waves are found to be closed to unity.

Chapter 4

Effect of thermal and micro-inertia on the refraction of elastic waves in micropolar thermoelastic materials with voids³

4.1 Introduction

The phenomena of reflection and refraction of elastic waves are very common in the field of Seismology, Geophysics and Earthquake engineering. Tomar and Gogna (1995) studied the problem of longitudinal waves at an interface between two micropolar elastic solids in welded contact and obtained amplitude and energy ratios of the reflected and refracted waves. Chakraborty and Singh (2011) discussed the problem of reflection and refraction of a plane thermoelastic wave at a solidsolid interface under perfect boundary condition in presence of normal initial stress. They obtained the amplitude ratios of various reflected and refracted waves using an ideal boundary for the incident SV -wave.

In the present work, the reflection and refraction of plane waves at the interface between two dissimilar half-spaces of micropolar thermoelastic materials with voids has been investigated. The amplitude and energy ratios of the reflected and refracted waves are obtained analytically

³*Communicated to International Journal of Computational Method for Engineering Sciences and Mechanics (2017)*

and numerically for a particular model. The effects of thermal and micro-inertia on these ratios are discussed for two separate cases, i.e., (i) incident longitudinal wave and (ii) incident shear wave. In the case of incident longitudinal wave, the effect of linear thermal expansion on the amplitude and energy ratios is discussed, while for the incident shear wave, we have discussed the effect of micro-inertia.

4.2 Basic Equations

The equations of motion for a homogeneous and isotropic micropolar thermoelastic materials with voids are written as

$$(c_1^2 + c_2^2)\nabla^2 p + c_3^2\psi - c_4^2\Theta = \ddot{p}, \quad (4.1)$$

$$c_8^2\nabla^2 p - (c_9^2\nabla^2 - c_{10}^2)\psi + c_{11}^2\Theta = -\ddot{\psi}, \quad (4.2)$$

$$K_0\nabla^2\Theta - (1 + \tau\frac{\partial}{\partial t})(c_d^2\dot{\Theta} + c_m^2\nabla^2\dot{p} - c_\xi^2\dot{\psi}) = 0, \quad (4.3)$$

$$(c_{13}^2 + c_6^2)\nabla^2\phi' - c_7^2\phi' = \ddot{\phi}', \quad (4.4)$$

$$c_{12}^2\nabla^2\mathbf{P} + c_2^2\nabla \times \phi'' = \ddot{\mathbf{P}}, \quad (4.5)$$

$$(c_6^2\nabla^2 - c_7^2)\phi'' + c_5^2\nabla \times \mathbf{P} = \ddot{\phi}'', \quad (4.6)$$

where

$$c_1^2 = \frac{\lambda + 2\mu}{\rho}, \quad c_2^2 = \frac{\kappa}{\rho}, \quad c_3^2 = \frac{s}{\rho}, \quad c_4^2 = \frac{m}{\rho}, \quad c_5^2 = \frac{\kappa}{\rho_1}, \quad c_6^2 = \frac{\gamma}{\rho_1}, \quad c_7^2 = \frac{2\kappa}{\rho_1}, \quad c_8^2 = \frac{s}{\rho_2}, \quad c_9^2 = \frac{a}{\rho_2},$$

$$c_{10}^2 = \frac{\zeta}{\rho_2}, \quad c_{11}^2 = \frac{\xi}{\rho_2}, \quad c_{12}^2 = \frac{\mu + \kappa}{\rho}, \quad c_{13}^2 = \frac{\alpha + \beta}{\rho_1}, \quad c_d^2 = \frac{d}{\rho_1}, \quad c_m^2 = \frac{m}{\rho_1}, \quad c_\xi^2 = \frac{\xi}{\rho_1}, \quad K_0 = \frac{k_0}{\rho_1\Theta_0}.$$

It may be notated that p , ψ and Θ are coupled dilatational waves and \mathbf{P} , ϕ'' are coupled shear waves obtained from the Helmholtz's decomposition of displacement (\mathbf{u}) and microrotation vectors (ϕ). The micropolar wave is given by Eq. (4.4) and it participates neither in reflection nor in refraction from any discontinuity in the material body (Parfitt and Eringen,

1969).

4.3 Wave propagation

Consider the Cartesian co-ordinate system with x and y -axis lying horizontally and z -axis vertically downward. The two dissimilar half-spaces of micropolar thermoelastic materials with voids are represented by $M = \{(x, z), x \in R, z \in (0, \infty)\}$ and $M' = \{(x, z), x \in R, z \in (-\infty, 0)\}$. The material parameters in M will denote without prime and the corresponding parameters in M' will be denoted with prime ($'$). A train of longitudinal wave or shear wave with amplitude constant A at an angle θ with the positive direction of z -axis be incident at the plane interface. This wave gives five reflected waves (three coupled longitudinal waves and two coupled shear waves) in M and five refracted waves (three coupled longitudinal waves and two coupled shear waves) in M' . The complete geometry of the problem is shown in Figure 4.1.

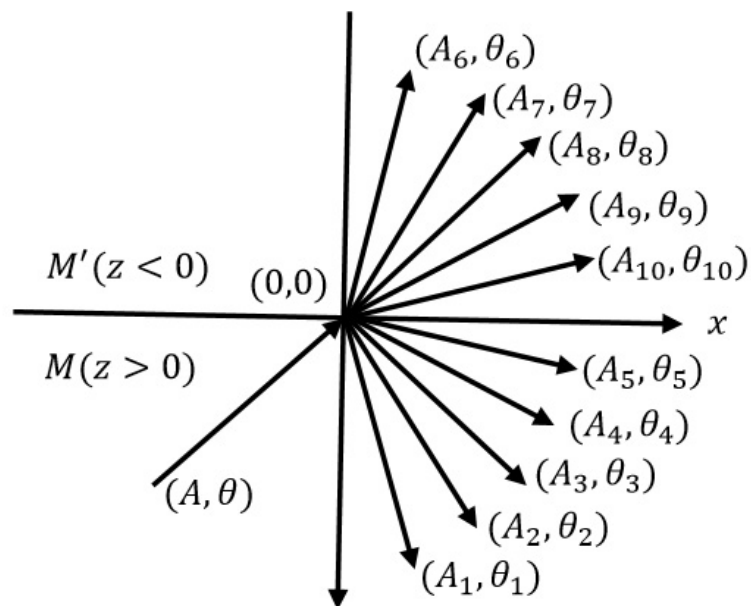


Figure 4.1: Geometry of the problem

The complete potential structures of the various reflected and refracted waves are given below.

For the reflected waves in the half-space, M

$$\{p, \psi, \Theta\} = \{1, \eta_0, \pi_0\}A \exp(Q_0) + \sum_{i=1}^3 \{1, \eta_i, \pi_i\}A_i \exp(Q_i), \quad (4.7)$$

$$\{P, \phi_2\} = \{1, \eta_{00}\}A \exp(Q_0) + \sum_{i=4}^5 \{1, \eta_i\}A_i \exp(Q_i), \quad (4.8)$$

where

$$Q_0 = \imath k(x \sin \theta + z \cos \theta - Vt), \quad Q_i = \imath k_i(x \sin \theta_i - z \cos \theta_i - V_i t),$$

ϕ_2 is the y -component of ϕ'' and P is the y -component of \mathbf{P} of the reflected waves, A_i is the amplitude constant of the reflected wave at angle θ_i with wavenumber k_i and V is the velocity of the incident wave with wavenumber, k .

For the refracted waves in the half-space M'

$$\{p', \psi', \Theta'\} = \sum_{i=6}^8 \{1, \eta_i, \pi_i\}A_i \exp(Q_i), \quad (4.9)$$

$$\{P', \phi'_2\} = \sum_{i=9}^{10} \{1, \eta_i\}A_i \exp(Q_i), \quad (4.10)$$

where

$$Q_i = \imath k_i(x \sin \theta_r + z \cos \theta_r - V_i t),$$

ϕ'_2 and P' are similar form of ϕ_2 and P respectively in the half-space M' and A_i is amplitude constant of the refracted wave with wavenumber, k_i .

The expressions of phase velocities, V_i are given in (2.20), (2.21), (2.22) and (2.28), and the coupling parameters, η_i and π_i ($i = 1, \dots, 10$) are given below.

$$\eta_i = \begin{cases} \left\{ \begin{aligned} & \{c_8^2 c_k^2 k_i^4 - (c_8^2 c_d^2 - c_{11}^2 c_m^2) k_i^2\} / \{c_9^2 c_k^2 k_i^4 - \\ & (\omega^2 c_k^2 - c_{10}^2 c_k^2 + c_9^2 c_d^2) k_i^2 - c_{11}^2 c_\xi^2 - c_{10}^2 c_d^2 + \omega^2 c_d^2\}, \quad (i = 1, 2, 3) \\ & c_5^2 / \{c_6^2 + c_7^2 / k_i^2 - V_i\}, \quad (i = 4, 5) \\ & \{c_8'^2 c_k'^2 k_i^4 - (c_8'^2 c_d'^2 - c_{11}'^2 c_m'^2) k_i^2\} / \{c_9'^2 c_k'^2 k_i^4 - \\ & (\omega^2 c_k'^2 - c_{10}'^2 c_k'^2 + c_9'^2 c_d'^2) k_i^2 - c_{11}'^2 c_\xi'^2 - c_{10}'^2 c_d'^2 + \omega^2 c_d'^2\}, \quad (i = 6, 7, 8) \\ & c_5'^2 / \{c_6'^2 + c_7'^2 / k_i^2 - V_i\}, \quad (i = 9, 10) \end{aligned} \right. \\ \\ \pi_i = \begin{cases} \left\{ \begin{aligned} & \{c_m^2 c_9^2 k_i^4 + (c_m^2 c_{10}^2 + c_8^2 c_\xi^2 - c_m^2 \omega^2) k_i^2\} / \{-c_9^2 c_k^2 k_i^4 + \\ & (\omega^2 c_k^2 - c_{10}^2 c_k^2 + c_9^2 c_d^2) k_i^2 + c_{11}^2 c_\xi^2 + c_{10}^2 c_d^2 - \omega^2 c_d^2\}, \quad (i = 1, 2, 3) \\ & \{c_m'^2 c_9'^2 k_i^4 + (c_m'^2 c_{10}'^2 + c_8'^2 c_\xi'^2 - c_m'^2 \omega^2) k_i^2\} / \{-c_9'^2 c_k'^2 k_i^4 + \\ & (\omega^2 c_k'^2 - c_{10}'^2 c_k'^2 + c_9'^2 c_d'^2) k_i^2 + c_{11}'^2 c_\xi'^2 + c_{10}'^2 c_d'^2 - \omega^2 c_d'^2\}, \quad (i = 6, 7, 8), \end{aligned} \right. \end{cases}$$

where

$$c_1'^2 = \frac{\lambda' + 2\mu'}{\rho'}, \quad c_2'^2 = \frac{\kappa'}{\rho'}, \quad c_3'^2 = \frac{s'}{\rho'}, \quad c_4'^2 = \frac{m'}{\rho'}, \quad c_5'^2 = \frac{\kappa'}{\rho_1'}, \quad c_6'^2 = \frac{\gamma'}{\rho_1'}, \quad c_7'^2 = \frac{2\kappa'}{\rho_1'}, \quad c_8'^2 = \frac{s'}{\rho_2'}, \quad c_9'^2 = \frac{a'}{\rho_2'},$$

$$c_{10}'^2 = \frac{\zeta'}{\rho_2'}, \quad c_{11}'^2 = \frac{\xi'}{\rho_2'}, \quad c_{12}'^2 = \frac{\mu' + \kappa'}{\rho'}, \quad c_{13}'^2 = \frac{\alpha' + \beta'}{\rho_1'}, \quad c_d'^2 = \frac{d'}{\rho_1'}, \quad c_m'^2 = \frac{m'}{\rho_1'}, \quad c_\xi'^2 = \frac{\xi'}{\rho_1'}, \quad K_0' = \frac{k_0'}{\rho_1' \Theta_0}.$$

It may be noted that when the incident wave is longitudinal wave (three coupled longitudinal waves), the coupling constants $(\eta_0, \pi_0, \eta_{00}, \theta) = (\eta_i, \pi_i, 0, \theta_i)$ for $i = 1$ as incident first coupled longitudinal wave (*FCLW*), $i = 2$ as incident second coupled longitudinal wave (*SCLW*) and $i = 3$ as incident third coupled longitudinal wave (*TCLW*). Similarly, $(\eta_0, \pi_0, \eta_{00}, \theta) = (0, 0, \eta_i, \theta_i)$ for incident two coupled shear waves, i.e., $i = 4$ corresponds for incident first coupled shear wave (*FCSW*) and $i = 5$ corresponds for incident second coupled shear wave (*SCSW*).

The Snell's law can be written for our problem as

$$\frac{\sin \theta}{V} = \frac{\sin \theta_i}{V_i} = \frac{\sin \theta_{i+5}}{V_{i+5}} \quad (i = 1, 2, \dots, 5). \quad (4.11)$$

4.4 Boundary conditions

The displacements, stress tensors, equilibrated stress vector, temperature gradient, change in void volume fraction, micro-rotation vector and change in temperature are continuous at $z = 0$. Mathematically, these conditions at $z = 0$ are

$$T_{zz} = T'_{zz}, \quad T_{zx} = T'_{zx}, \quad M_{zy} = M'_{zy}, \quad h_{,z} = h'_{,z}, \quad u_x = u'_x, \quad u_z = u'_z, \quad (4.12)$$

$$\Theta_{,z} = \Theta'_{,z}, \quad \psi = \psi', \quad \Theta = \Theta', \quad \phi_2 = \phi'_2, \quad (4.13)$$

Using Eq. (1.37) into (4.12), we have

$$\begin{aligned} & \lambda \frac{\partial^2 p}{\partial x^2} + (\lambda + 2\mu + \kappa) \frac{\partial^2 p}{\partial z^2} + (2\mu + \kappa) \frac{\partial^2 P}{\partial x \partial z} + s\psi - m\Theta = \\ & \lambda' \frac{\partial^2 p'}{\partial x^2} + (\lambda' + 2\mu' + \kappa') \frac{\partial^2 p'}{\partial z^2} + (2\mu' + \kappa') \frac{\partial^2 P'}{\partial x \partial z} + s'\psi' - m'\Theta', \end{aligned} \quad (4.14)$$

$$\begin{aligned} & (2\mu + \kappa) \frac{\partial^2 p}{\partial x \partial z} - (\mu + \kappa) \frac{\partial^2 P}{\partial z^2} + \mu \frac{\partial^2 P}{\partial x^2} - \kappa \phi_2 = \\ & (2\mu' + \kappa') \frac{\partial^2 p'}{\partial x \partial z} - (\mu' + \kappa') \frac{\partial^2 P'}{\partial z^2} + \mu' \frac{\partial^2 P'}{\partial x^2} - \kappa' \phi'_2, \end{aligned} \quad (4.15)$$

$$\gamma \frac{\partial \phi_2}{\partial z} = \gamma' \frac{\partial \phi'_2}{\partial z}, \quad a \frac{\partial \psi}{\partial z} = a' \frac{\partial \psi'}{\partial z}, \quad (4.16)$$

$$\frac{\partial p}{\partial x} - \frac{\partial P}{\partial z} = \frac{\partial p'}{\partial x} - \frac{\partial P'}{\partial z}, \quad \frac{\partial p}{\partial z} + \frac{\partial P}{\partial x} = \frac{\partial p'}{\partial z} + \frac{\partial P'}{\partial x}. \quad (4.17)$$

Inserting Equations (4.7)-(4.11) into (4.13)-(4.14), we get a system of equations

$$\sum_{j=1}^{10} a_{ij} Z_j = b_i \quad (i = 1, 2, \dots, 10) \quad (4.18)$$

where the non-zero a_{ij} are given as

$$a_{1j} = \{\lambda + (2\mu + \kappa) \cos^2 \theta_j - (s\eta_j - m\pi_j)/k_j^2\} k_j^2, \quad (j = 1, 2, 3);$$

$$a_{1j} = -(2\mu + \kappa) \sin \theta_j \cos \theta_r k_j^2, \quad (j = 4, 5);$$

$$\begin{aligned}
a_{1j} &= -\{\lambda' + (2\mu' + \kappa') \cos^2 \theta_j - (s'\eta_j - m'\pi_j)/k_j^2\}k_j^2, \quad (j = 6, 7, 8); \\
a_{1j} &= -(2\mu' + \kappa') \sin \theta_j \cos \theta_j k_j^2, \quad (j = 9, 10); \\
a_{2j} &= (2\mu + \kappa) \sin \theta_j \cos \theta_j k_j^2, \quad (j = 1, 2, 3); \\
a_{2j} &= \{\mu(\cos^2 \theta_j - \sin^2 \theta_j) + \kappa \cos^2 \theta_j - \kappa\eta_j/k_j^2\}k_j^2, \quad (j = 4, 5); \\
a_{2j} &= (2\mu' + \kappa') \sin \theta_j \cos \theta_j k_j^2, \quad (j = 6, 7, 8); \\
a_{2j} &= -\{\mu'(\cos^2 \theta_j - \sin^2 \theta_j) + \kappa' \cos^2 \theta_j - \kappa'\eta_j/k_j^2\}k_j^2, \quad (j = 9, 10); \\
a_{3j} &= \gamma\eta_j \cos \theta_j k_j \quad (j = 4, 5), \quad a_{3j} = \gamma'\eta_j \cos \theta_j k_j, \quad (j = 9, 10); \\
a_{4j} &= a\eta_j \cos \theta_j k_j \quad (j = 1, 2, 3), \quad a_{4j} = a'\eta_j \cos \theta_j k_j, \quad (j = 6, 7, 8); \\
a_{5j} &= \pi_j \cos \theta_j k_j \quad (j = 1, 2, 3), \quad a_{5j} = \pi_j \cos \theta_j k_j, \quad (j = 6, 7, 8); \\
a_{6j} &= \sin \theta_j k_j \quad (j = 1, 2, 3), \quad a_{6j} = \cos \theta_j k_j, \quad (j = 4, 5); \\
a_{6j} &= -\sin \theta_j k_j \quad (j = 6, 7, 8), \quad a_{6j} = \cos \theta_j k_j, \quad (j = 9, 10); \\
a_{7j} &= -\cos \theta_j k_j \quad (j = 1, 2, 3), \quad a_{7j} = \sin \theta_j k_j, \quad (j = 4, 5); \\
a_{7j} &= -\cos \theta_j k_j \quad (j = 6, 7, 8), \quad a_{7j} = -\sin \theta_j k_j, \quad (j = 9, 10); \\
a_{8j} &= \eta_j \quad (j = 1, 2, 3), \quad a_{8j} = -\eta_j \quad (j = 6, 7, 8), \quad a_{9j} = \pi_j \quad (j = 1, 2, 3); \\
a_{9j} &= -\pi_j \quad (j = 6, 7, 8), \quad a_{10j} = \eta_j \quad (j = 4, 5), \quad a_{10j} = -\eta_j \quad (j = 9, 10).
\end{aligned}$$

The non-zero b_i , ($i = 1, \dots, 10$) for the incident longitudinal waves are given as

$$b_1 = -a_{1j}, \quad b_2 = a_{2j}, \quad b_4 = a_{4j}, \quad b_5 = a_{5j}, \quad b_6 = -a_{6j},$$

$$b_7 = a_{7j}, \quad b_8 = -a_{8j}, \quad b_9 = -a_{9j}, \quad (j = 1, 2, 3).$$

Here, $j = 1$ corresponds for the incident first coupled longitudinal wave (*FCLW*), $j = 2$ corresponds for the incident second coupled longitudinal wave (*SCLW*) and $j = 3$ corresponds for the incident third coupled longitudinal wave (*TCLW*).

The non-zero b_i , ($i = 1, \dots, 10$) for the incident shear waves are given as

$$b_1 = a_{1j}, \quad b_2 = -a_{2j}, \quad b_3 = a_{3j}, \quad b_6 = a_{6j}, \quad b_7 = -a_{7j}, \quad b_{10} = -a_{10j}, \quad (j = 4, 5).$$

In this case, $j = 4$ corresponds for incident first coupled shear wave (*FCSW*) and $j = 5$ corresponds for incident second coupled shear wave (*SCSW*).

The amplitude ratios $Z_j(= A_j/A)$, $j = 1, 2, 3$ represent for the reflected coupled longitudinal waves and $Z_j(= A_j/A)$, $j = 4, 5$ represent reflected coupled shear waves, while $Z_j(= A_j/A)$, $j = 6, 7, 8$ represent for the refracted coupled longitudinal waves and $Z_j(= A_j/A)$, $j = 9, 10$ represent refracted coupled shear waves.

4.5 Energy partition

Consider the energy partitioning among the various reflected and refracted waves at the plane interface. Following Achenbach (1976), the energy distribution per unit area at the plane interface ($z = 0$) is given by

$$\wp = \langle T_{zz}, \dot{u}_z \rangle + \langle T_{zx}, \dot{u}_x \rangle + \langle M_{zy}, \dot{\phi}_y \rangle + \langle h_z, \dot{\psi} \rangle. \quad (4.19)$$

The expression of incident waves are given below:

(a) for incident longitudinal waves

$$\wp_{inc} = r_0 \omega k^3 \cos \theta A^2 \exp(2Q_0), \quad (4.20)$$

where $r_0 = \lambda + 2\mu + \kappa - (s\eta_0 + a\eta_0^2 - m\pi_0)/k^2$,

(b) for incident shear waves

$$\wp_{inc} = s_0 \omega k^3 \cos \theta A^2 \exp(2Q_0), \quad (4.21)$$

where $s_0 = \mu + \kappa - \eta_{00}(\gamma\eta_{00} + \kappa)/k^2$.

The expressions of energy ratios of various reflected and refracted waves are given by

(i) for incident longitudinal waves

$$E_i = \frac{r_i k_i^3 \cos \theta_i}{r_0 k^3 \cos \theta} Z_i^2, \quad (i = 1, 2, \dots, 10), \quad (4.22)$$

where

$$r_i = \lambda + 2\mu + \kappa - (s\eta_i + a\eta_i^2 - m\pi_i)/k_i^2, \quad (i = 1, 2, 3),$$

$$\begin{aligned}
r_i &= \mu + \kappa - \eta_i(\kappa + \gamma\eta_i)/k_i^2, \quad (i = 4, 5), \\
r_i &= \lambda' + 2\mu' + \kappa' - (s'\eta_i + a'\eta_i^2 - m'\pi_i)/k_i^2, \quad (i = 6, 7, 8), \\
r_i &= \mu' + \kappa' - \eta_i(\kappa' + \gamma'\eta_i)/k_i^2, \quad (i = 9, 10),
\end{aligned}$$

and (ii) for incident shear waves

$$E_i = \frac{r_i k_i^3 \cos \theta_i}{s_0 k^3 \cos \theta} Z_i^2, \quad (i = 1, 2, \dots, 10). \quad (4.23)$$

We note that the energy ratios E_i , ($i = 1, 2, 3$) corresponds for the reflected coupled longitudinal waves and E_i , ($i = 6, 7, 8$) corresponds for the refracted coupled longitudinal waves, while E_i , ($i = 4, 5$) corresponds for the reflected coupled shear waves and E_i , ($i = 9, 10$) corresponds for the refracted coupled shear waves.

4.6 Particular cases

Case 1: If we neglect the effect of micropolar in the two half-spaces M and M' , then the problem reduces to the reflection and refraction of elastic waves in two dissimilar half-spaces of thermoelastic materials with voids. Then, $\alpha = \beta = \gamma = \kappa = \alpha' = \beta' = \gamma' = \kappa' = 0$. Consequently,

$$V_5^2 = 0, \quad V_4^2 = \mu/\rho, \quad V_{10}^2 = 0, \quad V_9^2 = \mu'/\rho'.$$

There are one each reflected and refracted shear waves in this case. Eq. (4.18) reduces to 8 equations with the following non-zero a_{ij}

$$\begin{aligned}
a_{1j} &= \{\lambda + 2\mu \cos^2 \theta_j - (s\eta_j - m\pi_j)/k_j^2\}k_j^2, \quad (j = 1, 2, 3), \quad a_{14} = -2\mu \sin \theta_4 \cos \theta_4 k_4^2, \\
a_{1j} &= -\{\lambda' + 2\mu' \cos^2 \theta_j - (s'\eta_j - m'\pi_j)/k_j^2\}k_j^2, \quad (j = 6, 7, 8), \quad a_{19} = -2\mu' \sin \theta_9 \cos \theta_9 k_9^2, \\
a_{2j} &= 2\mu \sin \theta_j \cos \theta_j k_j^2, \quad (j = 1, 2, 3), \quad a_{24} = \mu(\cos^2 \theta_4 - \sin^2 \theta_4)k_4^2, \\
a_{2j} &= 2\mu' \sin \theta_j \cos \theta_j k_j^2, \quad (j = 6, 7, 8), \quad a_{29} = -\mu'(\cos^2 \theta_9 - \sin^2 \theta_9)k_9^2, \\
a_{4j} &= a\eta_j \cos \theta_j k_j, \quad (j = 1, 2, 3), \quad a_{4j} = a'\eta_j \cos \theta_j k_j, \quad (j = 6, 7, 8),
\end{aligned}$$

$$\begin{aligned}
a_{5j} &= \pi_j \cos \theta_j k_j, \quad (j = 1, 2, 3), & a_{5j} &= \pi_j \cos \theta_j k_j, \quad (j = 6, 7, 8), \\
a_{6r} &= \sin \theta_j k_j, \quad (j = 1, 2, 3), & a_{64} &= \cos \theta_4 k_4, & a_{6j} &= -\sin \theta_j k_j, \quad (j = 6, 7, 8), \\
a_{69} &= \cos \theta_9 k_9, & a_{7j} &= -\cos \theta_j k_j, \quad (j = 1, 2, 3), & a_{74} &= \sin \theta_4 k_4, \\
a_{7j} &= -\cos \theta_j k_j, \quad (j = 6, 7, 8), & a_{79} &= \sin \theta_9 k_9, & a_{8j} &= \eta_j, \quad (j = 1, 2, 3), \\
a_{8j} &= -\eta_j, \quad (j = 6, 7, 8), & a_{9j} &= \pi_j, \quad (j = 1, 2, 3), & a_{9j} &= -\pi_j, \quad (j = 6, 7, 8).
\end{aligned}$$

The corresponding energy ratios of the reflected and refracted waves for incident longitudinal and shear waves are given by Eqs. (4.22) and (4.23) with the following modified values

$$\begin{aligned}
r_0 &= \lambda + 2\mu - (s\eta_0 + a\eta_0^2 - m\pi_0)/k^2, & r_i &= \lambda + 2\mu - (s\eta_i + a\eta_i^2 - m\pi_i)/k_i^2, \quad (i = 1, 2, 3), \\
r_4 &= s_0 = \mu, & r_9 &= \mu', & r_i &= \lambda' + 2\mu' - (s'\eta_i + a'\eta_i^2 - m'\pi_i)/k_i^2, \quad (i = 6, 7, 8).
\end{aligned}$$

These results are exactly same as those of Singh (2011, 2013).

Case 2: If micropolar and voids effects are neglected, then M and M' reduce to two half-spaces of thermoelastic materials. In this case,

$$\alpha = \beta = \gamma = \kappa = a = s = \zeta = \xi = a' = s' = \zeta' = \xi' = \alpha' = \beta' = \gamma' = \kappa' = 0.$$

Then, Equation (4.18) reduces to six linear equations with the following non-zero a_{ij}

$$\begin{aligned}
a_{1j} &= (\lambda + 2\mu \cos^2 \theta_r + m\pi_j/k_j^2)k_j^2, \quad (j = 1, 2); & a_{14} &= -2\mu \sin \theta_4 \cos \theta_4 k_4^2, \\
a_{1j} &= -(\lambda' + 2\mu' \cos^2 \theta_j + m'\pi_j/k_j^2)k_j^2, \quad (j = 6, 7); & a_{19} &= -2\mu' \sin \theta_9 \cos \theta_9 k_9^2, \\
a_{2j} &= 2\mu \sin \theta_j \cos \theta_j k_j^2, \quad (j = 1, 2); & a_{24} &= \mu(\cos^2 \theta_4 - \sin^2 \theta_4)k_4^2, \\
a_{2j} &= 2\mu' \sin \theta_j \cos \theta_j k_j^2, \quad (j = 6, 7); & a_{29} &= -\mu'(\cos^2 \theta_9 - \sin^2 \theta_9)k_9^2, \\
a_{5j} &= \pi_j \cos \theta_r k_j, \quad (j = 1, 2); & a_{5j} &= \pi_j \cos \theta_j k_j, \quad (j = 6, 7); & a_{6j} &= \sin \theta_j k_j, \quad (j = 1, 2); \\
a_{64} &= \cos \theta_4 k_4, & a_{6j} &= -\sin \theta_j k_j, \quad (j = 6, 7); & a_{69} &= \cos \theta_9 k_9, \\
a_{7j} &= -\cos \theta_j k_j, \quad (j = 1, 2); & a_{74} &= \sin \theta_4 k_4, & a_{7j} &= -\cos \theta_j k_j, \quad (j = 6, 7);
\end{aligned}$$

$$a_{79} = \sin \theta_9 k_9, \quad a_{9j} = \pi_j, \quad (j = 1, 2); \quad a_{9j} = -\pi_j, \quad (j = 6, 7).$$

These results are similar with those of Kumar and Sarthi (2006).

The corresponding energy ratios of the reflected and refracted waves for incident longitudinal and shear waves are given by Eqs. (4.22) and (4.23) with the following modified values

$$r_0 = \lambda + 2\mu + m\pi_0/k^2, \quad r_i = \lambda + 2\mu + m\pi_i/k_i^2, \quad (i = 1, 2),$$

$$r_4 = s_0 = \mu, \quad r_9 = \mu', \quad r_i = \lambda' + 2\mu' + m'\pi_i/k_i^2, \quad (i = 6, 7).$$

Case 3: If we neglect micropolar, voids and thermal effect, then M and M' reduce to two half-spaces of isotropic elastic medium. In this case, $\alpha = \beta = \gamma = \kappa = a = s = \zeta = \xi = k_0 = \tau = m = \alpha' = \beta' = \gamma' = \kappa' = a' = s' = \zeta' = \xi' = k'_0 = \tau' = m' = 0$. Consequently,

$$V_1^2 = (\lambda + 2\mu)/\rho, \quad V_6^2 = (\lambda' + 2\mu')/\rho', \quad V_2 = V_7 = 0.$$

Equation (4.18) becomes a system of four linear equations with the following a_{ij} :

$$a_{11} = (\lambda + 2\mu \cos^2 \theta_1)k_1^2, \quad a_{14} = -2\mu \sin \theta_4 \cos \theta_4 k_4^2, \quad a_{16} = -(\lambda' + 2\mu' \cos^2 \theta_6)k_6^2,$$

$$a_{19} = -2\mu' \sin \theta_9 \cos \theta_9 k_9^2, \quad a_{21} = 2\mu \sin \theta_1 \cos \theta_1 k_1^2, \quad a_{24} = \mu(\cos^2 \theta_4 - \sin^2 \theta_4)k_4^2,$$

$$a_{26} = 2\mu' \sin \theta_6 \cos \theta_6 k_6^2, \quad a_{29} = -\mu'(\cos^2 \theta_9 - \sin^2 \theta_9)k_9^2, \quad a_{61} = \sin \theta_1 k_1,$$

$$a_{64} = \cos \theta_4 k_4, \quad a_{66} = -\sin \theta_6 k_6, \quad a_{69} = \cos \theta_9 k_9, \quad a_{71} = -\cos \theta_1 k_1,$$

$$a_{74} = \sin \theta_4 k_4, \quad a_{76} = -\cos \theta_6 k_6, \quad a_{79} = \sin \theta_9 k_9.$$

The corresponding energy ratios of the reflected and refracted waves for incident longitudinal and shear waves are given by Eqs. (4.22) and (4.23) with the following modified values

$$r_0 = r_1 = \lambda + 2\mu, \quad s_0 = r_4 = \mu, \quad r_6 = \lambda' + 2\mu', \quad r_9 = \mu'.$$

These results are exactly same with those of Achenbach (1976) for classical elasticity.

4.7 Numerical results and discussion

We are interested in computing the numerical values of amplitude and energy ratios of reflected and refracted waves for the incident longitudinal and shear waves. For this model, we consider two separate cases for incident first couple longitudinal wave (*FCLW*) and for incident first couple shear wave (*FCSW*). The parameters for half-spaces, M (Khurana and Tomar, 2007) and M' (Gauthier, 1982) are considered, shown below in table 4.1.

M			M'		
Symbol	Value	Unit	Symbol	Value	Unit
λ	7.85×10^{10}	N/m^2	λ'	7.59×10^{10}	N/m^2
μ	6.46×10^{10}	N/m^2	μ'	1.89×10^{10}	N/m^2
ρ	2.2×10^3	Kg/m^3	ρ'	2.19×10^3	Kg/m^3
κ	0.0139×10^{10}	N/m^2	κ'	0.0149×10^{10}	N/m^2
γ	0.386×10^6	N	γ'	0.268×10^6	N
χ	0.00791	m^2	χ'	0.00753	m^2
ζ	1.64×10^{10}	N/m^2	ζ'	1.49×10^{10}	N/m^2
s	1.02×10^{10}	N/m^2	s'	1.06×10^{10}	N/m^2
a	0.676×10^{-9}	N/m^2	a'	0.667×10^{-9}	N/m^2
ξ	1.375×10^6	N/m^2	ξ'	1.475×10^6	N/m^2
d	2.13×10^6	N/m^2	d'	2.16×10^6	N/m^2
k_0	1.6×10^2	$Jm^{-1}s^{-1}K^{-1}$	k'_0	1.7×10^2	$Jm^{-1}s^{-1}K^{-1}$
τ	0.25	s	τ'	0.12	s

Table 4.1: Numerical values of the parameters with $\Theta_0 = 293 K$ and $\omega = 5 s^{-1}$.

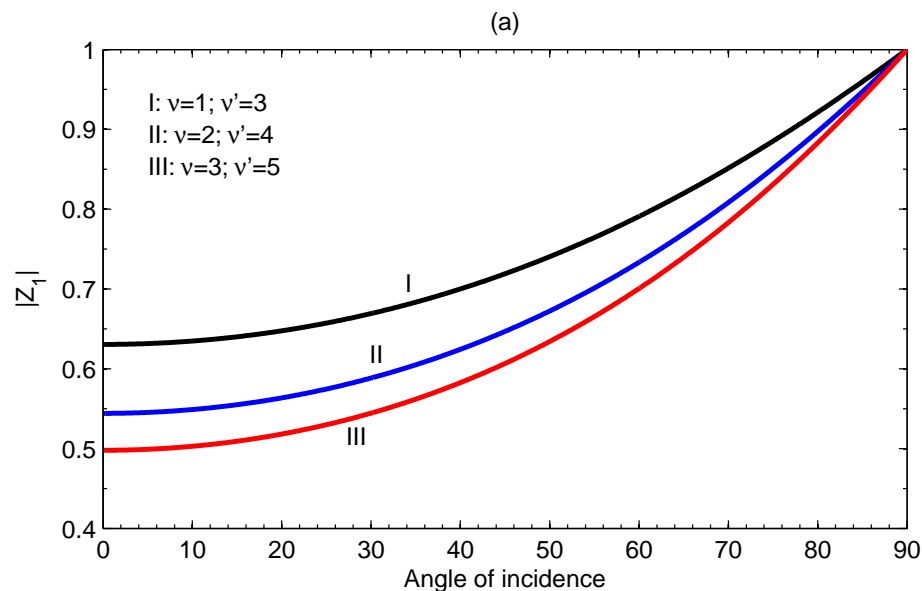
It may be noted that the following values of the micro-inertia and linear thermal expansion are used whenever not mentioned:

$$J = 0.0212 \times 10^{-4} m^2, J' = 0.0196 \times 10^{-4} m^2, \nu = 5 \times 10^{-4} K^{-1} \text{ and } \nu' = 3 \times 10^{-4} K^{-1}.$$

We developed a program on MATLAB for the computation of amplitude and energy ratios of reflected and refracted waves due to incident longitudinal and shear waves. Figures 4.2-4.9 shows the variation of modulus of amplitude and energy ratios due to incident longitudinal wave for different values of linear thermal expansions, while Figures 4.10-4.17 represent the variation of modulus of amplitude and energy ratios due to incident shear wave for different values of micro-inertia (J) and (J').

4.7.1 Effect of linear thermal expansion

The variation of amplitude ratios with angle of incidence (θ) for different values of ν and ν' are depicted in Figures 4.2-4.5 and those of energy ratios are represented by Figures 4.6-4.9. In all these figures, Curve I & IV : $(\nu, \nu') = (1, 3) \times 10^{-4} K^{-1}$; Curve II & V : $(\nu, \nu') = (2, 4) \times 10^{-4} K^{-1}$; Curve III & VI : $(\nu, \nu') = (3, 5) \times 10^{-4} K^{-1}$. In Figure 4.2(a), $|Z_1|$ increases with increase of θ from certain values at the normal incidence. The value of $|Z_1|$ decreases with the increase of linear thermal expansion. Figure 4.2(b) shows that the ratios $|Z_2|$ (Curves I, II, III) and $|Z_3|$ (Curves IV, V, VI) decrease with the increase θ to zero at the grazing angle of incidence. The value of $|Z_3|$ decreases with the increase of ν and ν' .



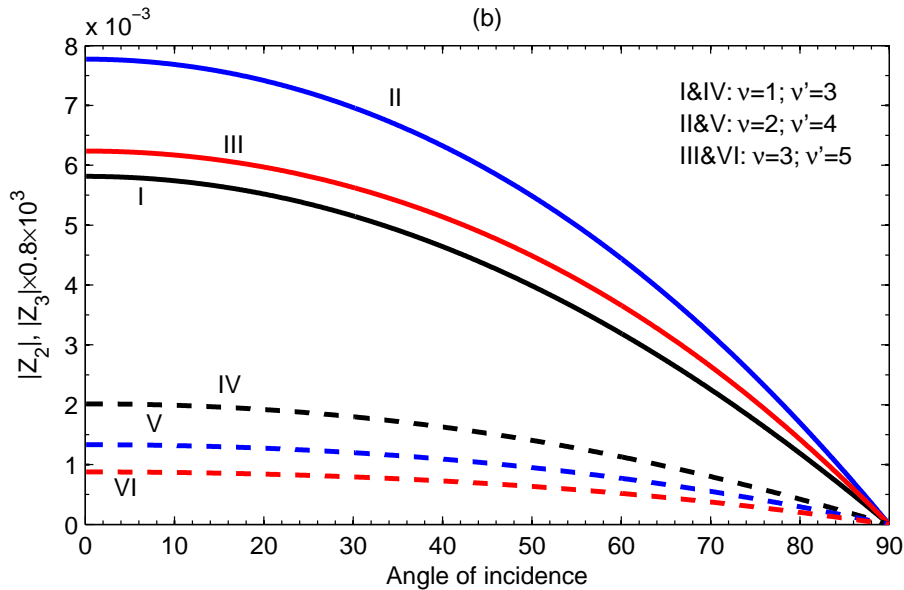


Figure 4.2: Variation of amplitude ratios, $|Z_1|$ in (a), $|Z_2|$ and $|Z_3|$ in (b) for incident longitudinal wave with θ at different values of ν and ν'

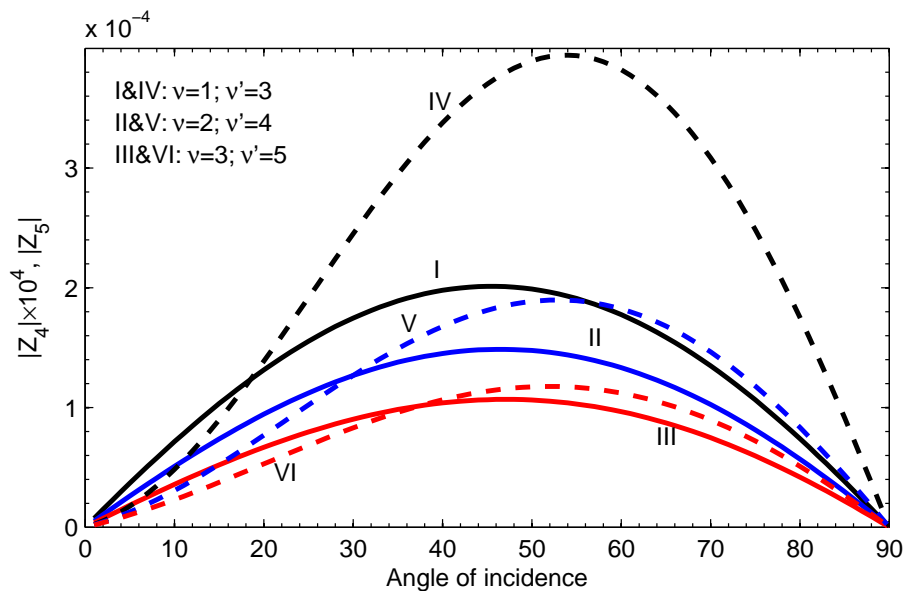


Figure 4.3: Variation of amplitude ratios, $|Z_4|$ and $|Z_5|$ for incident longitudinal wave with θ at different values of ν and ν'

In Figure 4.3, $|Z_4|$ (Curves I, II, III) and $|Z_5|$ (Curves IV, V, VI) are represented by parabolic curves between $\theta = 0^\circ$ and $\theta = 90^\circ$ with the maximum values at 45° and 54° respectively. It is observed that their values are decreased with the increase of ν and ν' . The variation of the

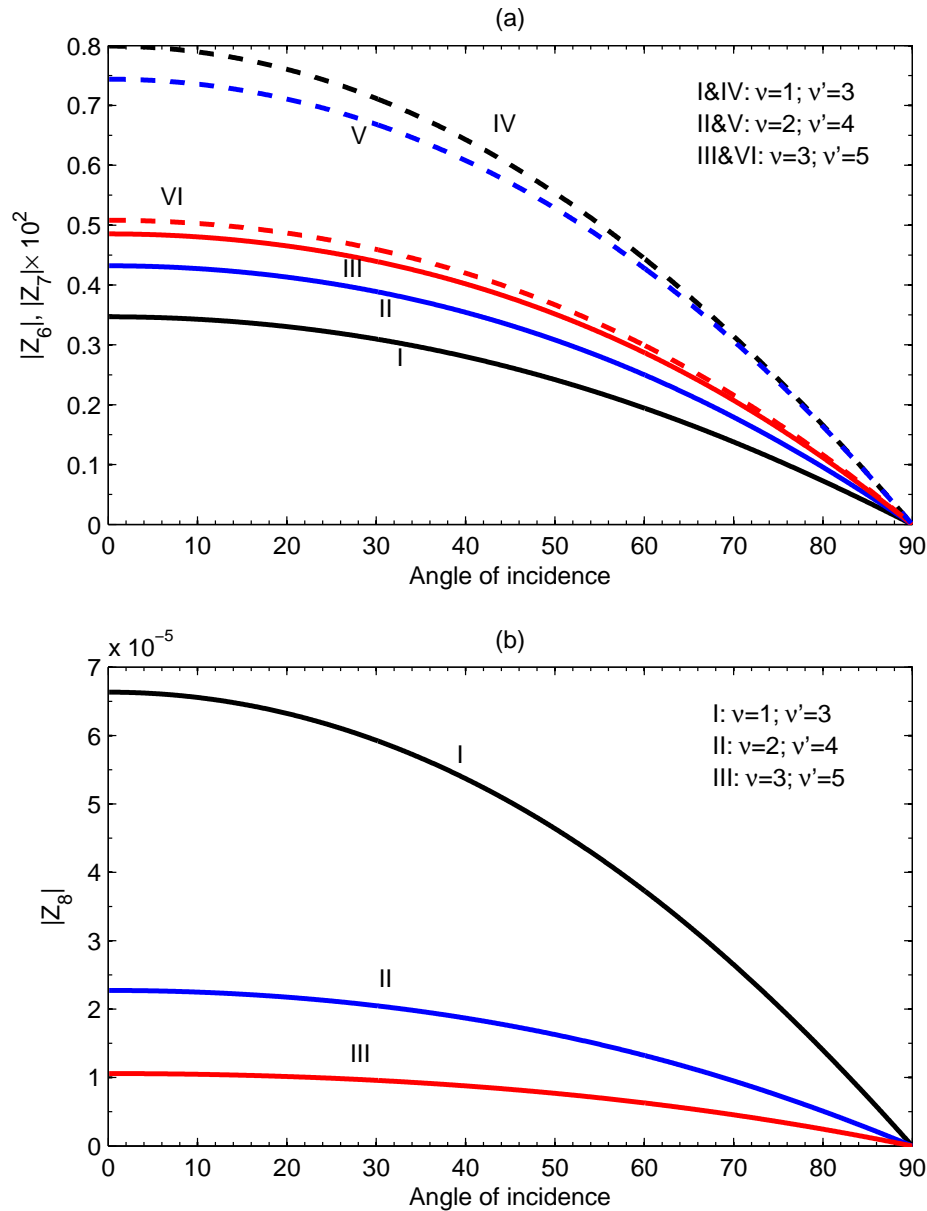


Figure 4.4: Variation of amplitude ratios, $|Z_6|$, $|Z_7|$ in (a) and $|Z_8|$ in (b) for incident longitudinal wave with θ at different values of ν and ν'

amplitude ratios, $|Z_6|$ (Curves I, II, III), $|Z_7|$ (Curves IV, V, VI) and $|Z_8|$ of the refracted coupled waves with θ have similar nature in Figures 4.4(a) and (b). They decrease with the increase of θ and obtain zero at the grazing angle of incidence. The value of $|Z_6|$ increases, while $|Z_7|$ and $|Z_8|$ decrease with the increase of linear thermal expansion. Similar nature of the ratios $|Z_9|$ (Curves I, II, III) and $|Z_{10}|$ (Curves IV, V, VI) with $|Z_4|$ is seen in Figure 4.5. In Figure 4.6(a), the energy ratio $|E_1|$ starts from certain value and increases with the

increase of angle of incidence with the maximum value at grazing angle of incidence. With the increase of ν and ν' , the value of $|E_1|$ decreases. Similar nature of $|E_2|$ (Curves I, II, III) and $|E_3|$ (Curves IV, V, VI) may be seen in Figure 4.6(b). They start from certain values, which decrease with the increase of θ and obtain the minimum value at the grazing angle of

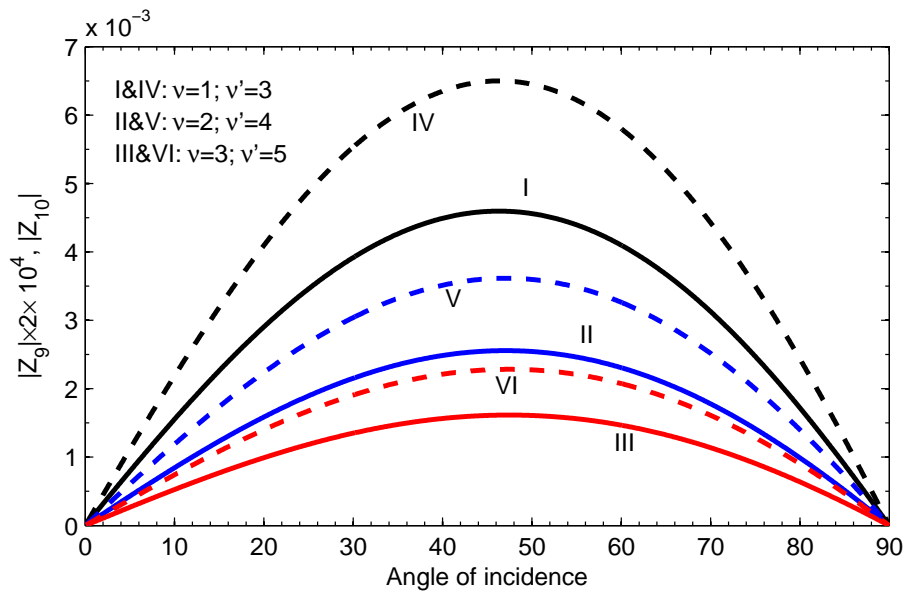
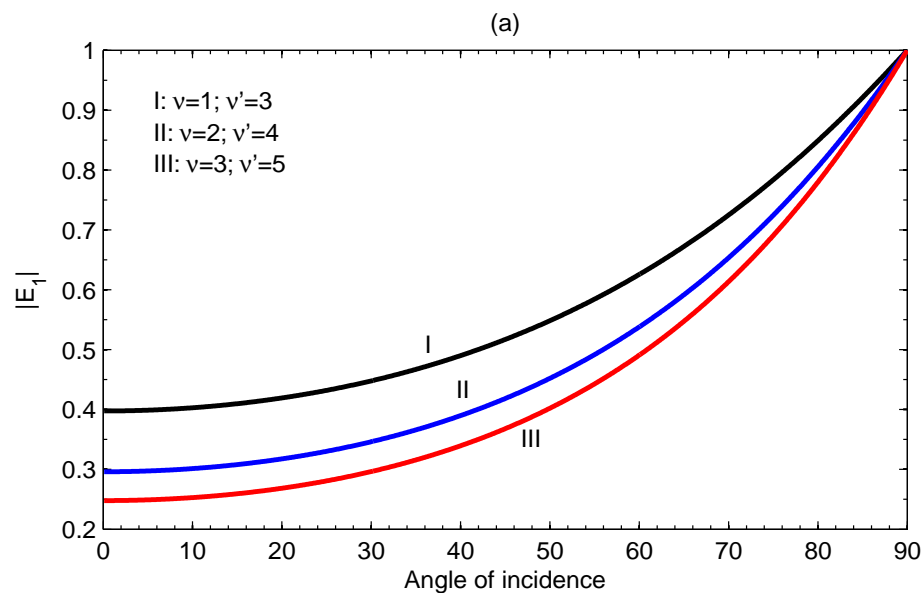


Figure 4.5: Variation of amplitude ratios, $|Z_9|$ and $|Z_{10}|$ for incident longitudinal wave with θ at different values of ν and ν'



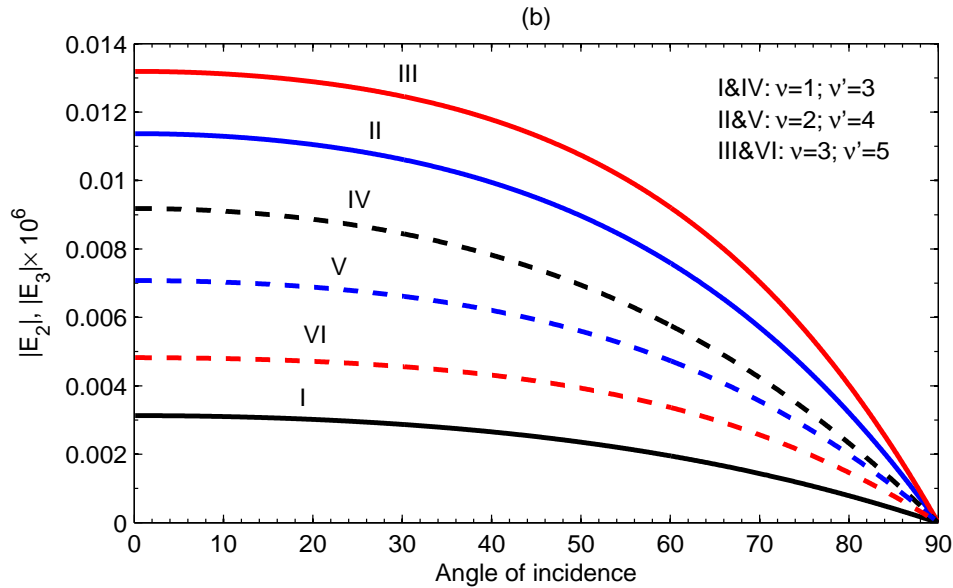


Figure 4.6: Variation of energy ratios, $|E_1|$ in (a), $|E_2|$ and $|E_3|$ in (b) for incident longitudinal wave with θ at different values of ν and ν'

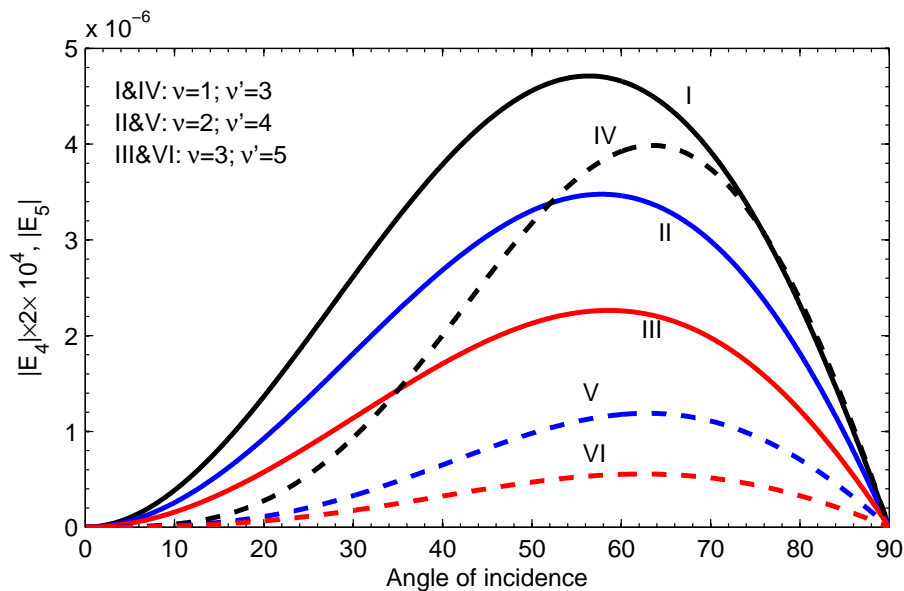


Figure 4.7: Variation of energy ratios, $|E_4|$ and $|E_5|$ for incident longitudinal wave with θ at different values of ν and ν'

incidence. The values of $|E_2|$ and $|E_3|$ increase and decrease respectively with the increase of ν and ν' . The energy ratios, $|E_4|$ (Curves I, II, III) and $|E_5|$ (Curves IV, V, VI) in Figure 4.7 increase initially and attain the maximum value at 55° and 63° respectively with the increase of θ . Then, they decrease again with the increase of θ . The values of $|E_4|$ and $|E_5|$

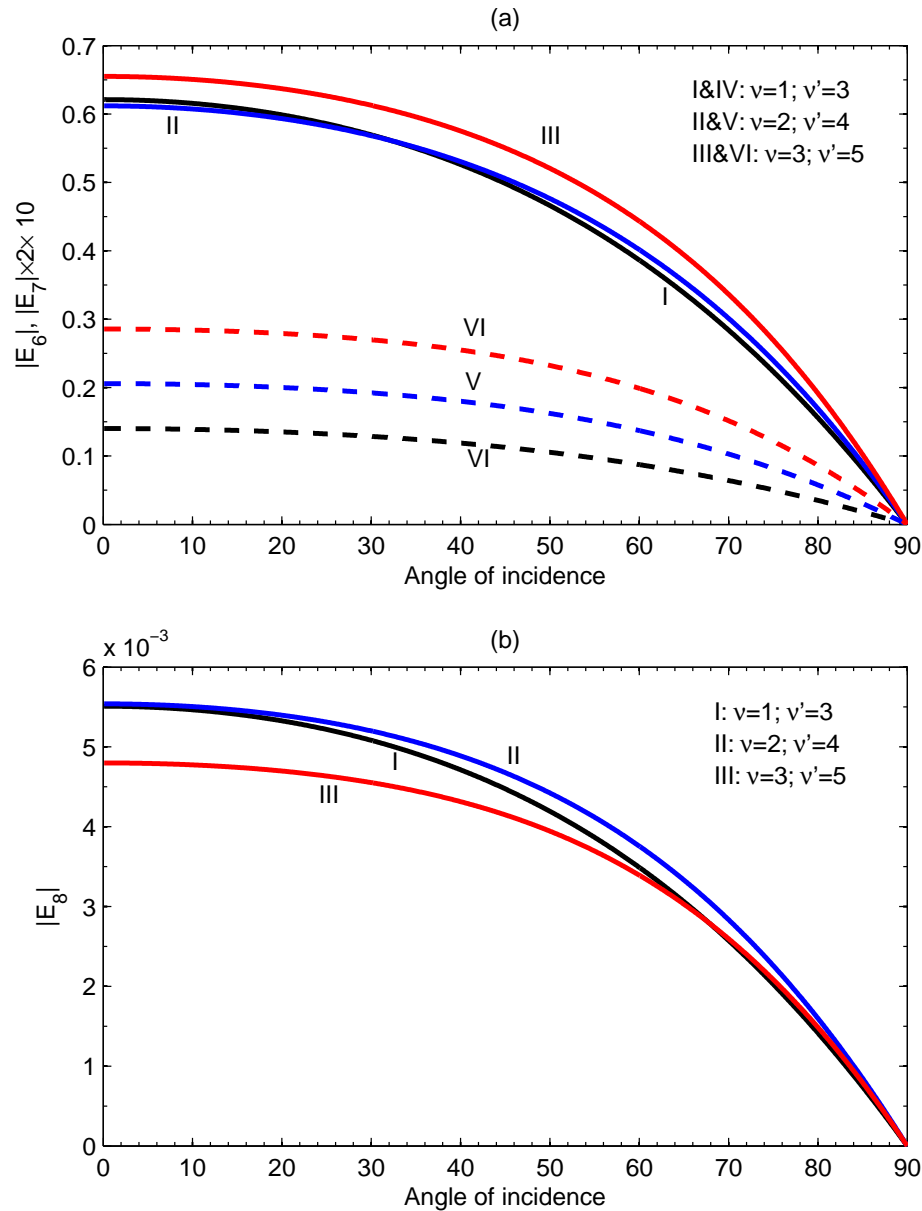


Figure 4.8: Variation of energy ratios, $|E_6|$, $|E_7|$ in (a) and $|E_8|$ in (b) for incident longitudinal wave with θ at different values of ν and ν'

decrease with the increase of ν and ν' . The values of $|E_6|$ (Curves I, II, III), $|E_7|$ (Curves IV, V, VI) and $|E_8|$ in Figures 4.8 (a) and (b), decrease with the increase of θ attaining the minimum value at grazing angle of incidence. The value of $|E_7|$ increase with the increase of ν and ν' . Similar nature of $|E_9|$ (Curves I, II, III) and $|E_{10}|$ (Curves IV, V, VI) with $|E_4|$ is seen in Figure 4.9. We have observed that the sum of energy ratios is close to unity. Thus,

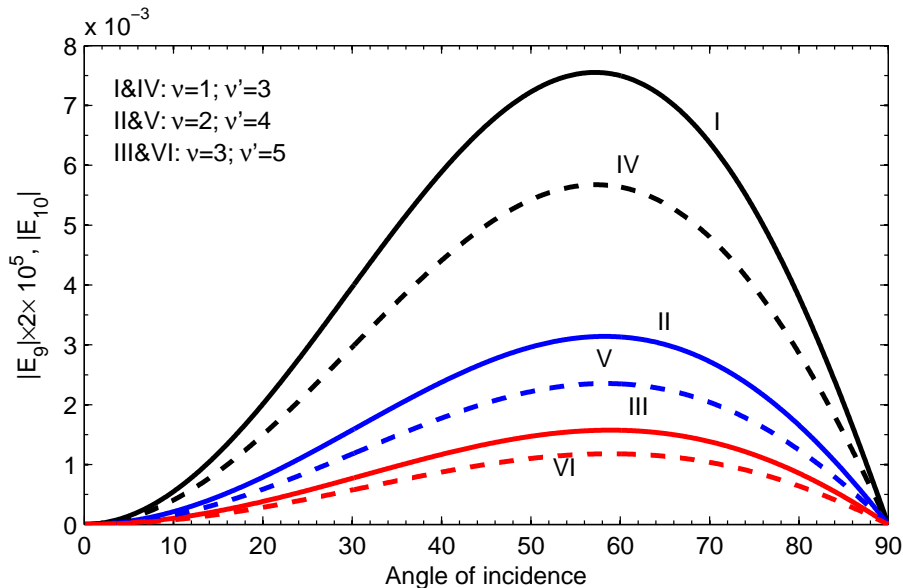


Figure 4.9: Variation of energy ratios, $|E_9|$ and $|E_{10}|$ for incident longitudinal wave with θ at different values of ν and ν'

we have seen that amplitude and energy ratios depend on angle of incidence (θ) and linear thermal expansion (ν and ν').

4.7.2 Effect of micro-inertia

We shall discuss the effects of micro-inertia on the amplitude and energy ratios of the reflected and refracted waves due to incident shear wave. In all figures, Curve I & IV $:(J, J') = (0.020, 0.015) \times 10^{-4} m^2$; Curve II & V $:(J, J') = (0.025, 0.020) \times 10^{-4} m^2$; Curve III & VI $:(J, J') = (0.030, 0.025) \times 10^{-4} m^2$. In Figure 4.10 (a), $|Z_1|$ increases initially upto certain value and then it decreases sharply with the increase of θ . The value of $|Z_1|$ increases again to the maximum value and thereafter, it decreases to zero with the increase of θ . We have observed similar nature $|Z_2|$ (Curves I, II, III) and $|Z_3|$ (Curves IV, V, VI) in Figure 4.10 (b). They increase initially, after that, decrease sharply and then increase again to the maximum value, which are followed by decreasing to zero with the increase of θ . The values of $|Z_2|$ and $|Z_3|$ increases with the increase of micro-inertia. Critical angles are observed for $|Z_1|$, $|Z_2|$ and $|Z_3|$. The value of $|Z_4|$ (Curves I, II, III), in Figure 4.11, starts slow decreases from a

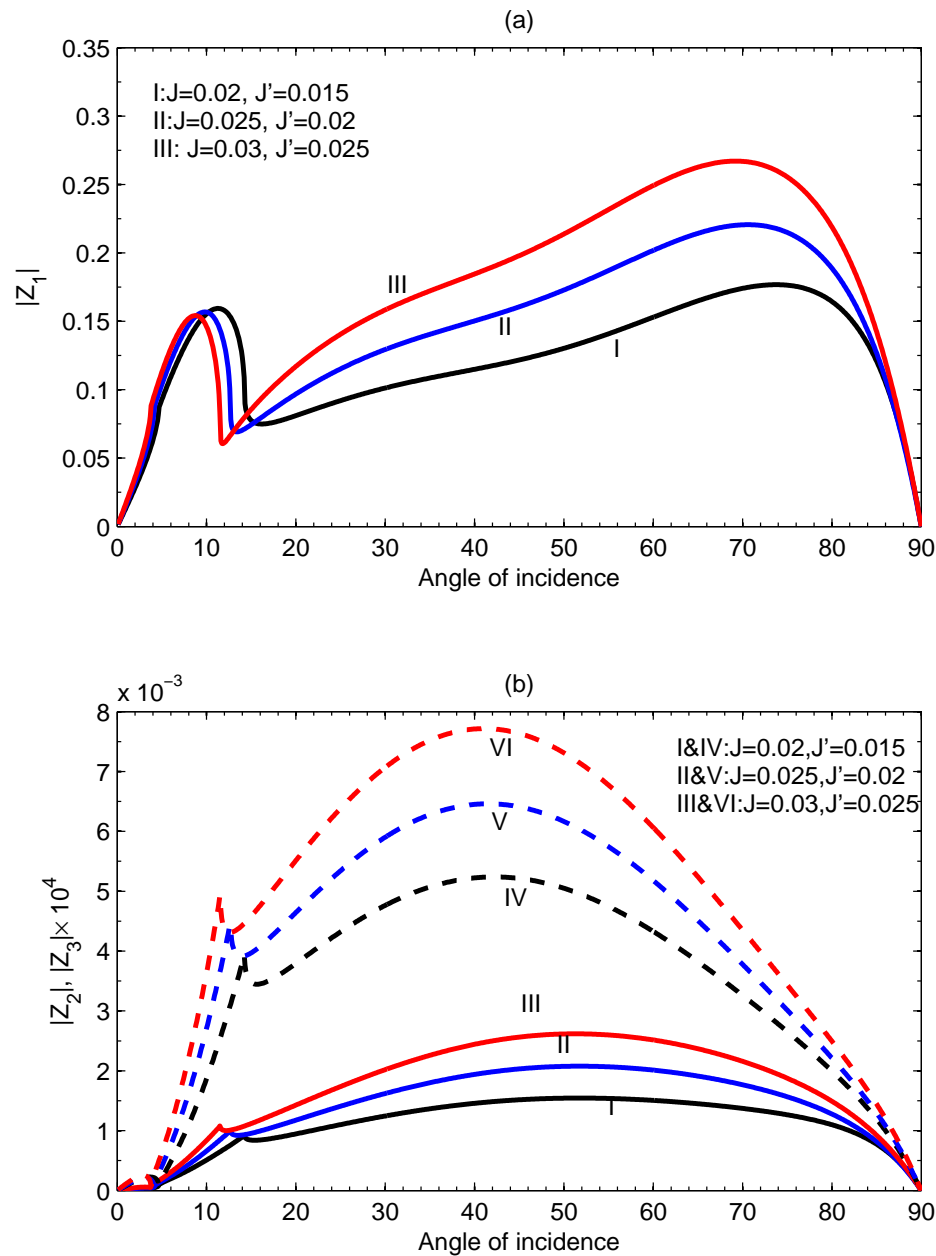


Figure 4.10: Variation of amplitude ratios, $|Z_1|$ in (a), $|Z_2|$ and $|Z_3|$ in (b) for incident shear wave with θ at different values of J and J'

certain value to zero and then it increases with the increase of θ attaining the maximum value at the grazing angle of incidence. In the same figure, $|Z_5|$ (Curves IV, V, VI) decreases from certain value to the minimum value at $\theta = 54^\circ$ for Curve IV, $\theta = 49^\circ$ for Curve V and $\theta = 45^\circ$ for Curve VI, thereafter, it increases upto certain value and then decreases to zero

with the increase of θ . Figures 4.12(a, b) show the similar natures of $|Z_6|$, $|Z_7|$ (Curves I, II, III) and $|Z_8|$ (Curves IV, V, VI). They increase initially upto certain value, followed by sharp decreasing nature and then, again they increase upto certain extend and thereafter, decrease to zero with the increase of θ . They increase with the increase of micro-inertia.

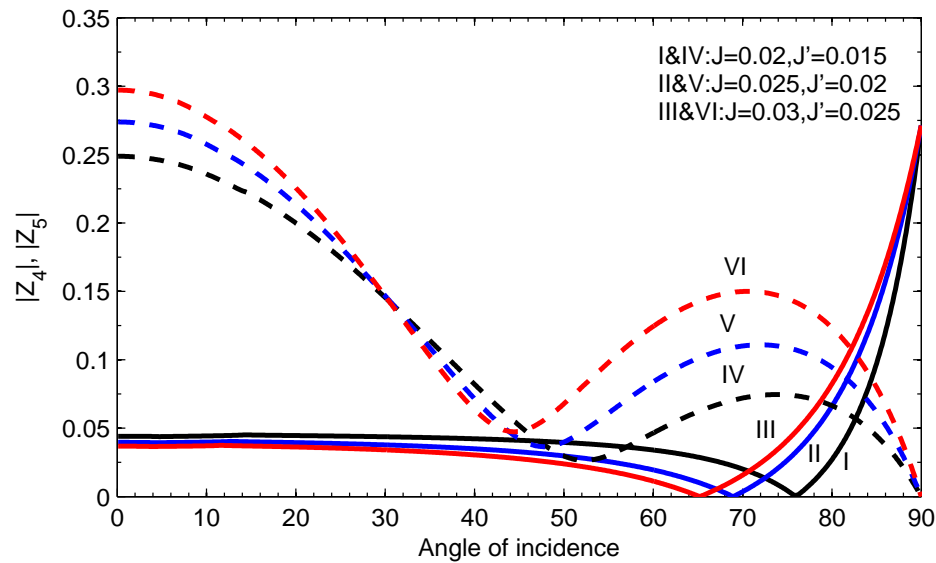
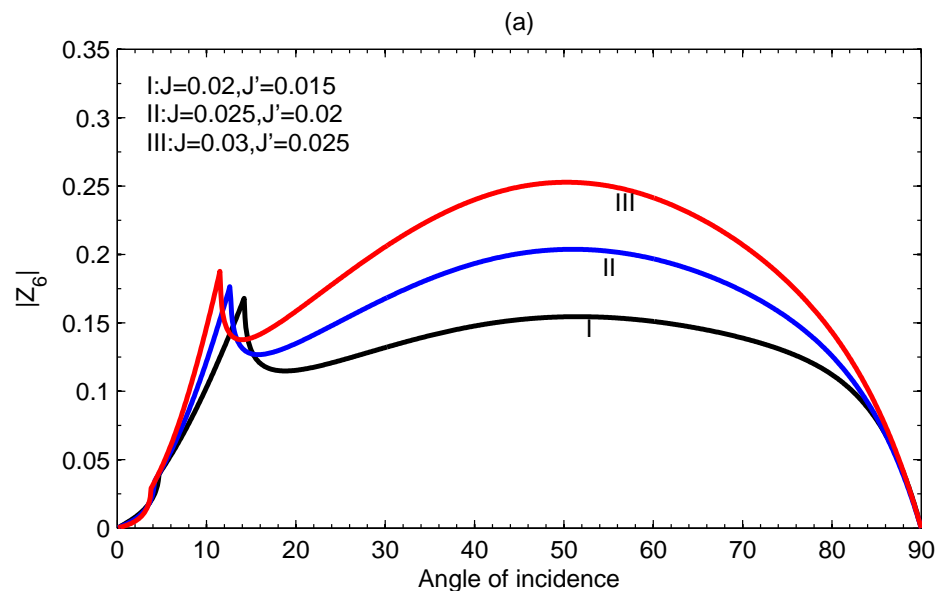


Figure 4.11: Variation of amplitude ratios, $|Z_4|$ and $|Z_5|$ for incident shear wave with θ at different values of J and J'



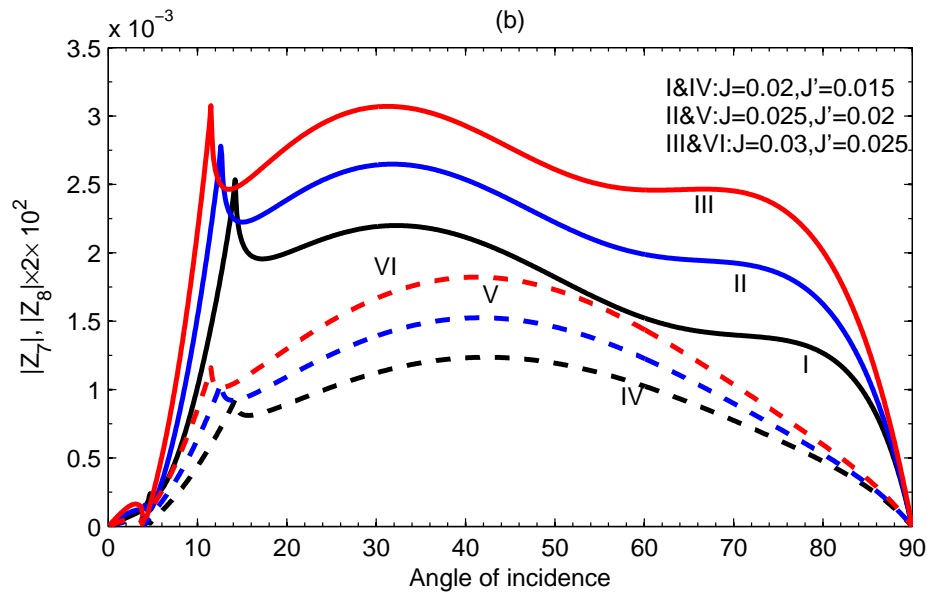


Figure 4.12: Variation of amplitude ratios, $|Z_6|$ in (a), $|Z_7|$ and $|Z_8|$ in (b) for incident shear wave with θ at different values of J and J'

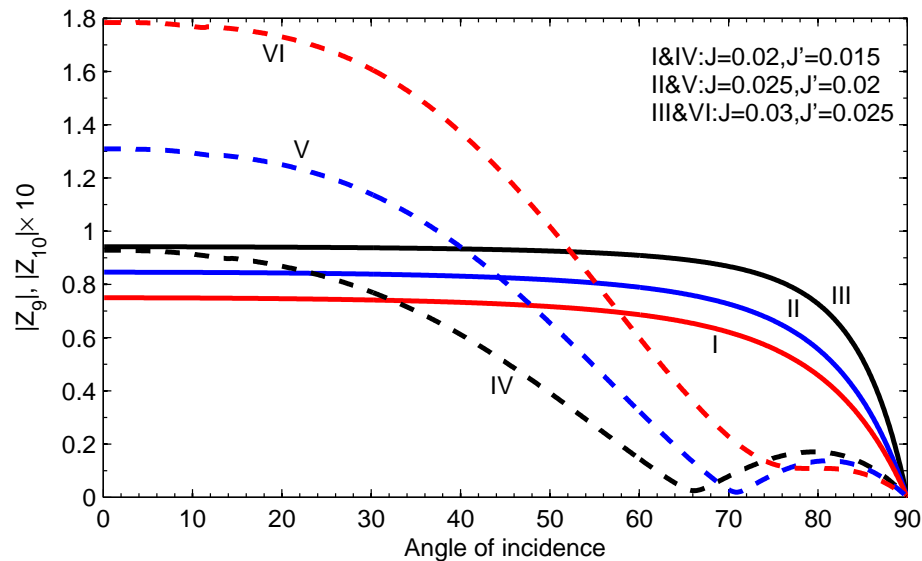


Figure 4.13: Variation of amplitude ratios, $|Z_9|$ and $|Z_{10}|$ for incident shear wave with θ at different values of J and J'

Here, also critical angles for $|Z_6|$, $|Z_7|$ and $|Z_8|$ are observed. The minimum effect of micro-inertia is observed near normal and grazing angle of incidence. In Figure 4.13, $|Z_9|$ (Curves I, II, III) starts from certain value and decreases to zero with the increase of θ . The minimum effect of J and J' is observed near the grazing angle of incidence and value of $|Z_9|$ decreases

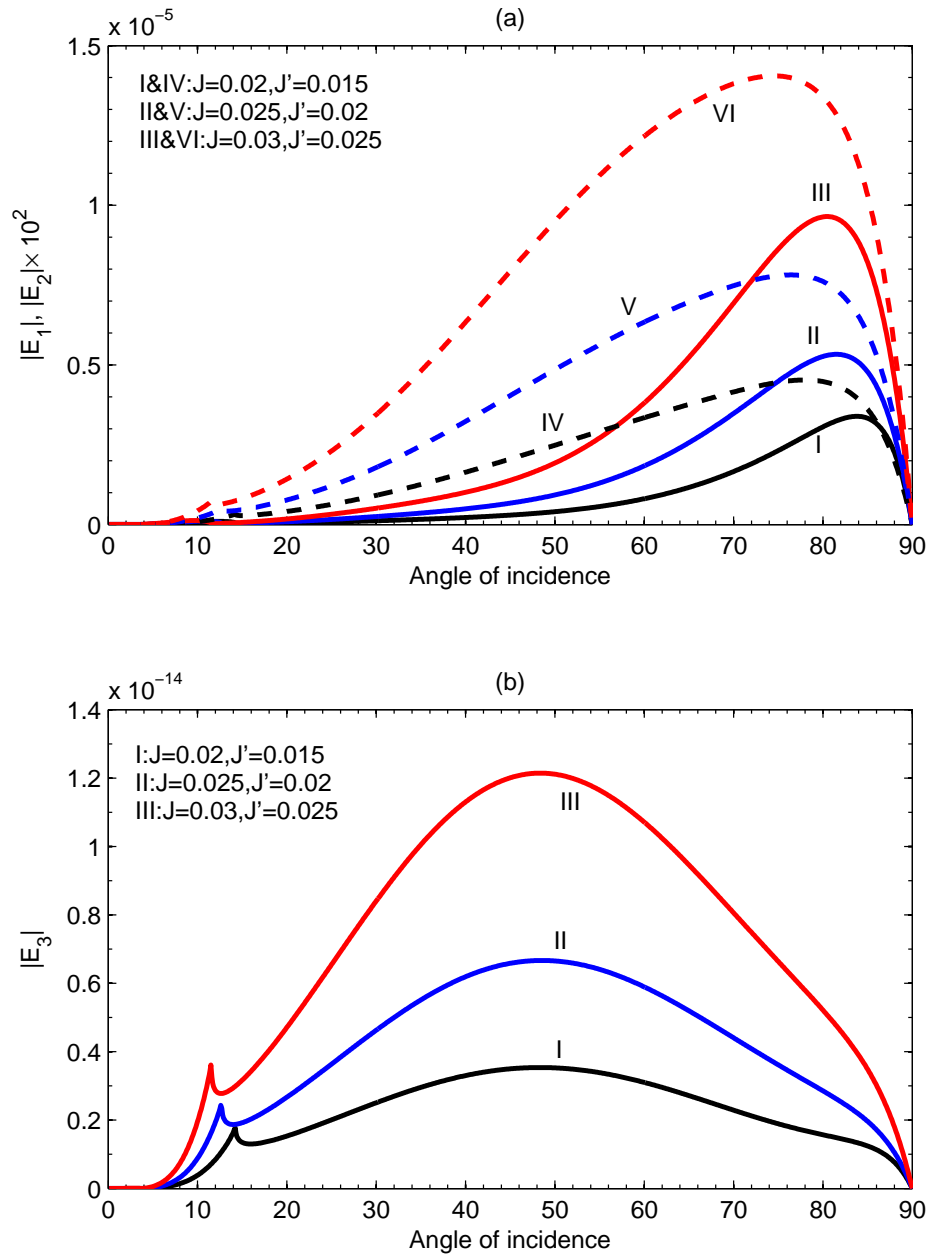


Figure 4.14: Variation of energy ratios, $|E_1|$, $|E_2|$ in (a) and $|E_3|$ in (b) for incident shear wave with θ at different values of J and J'

with the increase of micro-inertia. In the same figure, we have observed the decreasing nature of $|Z_{10}|$ (Curves IV, V, VI) upto $\theta = 63^\circ$ for Curve IV, $\theta = 69^\circ$ for Curve V and $\theta = 78^\circ$ for Curve VI. The maximum effect of micro-inertia is observed near the normal incidence. In Figures 4.14(a), $|E_1|$ (Curves I, II, III) and $|E_2|$ (Curves IV, V, VI) has similar nature.

They increase to the maximum value and decrease with the increase of θ . The effect of micro-inertia is minimum near the normal and grazing angle of incidence. The value of $|E_3|$ in Figure 4.14(b) increases initially upto certain value, which followed by sharp decrease and then, it increases to the maximum value, thereafter, it decreases again with the increase of

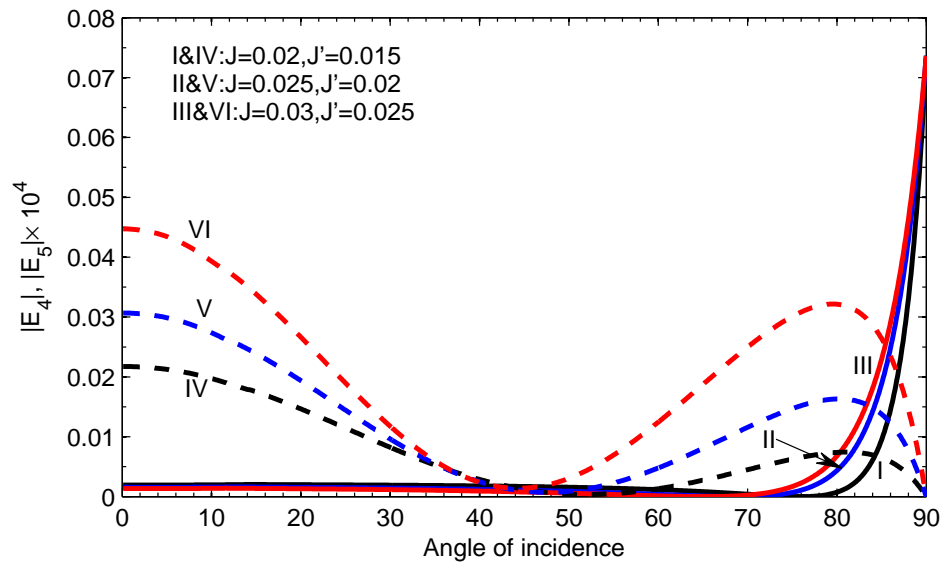
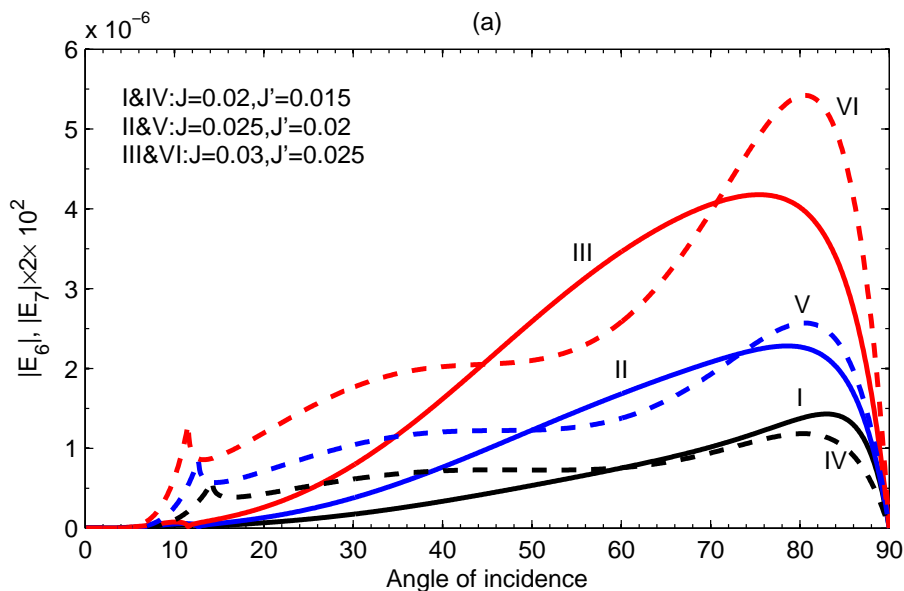


Figure 4.15: Variation of energy ratios, $|E_4|$ and $|E_5|$ for incident shear wave with θ at different values of J and J'



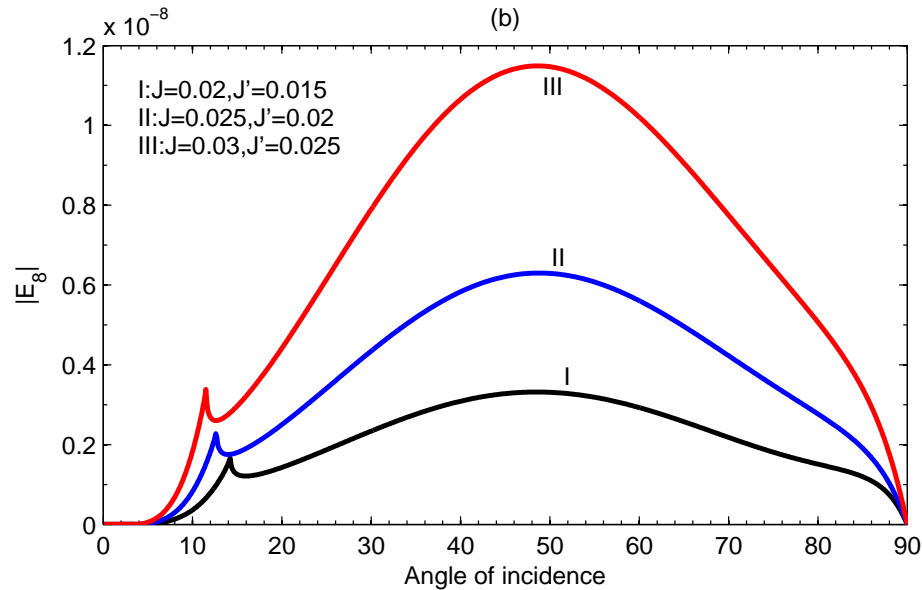


Figure 4.16: Variation of energy ratios, $|E_6|$, $|E_7|$ in (a) and $|E_8|$ in (b) for incident shear wave with θ at different values of J and J'

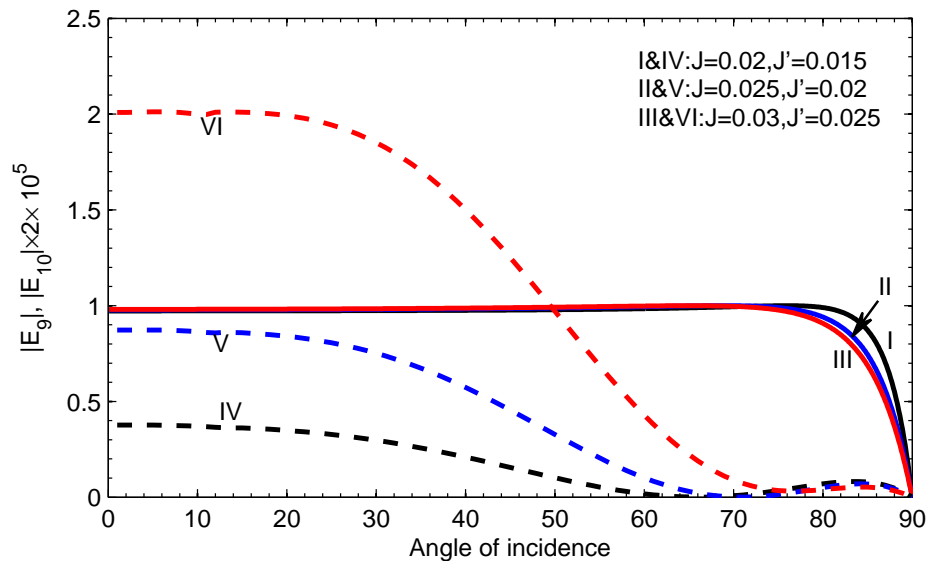


Figure 4.17: Variation of energy ratios $|E_9|$ and $|E_{10}|$ for incident shear wave with θ at different values of J and J'

θ . The value of $|E_4|$ (Curves I, II, III), in Figure 4.15, decreases initially and then increases with the increase of θ . In the same figure, $|E_5|$ (Curves IV, V, VI) starts from certain value and decreases upto $\theta = 52^\circ$ for Curve IV, $\theta = 48^\circ$ for Curve V and $\theta = 44^\circ$ for Curve VI with the increase of θ , which followed by a parabolic region. The minimum effect of micro-inertia

is found at $\theta = 35^0$ and $\theta = 90^0$. In Figure 4.16, it is noted that the energy ratio, $|E_6|$ (Curves I, II, III) is similar with that of $|E_2|$, while $|E_7|$ (Curves IV, V, VI) and $|E_8|$ are similar with that of $|E_3|$. The values of $|E_6|$, $|E_7|$ and $|E_8|$ increase with the increase of J and J' . In Figure 4.17, $|E_9|$ (Curves I, II, III) decreases to zero with the increase of θ , while $|E_{10}|$ (Curves IV, V, VI) decreases upto certain value of θ and then increases which is followed by decreasing again with the increase of θ . Here, also we see critical angles for $|E_1|$, $|E_2|$, $|E_3|$ of the reflected coupled longitudinal waves and $|E_6|$, $|E_7|$, $|E_8|$ of the refracted coupled longitudinal waves. The sum of the energy ratios of reflected and refracted waves is closed to unity.

4.8 Conclusions

The reflection and refraction of elastic waves from a plane interface between two dissimilar half-spaces of micropolar thermoelastic materials with voids has been analysed. The amplitude and energy ratios of the reflected and refracted waves due to incident longitudinal and shear waves are obtained. These ratios are the functions of angle of incidence, thermal, micropolar and voids parameters. These ratios are computed numerically for different values of the linear thermal expansion and micro-inertia. The effect of linear thermal expansion and micro-inertia on the amplitude and energy ratios are depicted graphically. We may summarize with the following concluding remarks:

- (i) The amplitude ratios, $|Z_1|$, $|Z_3|$, $|Z_4|$, $|Z_5|$, $|Z_7|$, $|Z_8|$, $|Z_9|$ and $|Z_{10}|$ of the reflected and refracted waves due to incident longitudinal wave decrease with the increase of linear thermal expansion, while $|Z_6|$ increases with the increase of ν and ν' .
- (ii) The energy ratios, $|E_1|$, $|E_3|$, $|E_4|$, $|E_5|$, $|E_9|$ and $|E_{10}|$ of the reflected and refracted waves due to incident longitudinal wave decrease with the increase of ν and ν' , while $|E_7|$ and $|E_2|$ increase with the increase of linear thermal expansion.
- (iii) The amplitude ratios, $|Z_2|$, $|Z_3|$, $|Z_6|$, $|Z_7|$ and $|Z_8|$ of the reflected and refracted waves due to incident shear wave increase with the increase of micro-inertia, while $|Z_9|$ decreases

with the increase of J and J' .

(iv) The energy ratios, $|E_1|$, $|E_2|$, $|E_3|$, $|E_6|$, $|E_7|$ and $|E_8|$ of the reflected and refracted waves due to incident shear wave increase with the increase of J and J' .

(v) The amplitude and energy ratios of the reflected and refracted coupled longitudinal waves due to incident shear wave are found to have critical angles.

(vi) The sum of energy ratios of the reflected and refracted waves is close to unity.

Chapter 5

Effect of micro-inertia on reflection/refraction of plane waves at the orthotropic and thermoelastic micropolar materials with voids⁴

5.1 Introduction

The problems of wave propagation in orthotropic micropolar materials and thermoelastic micropolar materials with voids are very important for the possibility of their extensive applications in various branches of sciences, particularly in optics, acoustics, geophysics and Seismology. Kumar and Choudhary (2002a, b) obtained the normal displacement, normal force stress and tangential couple stress in the physical domain with the help of integral transforms in orthotropic micropolar materials. Singh (2007c) studied two-dimensional problem of wave propagation in the orthotropic micropolar elastic medium and discussed the effects of anisotropy upon the velocities and reflection coefficients of the three coupled reflected waves.

In this chapter, the problem of the effect of micro-inertia on the reflection and refraction of plane waves at the orthotropic and thermoelastic micropolar materials with voids has been

⁴*Global Journal of Pure and Applied Mathematics*, 13(7), 2907-2921(2017)

investigated. We have obtained the amplitude and energy ratios of the reflected and refracted waves using appropriate boundary conditions. These ratios are numerically computed for a particular model and discussed the effect of micro-inertia.

5.2 Basic Equations

Let us consider the cartesian co-ordinate system with x -axis lying horizontally and y -axis vertically with positive direction pointing downward. We assume that an orthotropic micropolar elastic half-space, $M = \{(x, y); x \in R, y \in (0, \infty)\}$ and another half-space of micropolar thermoelastic materials with voids, $\bar{M} = \{(x, y); x \in R, y \in (-\infty, 0)\}$ are welded contact and are separated by $y = 0$.

Orthotropic micropolar elastic half-space, M :

The equations of motion in xy -plane for homogeneous orthotropic micropolar solid without body couples and forces are written as (Singh, 2007b)

$$A_{11}u_{1,11} + (A_{12} + A_{78})u_{2,12} + A_{88}u_{1,22} - K_1\phi_{3,2} = \rho\ddot{u}_1, \quad (5.1)$$

$$(A_{12} + A_{78})u_{1,12} + A_{77}u_{2,11} + A_{22}u_{2,22} - K_2\phi_{3,1} = \rho\ddot{u}_2, \quad (5.2)$$

$$B_{66}\phi_{3,11} + B_{44}\phi_{3,22} - K_3\phi_3 + K_1u_{1,2} + K_2u_{2,1} = \rho f\ddot{\phi}_3, \quad (5.3)$$

where $A_{11}, A_{12}, A_{22}, A_{77}, A_{78}, A_{88}, A_{44}, B_{44}$ and B_{66} are characteristic constants of the material, f is micro-inertia, ρ is density, $K_1 = A_{78} - A_{88}$, $K_2 = A_{77} - A_{78}$ and $K_3 = K_2 - K_1$. Here, the displacement vector and micro-rotation vector are respectively represented by $\mathbf{u} = (u_1, u_2, 0)$ and $\boldsymbol{\phi} = (0, 0, \phi_3)$. The subscripts preceded by coma indicate coordinate derivatives and superposed dots mean time derivatives.

Half-space of micropolar thermoelastic materials with voids, \bar{M} :

The equation of motions of homogeneous and isotropic micropolar thermoelastic materials with voids in the absence of body forces and body couples are (1.44)-(1.47)

$$(\lambda + 2\mu + \kappa)\nabla^2 u' + s\psi - m\Theta = \rho\ddot{u}', \quad (5.4)$$

$$s\nabla^2 u' - (a\nabla^2 - \zeta)\psi + \xi\Theta = -\rho_2\ddot{\psi}, \quad (5.5)$$

$$k_0\nabla^2\Theta - \Theta_0(1 + \tau\frac{\partial}{\partial t})(d\dot{\Theta} + m\nabla^2\dot{u}' - \xi\dot{\psi}) = 0, \quad (5.6)$$

$$(\alpha + \beta + \gamma)\nabla^2\phi' - 2\kappa\phi' = \rho_1\ddot{\phi}', \quad (5.7)$$

$$(\mu + \kappa)\nabla^2\mathbf{u}'' + \kappa\nabla \times \boldsymbol{\phi}'' = \rho\ddot{\mathbf{u}}'', \quad (5.8)$$

$$(\gamma\nabla^2 - 2\kappa)\boldsymbol{\phi}'' + \kappa\nabla \times \mathbf{u}'' = \rho_1\ddot{\boldsymbol{\phi}}'', \quad (5.9)$$

where λ, μ are lame's parameters, $\alpha, \beta, \gamma, \kappa$ are micropolar parameters, s, a, ζ, ξ are voids parameters and m, k_0, d, τ are thermal parameters, ρ is mass density, $\rho_1(= \rho J)$ and $\rho_2(= \rho \chi)$ are inertial coefficients, J, χ are micro-inertia and equilibrated inertia respectively. Here, ψ is the void volume fraction and Θ is temperature measured from a reference temperature Θ_0 . The displacement ($\bar{\mathbf{u}}$) and micro-rotation ($\bar{\boldsymbol{\phi}}$) vectors are represented as

$$\bar{\mathbf{u}} = \nabla u' + \nabla \times \mathbf{u}'', \quad \bar{\boldsymbol{\phi}} = \nabla \phi' + \nabla \times \boldsymbol{\phi}''. \quad (5.10)$$

Equations (5.2)-(5.2) are couple in u', ψ and Θ , while Equations (5.2) and (5.2) are also couple in \mathbf{u}'' and $\boldsymbol{\phi}''$. Equation (5.2) is uncouple longitudinal waves or micropolar waves (Parfitt and Eringen, 1969).

5.3 Wave propagation

A train of longitudinal wave with amplitude, A_0 is incident at the plane interface making an angle θ_0 with the normal. This wave gives three reflected coupled waves in the half-space, M and five refracted waves (three coupled longitudinal waves and two coupled shear waves)

in half-space, \bar{M} . The complete geometry of the problem is shown in Figure 5.1.

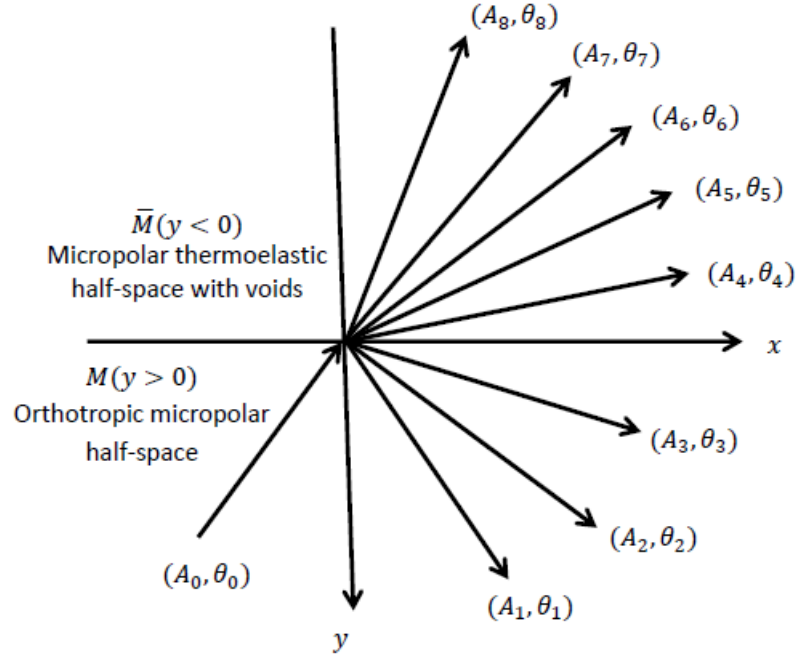


Figure 5.1: Geometry of the problem

The structures of the various reflected and refracted waves are given below.

(For the reflected waves in the half-space, M)

$$\{u_1, u_2, \phi_3\} = \sum_{i=0}^3 \{1, \eta_i, ik_i\pi_i\} k_i A_i \exp(Q_i), \quad (5.11)$$

(For the refracted waves in the half-space, \bar{M})

$$\{u', \psi, \Theta\} = \sum_{i=4}^6 \{1, \eta_i, \pi_i\} A_i \exp(Q_i), \quad (5.12)$$

$$\{u'', \Phi_3\} = \sum_{i=7}^8 \{1, \eta_i\} A_i \exp(Q_i), \quad (5.13)$$

where ϕ_3 is the z -component of ϕ , u'' and Φ_3 are the z -component of \mathbf{u}'' and ϕ'' respectively, $Q_i = ik_i(xp_1^{(i)} + yp_2^{(i)} - v_i t)$, $\mathbf{p}^{(i)} = (p_1^{(i)}, p_2^{(i)}, 0)$ is propagation vector, v_i is the phase velocity

and k_i is the wavenumber and A_i is the amplitude constant at angle θ_i with wavenumber k_i .

The coupling constants, η_i and π_i are defined as

$$\eta_i = \begin{cases} \{a_5^2(a_1^2 - v_i^2) - a_2^2 a_3^2\} / \{a_3^2(a_4^2 - v_i^2) - a_2^2 a_5^2\}, & (i = 0, 1, 2, 3) \\ \{c_4^2 c_k^2 k_i^4 - (c_4^2 c_d^2 - c_7^2 c_m^2) k_i^2\} / \{c_5^2 c_k^2 k_i^4 - (\omega^2 c_k^2 - c_6^2 c_k^2 + c_5^2 c_d^2) k_i^2 - \\ c_7^2 c_\xi^2 - c_6^2 c_d^2 + \omega^2 c_d^2\}, & (i = 4, 5, 6) \\ c_1^2 / \{c_2^2 + c_3^2 / k_i^2 - v_i^2\}, & (i = 7, 8) \end{cases}$$

$$\pi_i = \begin{cases} \{a_7^2 \eta_i + a_6^2\} / \{a_9^2 / v_i^2 + a_8^2 - 1\}, & (i = 0, 1, 2, 3) \\ \{c_m^2 c_5^2 k_i^4 + (c_m^2 c_6^2 + c_4^2 c_\xi^2 - c_m^2 \omega^2) k_i^2\} / \{-c_5^2 c_k^2 k_i^4 + (\omega^2 c_k^2 - c_6^2 c_k^2 + \\ c_5^2 c_d^2) k_i^2 + c_7^2 c_\xi^2 + c_6^2 c_d^2 - \omega^2 c_d^2\}, & (i = 6, 7, 8). \end{cases}$$

where

$$\begin{aligned} a_1^2 &= (A_{11} p_1^2 + A_{88} p_2^2) / \varrho, & a_2^2 &= p_1 p_2 (A_{12} + A_{78}) / \varrho, & a_3^2 &= K_1 p_2 / \varrho, & a_4^2 &= (A_{77} p_1^2 + A_{22} p_2^2) / \varrho, \\ a_5^2 &= K_2 p_1 / \varrho, & a_6^2 &= K_1 p_2 / \varrho j \omega^2, & a_7^2 &= K_2 p_1 / \varrho j \omega^2, & a_8^2 &= K_3 / \varrho j \omega^2, & a_9^2 &= (B_{66} p_1^2 + B_{44} p_2^2) / \varrho j \\ c_1^2 &= (\alpha + \beta) / \rho_1, & c_2^2 &= \gamma / \rho_1, & c_3^2 &= 2\kappa / \rho_1, & c_4^2 &= s / \rho_2, & c_5^2 &= a / \rho_2, & c_6^2 &= \zeta / \rho_2, & c_7^2 &= \xi / \rho_2, \\ c_m^2 &= m / \rho_1, & c_\xi^2 &= \xi / \rho_1, & c_d^2 &= d / \rho_1, & c_k^2 &= k_0 / \Theta_0 \rho_1 \omega (\omega \tau + \iota). \end{aligned}$$

The Snell's law in this problem may be written as

$$p_0^{(0)} k_0 = p_1^{(i)} k_i, \quad (i = 1, 2, \dots, 8). \quad (5.14)$$

It is also noted that θ_i ($i = 1, 2, 3$) correspond to angles of reflected waves in the half-space, M and θ_i ($i = 4, 5, 6, 7, 8$) correspond to angles of refracted waves in the half-space, \bar{M} .

5.4 Boundary conditions

The boundary conditions are the continuity of tensors (force stresses and couple stresses) at $y = 0$. Mathematically, these conditions at $y = 0$ may be written as

$$t_{22} = \bar{T}_{22}, \quad t_{21} = \bar{T}_{21}, \quad m_{23} = \bar{M}_{23}. \quad (5.15)$$

The displacement components, micro-rotation vectors, temperature gradient and the equilibrated stress vector are also continuous at $y = 0$ as

$$u_1 = \bar{u}_1, \quad u_2 = \bar{u}_2, \quad \phi_3 = \bar{\Phi}_3, \quad \Theta_{,2} = 0, \quad h_2 = 0. \quad (5.16)$$

With the help of Equations (1.33) and (1.37), Equation (5.15) may be written to

$$A_{12} \frac{\partial u_1}{\partial x} + A_{22} \frac{\partial u_2}{\partial y} = \lambda \frac{\partial^2 u'}{\partial x^2} + (\lambda + 2\mu + \kappa) \frac{\partial^2 u'}{\partial y^2} + (2\mu + \kappa) \frac{\partial^2 u''}{\partial x \partial y} + s\psi - m\Theta, \quad (5.17)$$

$$A_{78} \frac{\partial u_2}{\partial x} + A_{88} \frac{\partial u_1}{\partial y} + (A_{88} - A_{78})\phi_3 = (2\mu + \kappa) \frac{\partial^2 u'}{\partial x \partial y} - (\mu + \kappa) \frac{\partial^2 u''}{\partial y^2} + \mu \frac{\partial^2 u''}{\partial x^2} - \kappa \Phi_3, \quad (5.18)$$

$$B_{44} \frac{\partial \phi_3}{\partial y} = \gamma \frac{\partial \Phi_3}{\partial y}. \quad (5.19)$$

Using Equations (5.11)-(5.14) into the boundary conditions (5.16)-(5.19), we get a system of eight equations as

$$\sum_{j=1}^8 a_{ij} Z_j = b_i, \quad (i = 1, 2, \dots, 8). \quad (5.20)$$

The non-zero, a_{ij} are given as

$$a_{ij} = \begin{cases} (A_{12} p_1^{(j)} + A_{22} p_2^{(j)}) k_j^2, & (j = 0, 1, 2, 3) \\ \{\lambda + p_2^{(j)2} (2\mu + \kappa) - (s\eta_j - m\pi_j)/k_j^2\} k_j^2, & (i = 4, 5, 6) \\ (2\mu + \kappa) p_1^{(j)} p_2^{(j)} k_j^2, & (i = 7, 8) \end{cases}$$

$$\begin{aligned}
a_{2j} &= \begin{cases} (A_{78}\eta_j p_1^{(j)} + A_{88}p_2^{(j)} - K_1\pi_j)vk_j^2, & (j = 0, 1, 2, 3) \\ (2\mu + \kappa)p_1^{(j)}p_2^{(j)}k_j^2, & (i = 4, 5, 6) \\ -\{\mu(p_2^{(j)2} - p_1^{(j)2}) + \kappa p_1^{(j)2} - \kappa\eta_j/k_j^2\}, & (i = 7, 8) \end{cases} \\
a_{3j} &= \begin{cases} B_{44}\pi_j p_2^{(j)}k_j^3, & (j = 0, 1, 2, 3) \\ v\gamma\eta_j p_2^{(j)}k_j, & (j = 7, 8) \end{cases} \\
a_{4j} &= \begin{cases} k_j, & (j = 0, 1, 2, 3) \\ -ip_1^{(j)}k_j, & (j = 4, 5, 6) \\ ip_2^{(j)}k_j, & (j = 7, 8), \end{cases} \\
a_{5j} &= \begin{cases} \eta_j k_j, & (j = 0, 1, 2, 3) \\ p_2^{(j)}k_j, & (j = 4, 5, 6) \\ p_1^{(j)}k_j, & (j = 7, 8) \end{cases} \\
a_{6j} &= \begin{cases} \pi_j k_j^2, & (j = 0, 1, 2, 3) \\ \eta_j, & (7, 8) \end{cases}
\end{aligned}$$

$$a_{7j} = p_2^{(j)}\eta_j k_j, \quad (j = 4, 5, 6), \quad a_{8j} = p_2^{(j)}\pi_j k_j, \quad (j = 4, 5, 6), \quad b_i = -a_{i0}, \quad (i = 1, 2, \dots, 8)$$

and $Z_i (= A_i/A_0)$ are the amplitude ratios of the reflected and refracted waves for the incident longitudinal wave. It may be noted that Z_i , ($i = 1, 2, 3$) correspond to the amplitude ratios of reflected waves, while Z_i , ($i = 4, 5, 6, 7, 8$) correspond to the amplitude ratios of the refracted waves.

5.5 Energy partition

Let us consider energy partition between the reflected and refracted waves at the plane interface, $y = 0$. The rate of energy transmission per unit area at $y = 0$ is given by

$$P^* = \langle t_{22}, \dot{u}_2 \rangle + \langle t_{21}, \dot{u}_1 \rangle + \langle m_{23}, \dot{\phi}_3 \rangle + \langle h_2, \dot{\psi} \rangle. \quad (5.21)$$

The energy of the incident, reflected and refracted waves are given as

$$P_i = l_i \omega k_i^3 A_i^2 \exp(2Q_i), \quad (i = 0, 1, 2, 3, 4, 5, 6, 7, 8) \quad (5.22)$$

where

$$l_i = \begin{cases} (A_{12} + A_{78}\eta_i)p_1^{(i)} + (A_{22}\eta_i + A_{88} - B_{44}\pi_i^2 k_i^2)p_2^{(i)} - K_1\pi_i, & (i = 0, 1, 2, 3) \\ \{\lambda + 2\mu + \kappa - (s\eta_i + a\eta_i^2 - m\pi_i)/k_i^2\}p_2^{(i)}, & (i = 4, 5, 6) \\ \{\mu + \kappa - \eta_i(\kappa + \gamma\eta_i)/k_i^2\}p_2^{(i)}, & (i = 7, 8). \end{cases}$$

It may be noted that $i = 0$ represents for the energy of incident wave, $i = 1, 2, 3$ represent for the energy of reflected waves and $i = 4, 5, 6, 7, 8$ represent for the energy of refracted waves.

The energy ratios of the reflected and refracted waves are

$$E_i = \frac{P_i}{P_0}, \quad (i = 1, 2, \dots, 8) \quad (5.23)$$

Here, the energy ratios, E_i , ($i = 1, 2, 3$) correspond for the reflected waves and E_i , ($i = 4, 5, 6, 7, 8$) correspond for the refracted waves. We come to know that these ratios are functions of the angle of propagation, elastic, micropolar, thermal and void parameters.

5.6 Numerical results and discussion

We are interested in the computation of amplitude and energy ratios of reflected and refracted waves for the incident longitudinal wave. We have developed programs on MATLAB for the computation of amplitude and energy ratios and discussed the effects of micro-inertia

parameters, f and J . The following relevant parameters are considered.

For the orthotropic micropolar half-space, M (modified values of Singh, 2007c):

$$\begin{aligned} \rho &= 2290 \text{ Kg/m}^3, A_{11} = 1.165 \times 10^{11} \text{ N/m}^2, A_{22} = 1.265 \times 10^{11} \text{ N/m}^2, \\ A_{12} &= 7.69 \times 10^{10} \text{ N/m}^2, A_{77} = 1.669 \times 10^{10} \text{ N/m}^2, A_{78} = 1.59 \times 10^{10} \text{ N/m}^2, \\ A_{88} &= 2.29 \times 10^{10} \text{ N/m}^2, B_{44} = 4.9 \times 10^4 \text{ N}, B_{66} = 4.8 \times 10^4 \text{ N}. \end{aligned}$$

For the half-space, \bar{M} of thermoelastic micropolar materials with voids (Sharma and Kumar, 2009):

$$\begin{aligned} \rho &= 2190 \text{ Kg/m}^3, \lambda = 7.59 \times 10^{10} \text{ N/m}^2, \mu = 1.89 \times 10^{10} \text{ N/m}^2, \kappa = 1.49 \times 10^8 \text{ N/m}^2, \chi = \\ &0.00753 \text{ m}^2, \zeta = 1.49 \times 10^{10} \text{ N/m}^2, s = 1.05 \times 10^{10} \text{ N/m}^2, a = 6.68 \times 10^{-10} \text{ N/m}^2, \\ \gamma &= 2.68 \times 10^5 \text{ N}, \xi = 1.475 \times 10^6 \text{ N/m}^2, d = 2.16 \times 10^6 \text{ N/m}^2, k_0 = 1.7 \times 10^2 \text{ Jm}^{-1}\text{s}^{-1}\text{K}^{-1}, \\ \nu &= 0.02 \text{ K}^{-1}, \tau = 0.12 \text{ s}, \Theta_0 = 293 \text{ K}, \omega = 5 \text{ s}^{-1}. \end{aligned}$$

The variation of amplitude ratios with angle of incidence are depicted at Figures 5.2-5.6 and those of energy ratios are shown in Figures 5.7-5.11. In all the figures, we take

$$\text{Curve I \& IV: } (f, J) = (0.016, 0.014) \times 10^{-4} \text{m}^2,$$

$$\text{Curve II \& V: } (f, J) = (0.018, 0.016) \times 10^{-4} \text{m}^2 \text{ and}$$

$$\text{Curve III \& VI: } (f, J) = (0.020, 0.018) \times 10^{-4} \text{m}^2.$$

5.6.1 Effect of micro-inertia on amplitude ratios

In Figure 5.2, the value of $|Z_1|$ increases from a certain value with the increase of angle of incidence, θ_0 attaining the maximum value at the grazing angle of incidence. The values of $|Z_1|$ decrease with the increase of micro-inertia and the minimum effect of micro-inertia is found near $\theta_0 = 90^\circ$. In Figure 5.3, Curve I shows the decreasing nature of $|Z_2|$ thereby making local minimums at $\theta_0 = 77^\circ$ and $\theta_0 = 90^\circ$, but Curves II and III represent increasing $|Z_2|$ with the increase of θ_0 upto the maximum value at $\theta_0 = 15^\circ$ and $\theta_0 = 34^\circ$ respectively. In this figure, we come to know that the value $|Z_3|$ (Curves IV, V, VI) increases with the increase of θ_0 . The minimum and maximum effects of micro-inertia on $|Z_2|$ are observed near grazing and normal angle of incidence. But in the case of $|Z_3|$, the minimum effect is

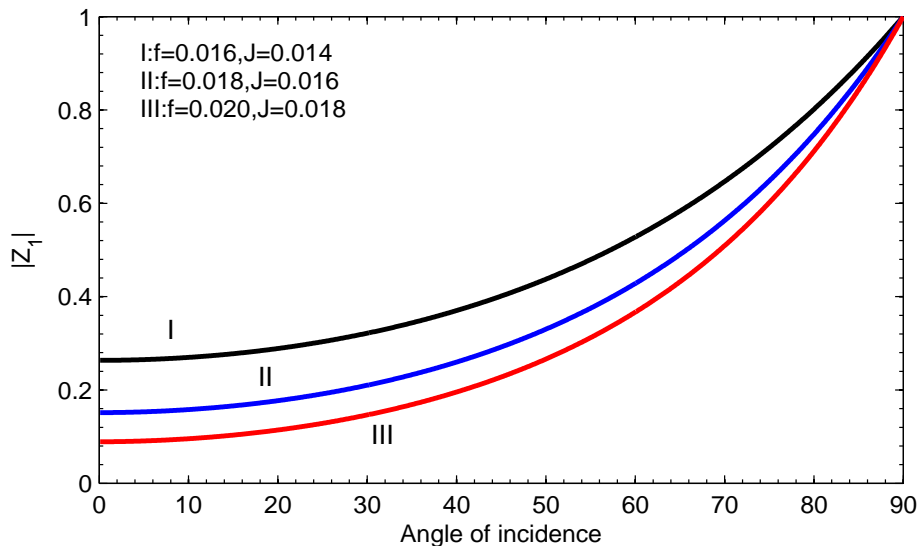


Figure 5.2: Variation of $|Z_1|$ with θ_0 at different values of f & J .

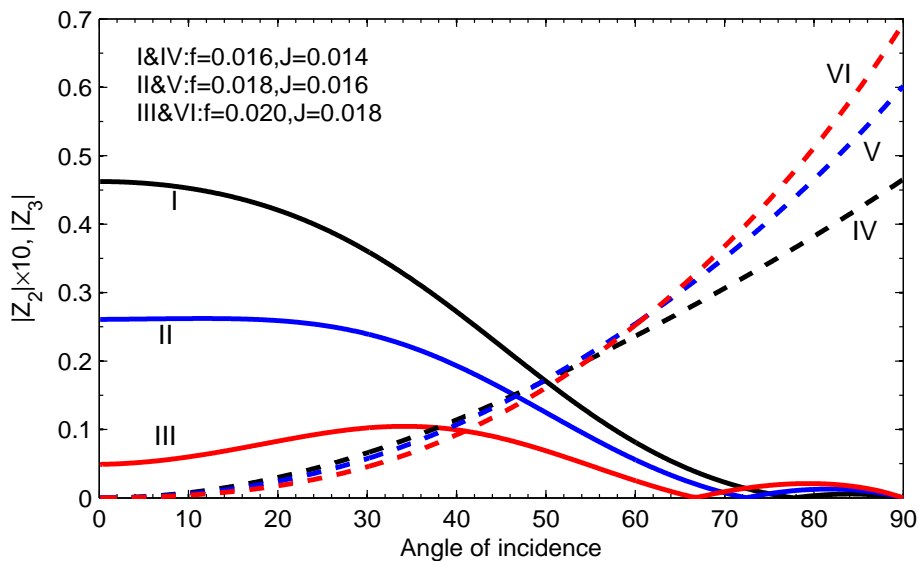


Figure 5.3: Variation of $|Z_2|$ (I, II, III) & $|Z_3|$ (IV, V, VI) with θ_0 at different values of f & J .

observed near normal angle of incidence. The amplitude ratios, $|Z_4|$ (Curves I, II, III) and $|Z_5|$ (Curves IV, V, VI) in Figure 5.4, and $|Z_6|$ in Figure 5.5 have similar nature. They increase to the maximum value and then decrease with the increase of θ_0 . The values of these amplitude ratios increase with the increase of the micro-inertia. The minimum effect

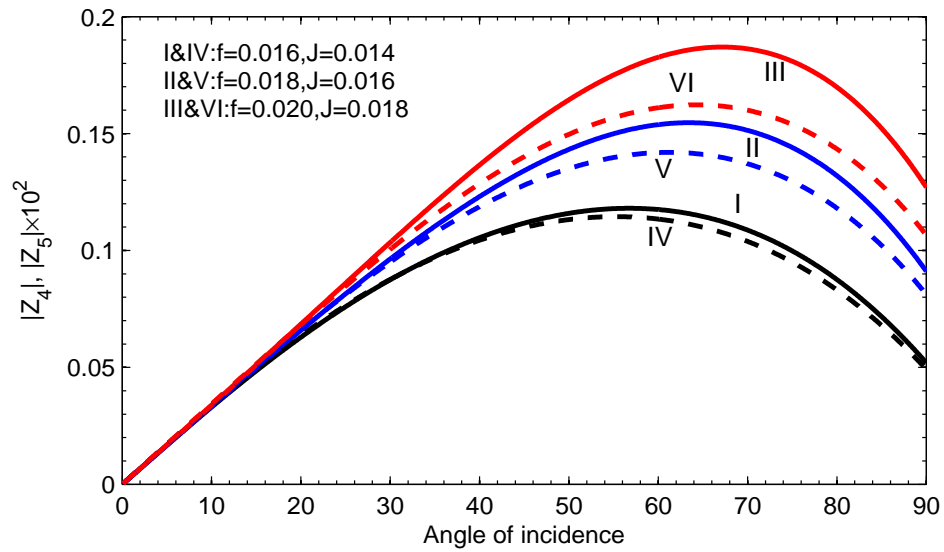


Figure 5.4: Variation of $|Z_4|$ (I, II, III) & $|Z_5|$ (IV, V, VI) with θ_0 at different values of f & J .

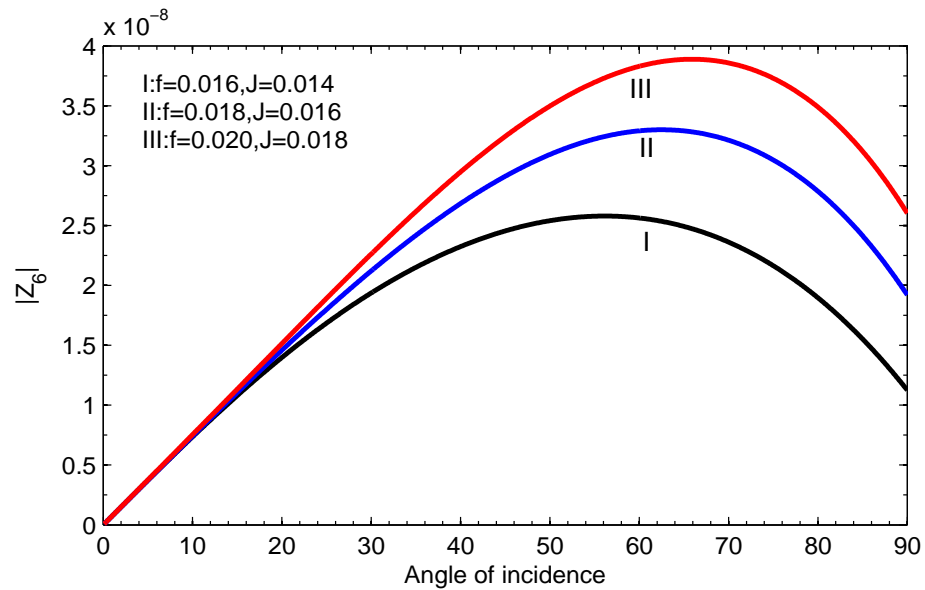


Figure 5.5: Variation of $|Z_6|$ with θ_0 at different values of f & J .

is observed near the normal angle of incidence. The similar nature of $|Z_7|$ and $|Z_8|$ is observed in Figure 5.6 and they increase with the increase of angle of incidence. The values of these amplitude ratios increase with the increase of micro-inertia.

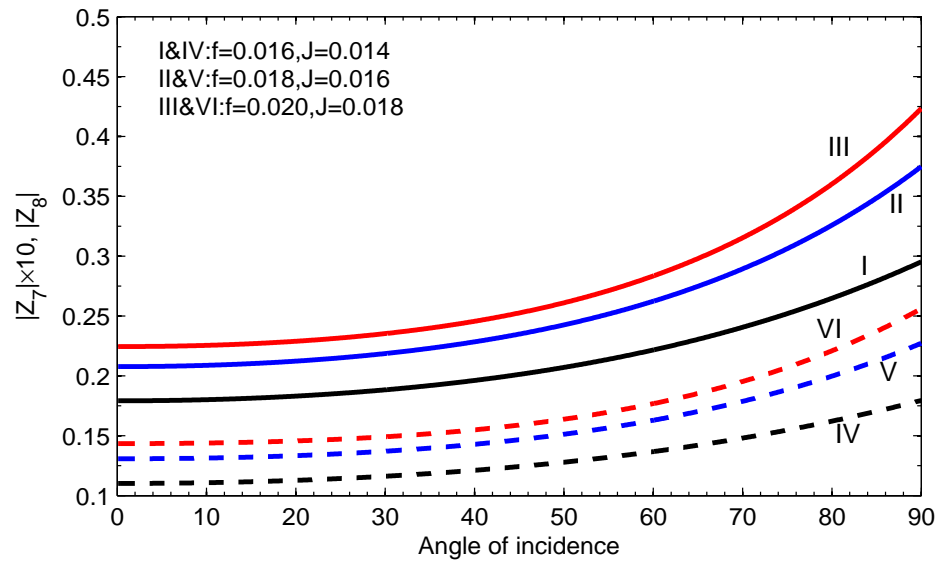


Figure 5.6: Variation of $|Z_7|$ (I, II, III) & $|Z_8|$ (IV, V, VI) with θ_0 at different values of f & J .

5.6.2 Effect of micro-inertia on energy ratios

In Figures 5.7, $|E_1|$ starts from certain values and increases with the increase of angle of incidence. The minimum effect of the micro-inertia is found near grazing angle of incidence.

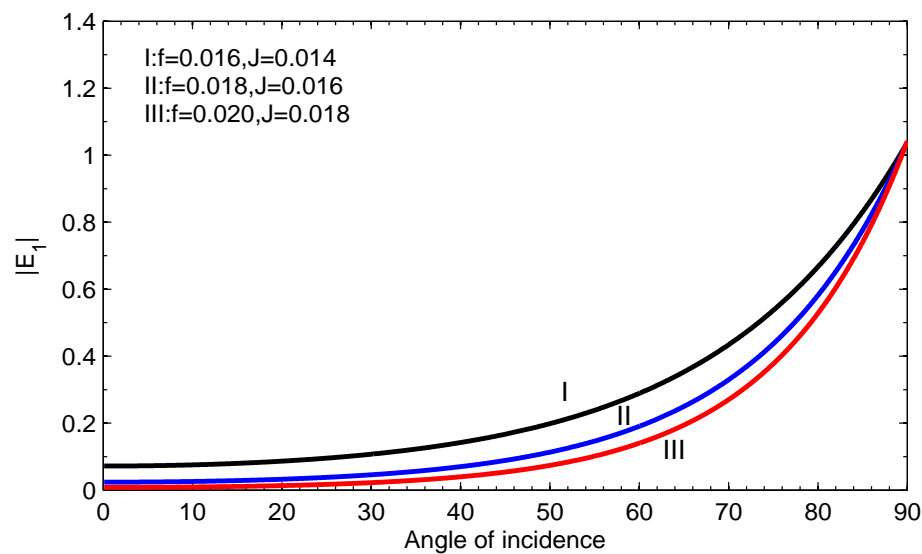


Figure 5.7: Variation of $|E_1|$ with θ_0 at different values of f & J .

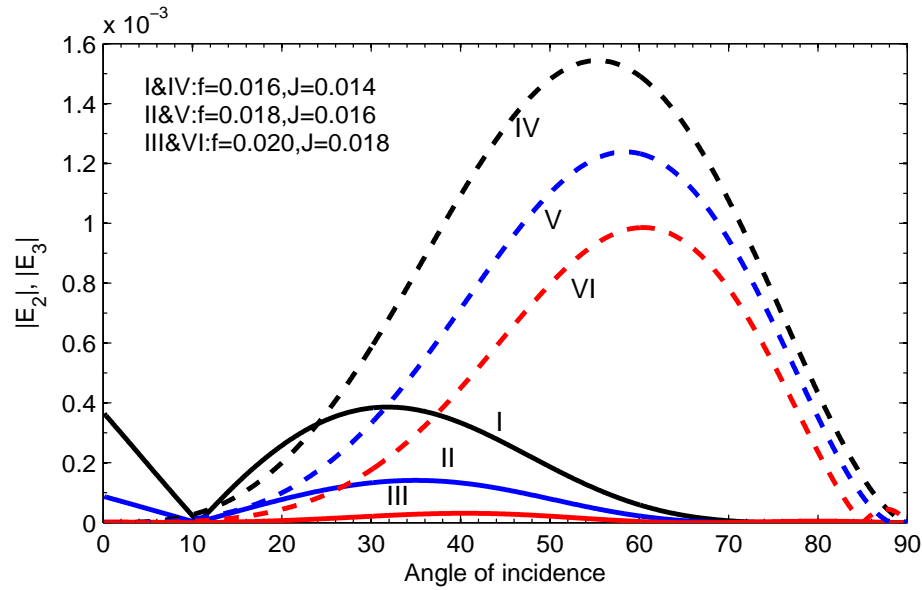


Figure 5.8: Variation of $|E_2|$ (I, II, III) & $|E_3|$ (IV, V, VI) with θ_0 at different values of f & J .

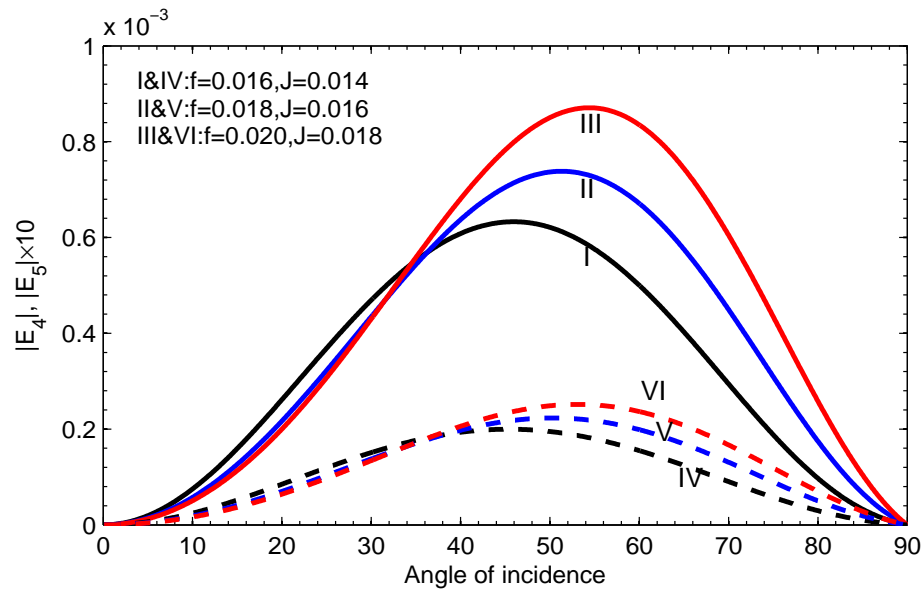


Figure 5.9: Variation of $|E_4|$ (I, II, III) & $|E_5|$ (IV, V, VI) with θ_0 at different values of f & J .

The Energy ratio, $|E_2|$ (Curves I, II, III) in Figure 5.8, decreases upto $\theta_0 = 11^\circ$ and thereafter, it increases to the maximum values with the increase of θ_0 . It may be noted that it decreases to the minimum value near grazing angle of incidence. In this figure, we have seen that $|E_3|$

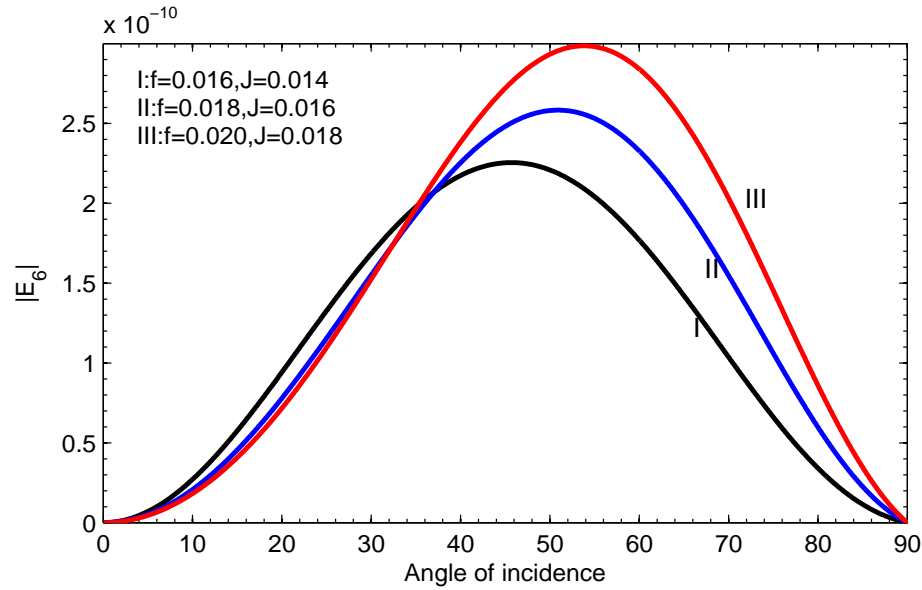


Figure 5.10: Variation of $|E_6|$ with θ_0 at different values of f & J .

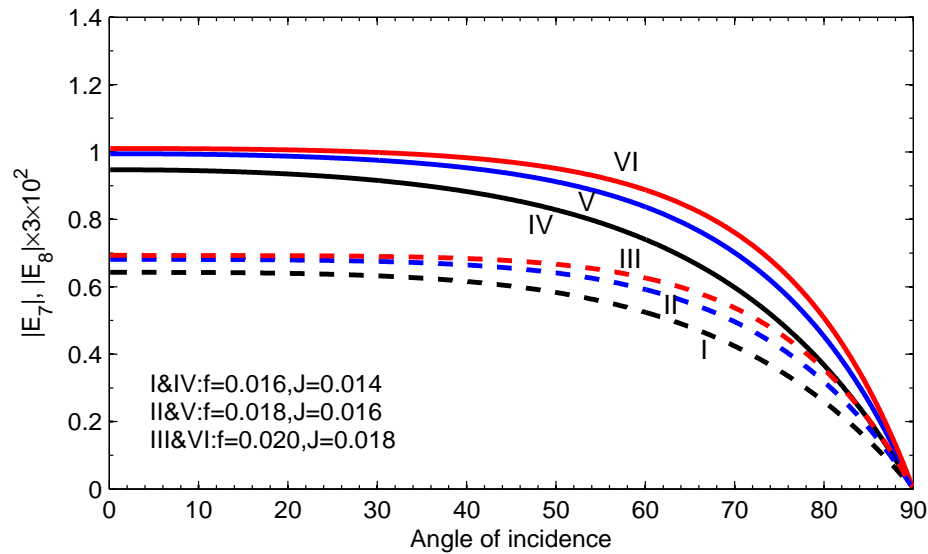


Figure 5.11: Variation of $|E_7|$ (I, II, III) & $|E_8|$ (IV, V, VI) with θ_0 at different values of f & J .

starts with very small values and it increases to the maximum value which leads to the decrease with the increase of θ_0 . The values of these energy ratios decrease with the increase of micro-inertia. The energy ratios, $|E_4|$ (Curves I, II, III), $|E_5|$ (Curves IV, V, VI) and $|E_6|$ have similar nature in Figures 5.9 and 5.10. They initially start from zero and increase to

the maximum value, which then decrease with the increase of θ_0 . The minimum effect of micro-inertia is observed near normal and grazing angle of incidence. The energy ratios, $|E_7|$ and $|E_8|$ in Figure 5.11 decrease with the increase of θ_0 . The values of these ratios increase with the increase of micro-inertia. The sum of the energy ratios due to reflected and refracted waves is close to unity.

5.7 Conclusions

The problem of the effect of micro-inertia on the reflection and refraction of elastic waves at a plane interface between two half-spaces of an orthotropic micropolar materials and micropolar thermoelastic materials with voids has been investigated. The amplitude and energy ratios of the reflected and refracted waves due to incident longitudinal wave are obtained. These ratios are computed numerically for different values of micro-inertia to study their effects. We may summarize with the following concluding remarks:

- (i) The amplitude and energy ratios are functions of angle of incidence, micropolar, thermal and voids parameters.
- (ii) The amplitude ratio, $|Z_4|$, $|Z_5|$, $|Z_6|$, $|Z_7|$ and $|Z_8|$ increase with increasing micro-inertia, while $|Z_1|$ decreases with the increase of micro-inertia.
- (iii) The energy ratios, $|E_7|$ and $|E_8|$ increase with the increase of micro-inertia, while $|E_1|$, $|E_2|$ and $|E_3|$ decrease with the increase of micro-inertia.
- (iv) The amplitude ratios, $|Z_3|$, $|Z_4|$, $|Z_5|$ and $|Z_6|$ have minimum effect of micro-inertia near normal angle of incidence, while $|Z_1|$ and $|Z_2|$ have minimum effect near grazing angle of incidence.
- (v) The energy ratios, $|E_1|$, $|E_2|$, $|E_7|$ and $|E_8|$ have minimum effect of micro-inertia near grazing angle of incidence, while $|E_4|$, $|E_5|$ and $|E_6|$ have minimum effect of micro-inertia near the normal and grazing angle of incidence.
- (vi) The sum of energy ratios is close to unity.

Chapter 6

Summary and Conclusions

In the present thesis, the problems of wave propagation in homogeneous isotropic micropolar thermoelastic materials with voids and orthotropic micropolar materials have been investigated. The phenomena of reflection and refraction of longitudinal and transverse waves are discussed with the help of appropriate boundary conditions. Amplitude and energy ratios are obtained analytically and numerically for a particular model.

Chapter 1 is the general introduction of the thesis. It consists of microcontinuum theories, linear micropolar theory, Hookes law, elastic waves, helmholtz decomposition theorem, applications of wave propagation and review of literatures.

In Chapter 2, the problem of plane wave in micropolar thermoelastic materials with voids is attempted. There exist six plane waves which are three coupled dilatational waves ($FCDW$, $SCDW$, $TCDW$), two coupled shear waves ($FCSW$, $SCSW$) and one uncoupled dilatational wave (FDW). The phase velocities of these waves are obtained analytically and numerically for a particular model. We may conclude with the following remarks:

- (i) The phase velocity of micropolar wave (FDW) is a function of micropolar parameters.
- (ii) The shear waves ($FCSW$, $SCSW$) are independent of thermal and void parameters.
- (iii) The phase velocity of dilatational waves depend on the Lamé's constants, micropolar, thermal and void parameters.
- (iv) All the coupled dilatational waves are attenuated only when $G \neq 0$.

- (v) One of the coupled dilatational waves is non-attenuated for $G = 0$.
- (vi) The phase velocities corresponding to $SCDW$, $TCDW$ and attenuation coefficient of $FCDW$ increase with the increase of angular frequency (ω).
- (vii) The attenuation coefficient of $SCDW$ decreases with the increase of ω .
- (viii) The values of phase velocity of $FCDW$ increase with the increase of J .
- (ix) The values of phase velocity of $SCDW$ and $TCDW$ decrease and increase respectively with the increase of J .
- (x) The values of the attenuation coefficients of $FCDW$ and $SCDW$, $TCDW$ increase and decrease respectively with the increase of J .

In Chapter 3, the problem of reflection of elastic waves due to incident longitudinal and shear waves at a plane free boundary of a micropolar thermoelastic materials with voids has been investigated. The micropolar wave is not reflected for the incident coupled longitudinal/shear wave. The expressions of the amplitude and energy ratios of the reflected waves are obtained analytically and numerically. These ratios are the functions of elastic, micropolar, thermal and void parameters and angle of incidence. We conclude with the following points:

- (i) Amplitude and energy ratios are the functions of elastic, micropolar, thermal and void parameters and angle of incidence.
- (ii) The micropolar wave is not reflected for the incident coupled longitudinal/shear wave.
- (iii) Amplitude ratios, $|Z_1|$, $|Z_2|$, $|Z_3|$, $|Z_4|$ for the incident coupled longitudinal wave increase with the increase of J , while $|Z_5|$ decrease with the increase of J .
- (iv) Energy ratios of the reflected coupled longitudinal waves for incident coupled waves increase with the increase of J .
- (v) We have observed that the effect of J on the amplitude and energy ratios for the incident shear wave are more than that of incident longitudinal wave.
- (vi) The sum of energy ratios of reflected waves for the incident coupled longitudinal and coupled shear waves are found to be closed to unity.

In Chapter 4, the problem of reflection and refraction of elastic waves at a plane interface between two dissimilar half-space of micropolar thermoelastic materials with voids has been studied. The amplitude and energy ratios of the reflected and refracted waves are obtained separately for the cases of incident longitudinal and shear waves. We have observed that these ratios are functions of angle of incidence, thermal, micropolar and voids parameters. These ratios are computed numerically for different values of the linear thermal expansion and micro-inertia. The following concluding remarks may be mentioned:

- (i) The amplitude ratios, $|Z_1|$, $|Z_3|$, $|Z_4|$, $|Z_5|$, $|Z_7|$, $|Z_8|$, $|Z_9|$ and $|Z_{10}|$ of the reflected and refracted waves due to incident longitudinal wave decrease with the increase of linear thermal expansion, while $|Z_6|$ increases with the increase of ν and ν' .
- (ii) The energy ratios, $|E_1|$, $|E_3|$, $|E_4|$, $|E_5|$, $|E_9|$ and $|E_{10}|$ of the reflected and refracted waves due to incident longitudinal wave decrease with the increase of ν and ν' , while $|E_7|$ and $|E_2|$ increase with the increase of linear thermal expansion.
- (iii) The amplitude ratios, $|Z_2|$, $|Z_3|$, $|Z_6|$, $|Z_7|$ and $|Z_8|$ of the reflected and refracted waves due to incident shear wave increase with the increase of micro-inertia, while $|Z_9|$ decreases with the increase of J and J' .
- (iv) The energy ratios, $|E_1|$, $|E_2|$, $|E_3|$, $|E_6|$, $|E_7|$ and $|E_8|$ of the reflected and refracted waves due to incident shear wave increase with the increase of J and J' .
- (v) The amplitude and energy ratios of the reflected and refracted coupled longitudinal waves due to incident shear wave are found to have critical angles.
- (vi) The sum of energy ratios of the reflected and refracted waves is close to unity.

In Chapter 5, the problem of the effect of micro-inertia on reflection/refraction of plane waves at the orthotropic and thermoelastic micropolar materials with voids has been investigated. The amplitude and energy ratios of the reflected and refracted waves due to incident longitudinal wave are obtained using appropriate boundary conditions. These ratios are computed numerically for a particular model. These ratios are found to be functions of angle of incidence, micropolar, thermal and voids parameters. We summarize with the

following concluding remarks:

- (i) The amplitude ratio, $|Z_4|$, $|Z_5|$, $|Z_6|$, $|Z_7|$ and $|Z_8|$ increase, while $|Z_1|$ decreases with the increase of micro-inertia. The energy ratios, $|E_7|$ and $|E_8|$ increase, while $|E_1|$, $|E_2|$ and $|E_3|$ decrease with the increase of micro-inertia.
- (ii) The amplitude ratios, $|Z_3|$, $|Z_4|$, $|Z_5|$ and $|Z_6|$ have minimum effect of micro-inertia near normal angle of incidence, while $|Z_1|$ and $|Z_2|$ have minimum effect near grazing angle of incidence.
- (iii) The energy ratios, $|E_1|$, $|E_2|$, $|E_7|$ and $|E_8|$ have minimum effect of micro-inertia near grazing angle of incidence, while $|E_4|$, $|E_5|$ and $|E_6|$ have minimum effect of micro-inertia near the normal and grazing angle of incidence.

Future scopes of the work

The works in the present thesis may be useful in the field of Earthquake Engineering, Seismology, Explorations of oil and minerals, etc.

The following problems may be extended:

- (i) Plane waves at the interface between a micropolar fluid and micropolar thermoelastic materials with voids.
- (ii) Symmetric and Anti-symmetric vibration in the plate of micropolar thermoelastic materials with voids.

Bibliography

- Abd-Alla, A.M. (1999). "Propagation of Rayleigh waves in an elastic half-space of orthotropic material", *Appl. Math. Comp.* 99(1), 61-69.
- Abd-Alla, A.M. and Ahmad, S.M. (2003). "Stoneley and Rayleigh waves in a non-homogeneous orthotropic elastic medium under the influence of gravity", *Appl. Math. Comp.* 135(1), 187-200.
- Abd-Alla, A.N. and Al Dawy, A.A.S. (2000). "The reflection phenomena of SV waves in a generalized thermoelastic medium", *Int. J. Math. Math. Sci.* 23(8), 529-546.
- Acharya, D.P. and Sengupta, P.R. (1976). "Surface waves in the micropolar thermoelasticity", *Acta Geophys. Pol.* 24, 289-299.
- Achenbach, J.D. (1976). *Wave propagation in elastic solids*, North-Holland Publishing Company, New York.
- Ailawalia, P. and Kumar, R. (2011). "Thermomechanical deformation in micropolar porous thermoelastic material", *Mech. Adv. Mater. Struct.* 18(4), 255-261.
- Aouadi, M. (2007). "A problem for an infinite elastic body with a spherical cavity in the theory of generalized thermoelastic diffusion", *Int. J. Solids Struct.* 44(17), 5711-5722.
- Aouadi M. (2008). "Generalized theory of thermoelastic diffusion for anisotropic media", *J. Therm. Stresses* 31(3), 270-285.

- Aouadi, M. (2009). "Theory of generalized micropolar thermoelastic diffusion under Lord-Shulman model", *J. Therm. Stresses* 32(9), 923-942.
- Aouadi, M. (2010). "A theory of thermoelastic diffusion materials with voids", *J. Appl. Math. Phys.* 61(2), 357-379.
- Ariman, T. (1972). "Wave propagation in a micropolar elastic half space", *Acta Mech.* 13(1-2), 11-20.
- Ben-Menahem, A. and Singh, S.J. (1981). *Seismic Waves and Sources*, Springer-Verlag, New York.
- Biot, M.A. (1956). "Thermoelasticity and irreversible thermodynamics", *J. Appl. Phys.* 27(3), 240-253.
- Boccur, A.V., Prassarella, F. and Thibullo, V. (2014). "Rayleigh surface waves in the theory of thermoelastic materials with voids", *Mecc.* 49(9), 2069-2078.
- Boffils, F. and Quintanilla, R. (1995). "Some qualitative results for the linear theory of thermo-microstretch elastic solids", *Int. J. Engng. Sci.* 33(14), 2115-2125.
- Boschi, E. and Iesan, D. (1973). "A generalized theory of linear micropolar elasticity", *Mecc.* 8(3), 154-157.
- Brekhoviskikh, L.M. (1960). *Waves in Layered Media*, Academic Press, New York.
- Bullen, K.E. and Bolt, B.A. (1985). *Introduction to the Theory of Seismology*, Cambridge University Press, London.
- Chakraborty, N. and Singh, M.C. (2011). "Reflection and refraction of a plane thermoelastic wave at a solid-solid interface under perfect boundary condition, in presence of normal initial stress", *Appl. Math. Modelling* 35(11), 5286-5301.

- Chandrasekhariah, D.S. (1981). "Wave propagation in a thermoelastic half-space", *Indian J. Pure Appl. Math.* 12(2), 226-241.
- Chandrasekharaiah, D.S. (1986a). "Surface waves in an elastic half-space with voids", *Acta Mech.* 62(1-4), 77-85.
- Chandrasekharaiah, D.S. (1986b). "Heat-flux dependent micropolar thermoelasticity", *Int. J. Engng. Sci.* 24(8), 1389-1395.
- Chanrasekhariah, D.S. (1987a). "Variational and reciprocal principles in micropolar thermoelasticity", *Int. J. Engng. Sci.* 25(1), 55-63.
- Chanrasekhariah, D.S. (1987b). "A uniqueness theorem in the theory of elastic materials with voids", *J. Elasticity* 18(2), 173-179.
- Chandrasekharaiah, D.S. (1991). "Thermoelastic plane waves in a transversely isotropic body", *Acta Mech.* 87(1-2), 11-22.
- Chirita, S. (2011). "On the harmonic vibrations in linear theory of thermoelasticity of type III", *Mech. Res. Comm.* 38(5), 393-398.
- Chirita, S., Ciarletta, M. and Straughan, B. (2006). "Structural stability in porous elasticity", *Proc. Roy. Soc. A* 462(2073), 2593-2605.
- Chirita, S. and Ghiba, I.D. (2010). "Inhomogeneous plane waves in elastic materials with voids", *Wave Motion* 47(6), 333-342.
- Ciarletta, M., Chirita, S. and Passarella, F. (2005). "Some results on the spatial behaviour in linear porous elasticity", *Arch. Mech.* 57(1), 43-65.
- Ciarletta, M. and Iesan, D. (1993). *Non-classical elastic solids*, Longman Group of UK Limited, England.

- Ciarletta, M., Passarella, F. and Svanadze, M. (2014). "Plane waves and uniqueness theorems in the coupled linear theory of elasticity for solids with double porosity", *J. Elasticity* 114(1), 55-68.
- Ciarletta, M. and Scalia, A. (1990). "Thermoelasticity of non simple materials with voids", *Rev. Roum. Sci. Techn. Mec. Appl.* 35, 115-125.
- Ciarletta, M. and Scalia, A. (1993a). "On the nonlinear theory of non simple thermoelastic materials with voids", *ZAMM* 73(2): 67-75.
- Ciarletta, M. and Scalia, A. (1993b). "Thermodynamic theory for porous pizelectric materials", *Mecc.* 28(4): 303-308.
- Ciarletta, M., Scalia, A. and Svanadze, M. (2007a). "Fundamental solution in the theory of micropolar thermoelasticity for materials with voids", *J. Therm. Stresses* 30(3), 213-229.
- Ciarletta, M. and Straughan, B. (2006). "Poroacoustic acceleration waves", *Proc. Roy. Soc. London A* 462(2075), 3493-3499.
- Ciarletta, M. and Straughan, B. (2007a). "Poroacoustic acceleration waves with second sound", *J. Sound Vib.* 306(3-5), 725-731.
- Ciarletta, M. and Straughan, B. (2007b). "Thermo-poro acceleration waves in elastic materials with voids", *J. Math. Anal. Appl.* 333(1), 142-150.
- Ciarletta, M., Straughan, B. and Zampoli, V. (2007b). "Thermo-poroacoustic acceleration waves in elastic materials with voids without energy dissipation", *Int. J. Engng. Sci.* 45(9), 736-743.
- Ciarletta, M. and Sumbatyan, M.A. (2003). "Reflection of plane waves by the free boundary of a porous elastic half-space", *J. Sound Vib.* 259(2), 253-264.

- Ciarletta, M., Svanadze, M. and Buonanno, L. (2009). "Plane waves and vibrations in the theory of micropolar thermoelasticity for materials with voids", *Eur. J. Mech. A/Solids* 28(4), 897-903.
- Cosserat, E. and Cosserat, F. (1909). *Theory of deformable bodies*, Translated by Delphenich, D.H., Hermann and sons, Paris.
- Cowin, S.C. and Nunziato, J.W. (1983). "Linear elastic materials with voids", *J. Elasticity* 13(2), 125-147.
- Cruz, V., Hube, J. and Spanos, T.J.T. (1992). "Reflection and transmission of seismic waves at the boundaries of porous media", *Wave Motion* 16(4), 323-338.
- Das, N.C., Lahiri, A., Sarkar, S. and Basu, B. (2008). "Reflection of generalized thermoelastic waves from isothermal and insulated boundaries of a half space", *Comp. Math. Appl.* 56(11), 5795-2805.
- Das, P.S. and Sengupta, P.R. (1990). "Surface waves in micropolar thermoelasticity under the influence of gravity", *Proc. Indian Natn. Sci. Acad.* 56(5), 459-471.
- Deresiewicz, H. and Rice, J.T. (1962). "The effect of boundaries on wave propagation in a liquid-filled porous solid", *Bull. Seismol. Soc. Am.* 52(3), 595-625.
- Dhaliwal, R.S. and Wang, J. (1995). "A heat-flux dependent theory of thermoelasticity with voids", *Acta Mech.* 110(1-4), 33-39.
- Diebel, S. (1999). "A micropolar theory of porous media: Constitutive modelling", *Trans. Porous Med.* 34(1-3), 193-208.
- Duhamel, J.M.C. (1837). "Second memorie sur les phenomenes thermo mecanique", *J. de l'Ecole Polytechnique* 15(25), 1-57.

- Eringen, A.C. (1964). *Mechanics of micromorphic materials*, in Proceedings of 11th International Congress of Applied Mechanics (Gortler, H., ed.), Springer-Verlag, New York.
- Eringen, A.C. (1966). "Linear theory of micropolar elasticity", *J. Math. Mech.* 15(6), 909-923.
- Eringen, A.C. (1968). *Theory of micropolar elasticity*, Academic Press, New York.
- Eringen, A.C. (1970). *Foundation of micropolar thermoelasticity*, Springer Verlag, Vienna.
- Eringen, A.C. (1980). *Mechanics of Continua, 2nd ed.*, Krieger, Melbourne, Florida.
- Eringen, A.C. (1984). "Plane waves in nonlocal micropolar elasticity", *Int. J. Engng. Sci.* 22(8-10), 1113-1121.
- Eringen, A.C. (1990a). "Theory of thermo-microstretch elastic solids", *Int. J. Engng. Sci.* 28(12), 1291-1301.
- Eringen, A.C. (1990b). "Theory of thermo-microstretch fluids and bubbly liquids", *Int. J. Engng. Sci.* 28(2), 133-143.
- Eringen, A.C. (1999). *Microcontinuum Field theories I: Foundation and Solids*, Springer-Verlag, New York.
- Eringen, A.C. (2003). "Micropolar mixture theory of porous media", *J. Appl. Phys.* 94(6), 4184-4190.
- Eringen, A.C. and Suhubi, E.S. (1964). "Nonlinear theory of simple micro-elastic solids-I", *Int. J. Engng. Sci.* 2(2), 189-203.
- Ewing, W.M., Zardetzky, W.S. and Press, F. (1957). *Elastic Waves in Layered Media*, McGraw Hill Book Co., New York.

- Gauthier, R.D. (1982). *Experimental investigation on micropolar media*, Mechanics of Micropolar Media (eds. O. Brien and R.K.T. Hsieh), World Scientific, Singapore.
- Goodman, M.A. and Cowin, S.C. (1972). "A continuum theory of granular materials", *Arch. Rat. Mech. Anal.* 44(4), 249-266.
- Graff, K.F. (1991). *Wave Motion in Elastic Solids*, Dover Publications, New York.
- Green, A.E. (1965). "Micro-materials and multipolar continuum mechanics", *Int. J. Engng. Sci.* 3(5), 533-537.
- Green, A.E. and Laws, N. (1972). "On the entropy production inequality", *Arch. Rat. Mech. Anal.* 45(1), 47.
- Green, A.E. and Lindsay, K.A. (1972). "Thermoelasticity", *J. Elasticity* 2(1), 1-7.
- Green, A.E. and Naghdi, P.M. (1993). "Thermoelasticity without energy dissipation", *J. Elasticity* 31(3), 189-208.
- Green, A.E. and Rivlin, R.S. (1964). "On Cauchy's equation of motion", *J. Appl. Math. Phys.* 15(3), 290-294.
- Hosten, B. (1991). "Reflection and transmission of acoustic plane waves on an immersed orthotropic and viscoelastic solid layer", *J. Acoust. Soc. Am.* 89(6), 2745-2752.
- Huang, K.Y. and Liang, K.Z. (1997) "Boundary element analysis of stress concentration in micropolar elastic plate", *Int. J. Numer. Meth. Engng.* 40(9), 1611-1622.
- Iesan, D. (1969). "On the linear theory of micropolar elasticity", *Int. J. Engng. Sci.* 7(12), 1213-1220.
- Iesan, D. (1973). "The plane micropolar strain of orthotropic elastic solids", *Arch. Mech.* 25, 547-561.
- Iesan, D. (1974). "Torsion of anisotropic elastic cylinders", *ZAMM* 54(11), 773-779.

- Iesan, D. (1985). "Some theorems in the theory of elastic materials with voids", *J. Elasticity* 15(2), 215-224.
- Iesan, D. (1986). "A Theory of thermoelastic materials with voids", *Acta Mech.* 60(1-2), 67-89.
- Iesan, D. (2010). "Deformation of orthotropic porous elastic bars under lateral loading", *Arch. Mech.* 62(1), 3-20.
- Iesan, D. (2004). *Thermoelastic model of continua*, Springer, Netherlands.
- Inan, E. and Eringen, A.C. (1991). "Nonlocal theory of wave propagation in thermoelastic plates", *Int. J. Engng. Sci.* 29(7), 831-843.
- Ivanov, Ts.P. (1988). "On the propagation of thermoelastic Rayleigh waves", *Wave Motion* 10(1), 73-82.
- Khurana, A. and Tomar, S.K. (2007). "Propagation of plane elastic waves at a plane interface between two electro-microelastic solid half-spaces", *Int. J. Solid Struct.* 44(11-12), 3773-3795.
- Kumar, R., Ahuja, S. and Grag, S.K. (2014). "Rayleigh waves in isotropic microstretch thermoelastic diffusion solid half space", *Latin Am. J. Solids Struct.* 11(2), 299- 319.
- Kumar, R. and Ailawalia, P. (2005). "Deformation in micropolar cubic crystal in various sources", *Int. J. Solid Struct.* 42(23), 5931-5944.
- Kumar, R. and Choudhary, S. (2002a). "Dynamical behaviour of orthotropic micropolar elastic medium", *J. Vib. Control* 8(8), 1053-1069.
- Kumar, R. and Choudhary, S. (2002b). "Mechanical sources in orthotropic micropolar continua", *Proc. Indian Acad. Sci.* 111(2), 133-141.

- Kumar, R. and Choudhary, S. (2003). "Interaction due to mechanical sources in micropolar elastic medium with voids", *J. Sound Vib.* 266(4), 889-904.
- Kumar, R. and Choudhary, S. (2004). "Response of orthotropic micropolar elastic medium due to time harmonic source," *Sadhana* 29(1), pp. 83-92.
- Kumar, R. and Partap, G. (2006). "Rayleigh Lamb waves in micropolar isotropic elastic plate", *Appl. Math. Mech.* 27(8), 1049-1059.
- Kumar, R. and Partab, G. (2007). "Axisymmetric free vibrations of infinite micropolar thermoelastic plate", *Appl. Math. Mech.* 28(3), 369-383.
- Kumar, R. and Sarthi, P. (2006). "Reflection and refraction of thermoelastic plane waves at an interface between two thermoelastic media without energy dissipation", *Arch. Mech.* 58(1), 155-185.
- Kumar, R. and Sharma, N. (2008). "Propagation of waves in micropolar viscoelastic generalized thermoelastic solids having interfacial imperfections", *Theor. Appl. Frac. Mech.* 50(3), 226-234.
- Kumar, R. and Gupta, R.R. (2009). "Plane strain deformation in an orthotropic micropolar thermoelastic solid with a heat source", *J. Engng. Phys. Thermophys.* 82(3), 556-565.
- Kumar, R. and Kaur, M. (2014). "Reflection and refraction of plane waves at the interface of an elastic solid and microstretch thermoelastic solid with microtemperatures", *Arch. Appl. Mech.* 84(4), 571-590.
- Lamb, H. (1917). "On waves in an elastic plate", *Proc. Roy. Soc. London A* 93(648), 114-128.
- Lord, H.W. and Shulman, Y. (1967) "A generalized dynamical theory of thermoelasticity", *J. Mech. Phys. Solids* 15(5), 299-309.

- Love, A.E.H. (1892). *A treatise on the mathematical theory of elasticity*, Cambridge University Press, London.
- Love, A.E.H. (1911). *Some problems of geodynamics*, Cambridge University Press, London.
- Marin, M. (1996). "Some basic theorems in elastostatics of micropolar materials with voids", *J. Comp. Appl. Math.* 70(1), 115-126.
- Marin, M. (2010). "A domain of influence theorem for microstretch elastic materials", *Nonlinear Anal.: Real World Appl.* 11(5), 3446-3452.
- Marin, M. (2016). "An approach of a heat-flux dependent theory for micropolar porous media", *Mecc.* 51(5), 1127-1133.
- Mindlin, R.D. (1964). "Micro-structure in linear elasticity", *Arch. Rat. Mech. Anal.* 16(1), 51-78.
- Mindlin, R.D. and Tiersten, H.F. (1962). "Effects of couple-stresses in linear elasticity", *Arch. Rat. Mech. Anal.* 11(1), 415-448.
- Mondal, A.K. and Acharya, D.P. (2006). "Surface waves in a micropolar elastic solid containing voids", *Acta Geophys.* 54(4), 430-452.
- Muller, G. (2007). *Theory of elastic waves*, Geo Forschungs Zentrum, Potsdam.
- Nakamura, S., Benedict, R. and Lakes, R. (1984). "Finite element method for orthotropic micropolar elasticity", *Int. J. Engng. Sci.* 22(3), 319-330.
- Neumann, F. (1885). *Theorie der Elasticitat der festen korper und des lichtathers*, Teubner, Leipzig.
- Nield, D.A. and Bejan, A. (2017). *Convection in porous media*, Springer International Publishing, 5th Edition.

- Nowacki, W. and Nowacki, W.K. (1969). "Propagation of monochromatic waves in an infinite micropolar elastic plate", *Bull. Pol. Acad. Sci. Ser. Sci. Techn.* XVII, 45-53.
- Nunziato, J.W. and Cowin, S.C. (1979). "A nonlinear theory of elastic material with voids", *Arch. Rat. Mech. Anal.* 72(2), 175-201.
- Othman, M.I.A. and Atwa, S.Y. (2012). "Response of micropolar thermoelastic solid with voids due to various sources under Green Nagdhi theory", *Acta Mech. Solida Sinica* 25(2), 197-209.
- Othman, M.I.A. and Song, Y. (2008). "Reflection of magneto-thermoelastic waves with two relaxation times and temperature dependent elastic moduli", *Appl. Math. Modelling* 32(4), 483-500.
- Othman, M.I.A. and Singh, B. (2007). "The effect of rotation on generalized micropolar thermoelasticity for a half-space under five theories", *Int. J. Solids Struct.* 44(2), 2748-2762.
- Pabst, W. (2005). "Micropolar materials", *Ceram. Silikaty* 49(3), 170-180.
- Pamplona, P.X., Rivera, J.E.M. and Quintanilla, R. (2009). "Stabilization in elastic solids with voids", *J. Math. Anal. Appl.* 350(1), 37-49.
- Parfitt, V.R. and Eringen, A.C. (1969). "Reflection of plane waves from the flat boundary of a micropolar elastic half-space", *J. Acoust. Soc. Am.* 45(5), 1258-1272.
- Passarella, F. (1996). "Some results in micropolar thermoelasticity", *Mech. Res. Comm.* 23(4), 349-357.
- Passarella, F., Tibullo, V. and Zampoli, V. (2011a). "On the heat-flux dependent thermoelasticity for micropolar porous media", *J. Therm. Stresses* 34(8), 778-794.

- Passarella, F., Tibullo, V. and Zampoli, V. (2011b). "On the strong ellipticity for orthotropic micropolar elastic bodies in a plane strain state", *Mech. Res. Comm.* 38(7), 512-517.
- Passarella, F. and Zampoli, V. (2010). "On the theory of micropolar thermoelasticity without energy dissipation", *J. Therm. Stresses* 33(4), 305-317.
- Pompei, A. and Scalia, A. (1994). "On the steady vibrations of the thermoelastic porous materials", *Int. J. Solids Struct.* 31(20), 2819-2834.
- Pujol, J. (2003). *Elastic wave propagation and generation in seismology*, Cambridge University Press, UK.
- Puri, P. and Cowin, S.C. (1985). "Plane waves in linear elastic materials with voids", *J. Elasticity* 15(2), 167-183.
- Raiser, G.F., Wise, J.L., Clifton, R.J., Grady, D.E. and Cox, D.E. (1994). "Plate impact response of ceramics and glasses", *J. Appl. Phys.* 75(8), 3862-3869.
- Ramezani, S. and Naghdabadi, R. (2007). "Energy pairs in the micropolar continuum", *Int. J. Solids Struct.* 44(14-15), 4810-4818.
- Rayleigh, L. (1877). "On progressive waves", *Proc. London Math. Soc.* s1-9, 21-26.
- Rayleigh, L. (1885). "On waves propagated along the plane surface of an elastic solid", *Proc. London Math. Soc.* 1-17(1), 4-11.
- Saggio-Woyansky, J., Scott, C.E. and Minnear, W.P. (1992). "Processing of porous ceramics", *Am. Ceram. Soc. Bull.* 71(11), 1674-1682.
- Scalia, A. (1992). "A grade consistent micropolar theory of thermoelastic materials with voids", *J. Appl. Math. Mech.* 72(2), 133-140.

- Sharma, J.N. (1988). "Reflection of thermoelastic waves from the stress-free insulated boundary of an anisotropic half-space", *Indian J. Pure Appl. Math.* 19(3), 294-304.
- Sharma, J.N. (2001). "On the propagation of thermoelastic waves in homogeneous isotropic plates", *Indian J. Pure Appl. Math.* 32(9), 1329-1341.
- Sharma, M.D. (2006). "Wave propagation in anisotropic generalized thermoelastic media", *J. Therm. Stresses* 29(7), 629-642.
- Sharma, M.D. (2007). "Wave propagation in a general anisotropic poroelastic medium: Biots theories and homogenisation theory", *J. Earth Syst. Sci.* 116(4), 357-367.
- Sharma, M.D. (2008). "Wave propagation in thermoelastic saturated porous medium", *J. Earth Syst. Sci.* 117(6), 951-958.
- Sharma, J.N. and Kaur, R. (2014). "Study of reflection and transmission of plane waves at thermoelastic-diffusive solid/liquid interface", *Latin Am. J. Solids Struc.* 11(12), 2141-2170.
- Sharma, J.N., Kumar, V. and Chand, D. (2003a). "Reflection of generalized thermoelastic waves from the boundary of a half-space", *J. Therm. Stresses* 26(10), 925-942.
- Sharma, J.N. and Kumar, S. (2009). "Lamb waves in micropolar thermoelastic solid plates immersed in liquid with varying temperature", *Mecc.* 44(3), 305-319.
- Sharma, K. and Marin, M. (2014). "Reflection and transmission of waves from imperfect boundary between two heat conducting micropolar thermoelastic solids", *An. St. Univ. Ovidius Constanta* 22(2), 151-176.
- Sharma, J.N. and Sharma, R. (2009). "Modelling of thermoelastic Rayleigh waves in a solid underlying a fluid layer with varying temperature", *Appl. Math. Modelling* 33(3), 1683-1695.

- Sharma, J.N., Singh, D. and Kumar, R. (2003b). "Generalized thermoelastic waves in transversely isotropic plates", *Indian J. Pure Appl. Math.* 34(6), 841-852.
- Shaw, S. and Mukhopadhyay, B. (2011). "Thermo elastic waves with thermal relaxation in isotropic micropolar plate", *Sadhana* 369(2), 209-221.
- Singh, B. (2000). "Reflection of plane sound wave from a micropolar generalized thermoelastic solid half-space", *J. Sound Vib.* 235(4), 685-696.
- Singh, B. (2001). "Reflection and refraction of micropolar thermoelastic waves at a liquid-solid interface", *Indian J. Pure Appl. Math.* 32(8), 1229-1236.
- Singh, B. (2002). "Reflection of plane waves from free surface of a microstretch elastic solid", *Proc. Indian Acad. Sci.* 111(1), 29-37.
- Singh, B. (2003). "Wave propagation in anisotropic generalized thermoelastic solid", *Indian J. Pure Appl. Math.* 34(10), 1479-1485.
- Singh, B. (2005). "Reflection of P and SV waves from free surface of an elastic solid with generalized thermodiffusion", *J. Earth Syst. Sci.* 114(2), 159-168.
- Singh, B. (2007a). "Reflection coefficients and energy ratios in a micropolar thermoelastic medium without energy dissipation", *ANZIAM J.* 48(3), 433-447.
- Singh, B. (2007b). "Wave propagation in a generalized thermoelastic material with voids", *Appl. Math. Comp.* 189(1), 698-709.
- Singh, B. (2007c). "Wave propagation in an orthotropic micropolar elastic solid", *Int. J. Solids Struct.* 44(11-12), 3638-3645.
- Singh, B. (2010). "Propagation of thermoelastic waves in micropolar mixture of porous media", *Int. J. Thermophys.* 31(3), 637-647.

- Singh, B. (2011). "On theory of generalized thermoelastic solids with voids and diffusion", *Eur. J. Mech. A/ Solids* 30(6), 976-982.
- Singh, S.S. (2011). "Reflection and transmission of couple longitudinal waves at a plane interface between two dissimilar half-spaces of thermo-elastic materials with voids", *Appl. Math. Comp.* 218(7), 3359-3371.
- Singh, S.S.(2013). "Transverse wave at a plane interface in thermo-elastic materials with void", *Mecc.* 48(3), 617-630.
- Singh, M.C. and Chakraborty, N. (2013). "Reflection and refraction of P -, SV - and thermal wave at an initially stressed solid-liquid interface in generalized thermoelasticity", *Appl. Math. Modelling* 37(1-2), 463-475.
- Singh, B., Singh, J. and Ailawalia, P. (2010). "Thermoelastic waves at an interface between two solid half-spaces under hydrostatic initial stress", *Arch. Mech.* 62(3), 177-193.
- Singh, B., Singh, L. and Deswal, S. (2011). "Propagation of waves at an interface between two thermoelastic half-spaces with diffusion", *J. Theor. Appl. Mech.* 41(1), 61-80.
- Singh, J. and Tomar, S.K. (2006a). "Reflection and transmission of transverse waves at a plane interface between two different porous elastic solid half-spaces", *Appl. Math. Comp.* 176(1), 364-378.
- Singh, D. and Tomar S.K. (2006b). "Wave propagation in micropolar mixture of porous media", *Int. J. Engng. Sci.* 44(18-19), 1304-1323.
- Singh, J. and Tomar, S.K. (2007). "Plane waves in thermo-elastic material with voids", *MoM.* 39(10), 932-940.
- Singh, J. and Tomar, S.K. (2011). "Plane waves in a rotating generalized thermo-elastic solid with voids", *Int. J. Engng. Sci. Tech.* 3(2), 34-41.

- Sinha, S.B. and Elsibai, K.A. (1996). "Reflection of thermoelastic waves at a solid half-space with two relaxation times", *J. Therm. Stresses* 19(8), 749-762.
- Sinha, S.B. and Elsibai, K.A. (1997). "Reflection and refraction of thermoelastic waves at an interface of two semi infinite media with two relaxation times", *J. Therm. Stresses* 20(2), 129-145.
- Smith, A.C. (1967). "Waves in micropolar elastic solids", *Int. J. Engng. Sci.* 5(10), 741-746.
- Sokolnikof, I.S. (1956). *Mathematical theory of elasticity*, McGraw-Hill Book Company, Inc, New York.
- Straughan, B. (2008). *Stability and wave motion in porous media*, Springer-Verlag, New York.
- Straughan, B. (2009). "Nonlinear acceleration waves in porous media", *Math. Comp. Simul.* 80(4), 763-769.
- Suhubi, E.S. and Eringen, A.C. (1964). "Nonlinear theory of micro-elastic solids-II", *Int. J. Engng. Sci.* 2(4), 389-404.
- Svanadze, M. and De Cicco, S. (2005). "Fundamental solution in the theory of thermomicrostretch elastic solids", *Int. J. Engng. Sci.* 43(5-6), 417-431.
- Tauchert, T.R. Claus, W.D. and Ariman, T. (1968). "The linear theory of micropolar thermoelasticity", *Int. J. Engng. Sci.* 6(1), 37-47.
- Tomar, S.K. (2005). "Wave propagation in micropolar elastic plate with voids", *J. Vib. Control* 11(6), 849-863.
- Tomar, S.K. and Gogna, M.L. (1995). "Reflection and refraction of longitudinal waves at an interface between two micropolar elastic solids in welded contact", *J. Acoust. Soc. Am.* 97(2), 822-830.

- Tomar, S.K. and Kumar, R. (1995). "Reflection and refraction of longitudinal displacement wave at a liquid-micropolar solid interface", *Int. J. Engng. Sci.* 33(10), 1507-1515.
- Tomar, S.K., Kumar, R. and Kaushik, V.P. (1998), "Wave propagation of micropolar elastic medium with stretch", *Int. J. Engng. Sci.* 36(5-6), 683-698.
- Tomar, S.K. and Singh, J. (2006). "Plane waves in micropolar porous elastic solid", *Int. J. Appl. Math. Mech.* 2(3), 52-70.
- Toupin, R.A. (1962). "Elastic materials with couple stresses", *Arch. Rat. Mech. Anal.* 11(1), 385-414.
- Tsaklis, P.V. (2010). "Presentation of acoustic waves propagation and their effects through human body tissues", *Human Movement* 11(1), 58-65.
- Udias, A. (1999). *Principles of Seismology*, Cambridge University Press, UK.
- Vashishth, A.K. and Sukhija, H. (2015). "Reflection and transmission of plane waves from fluid-piezothermoelastic solid interface", *Appl. Math. Mech.* 36(1), 11-36.
- Vinh, P.C. (2013). "Scholte-wave velocity formulae", *Wave Motion* 50(2), 180-190.
- Vinh, P.C. and Ogden, R.W. (2004). "Formulas for the Rayleigh wave speed in orthotropic elastic solids", *Arch. Mech.* 56(3), 247-265.
- Voigt, W. (1887). "Theoretische studien uber die elastizitats verhaltnisse der krystalle", *Abh. Ges. Wiss. Gottingen* 34, 3-51.
- Wang, J. and Dhaliwal, R.S. (1993). "On some theorem in the nonlocal theory of micropolar elasticity", *Int. J. Solid Struct.* 30(10), 1331-1338.
- Xia, J., Miller, R.D. and Park, C.B. (1999). "Estimation of near surface shear wave velocity by inversion of Rayleigh waves", *Geophys.* 64(3), 691-700.

Zhu, Y. and Tsvankin, I. (2006). "Plane-wave propagation in attenuative transversely isotropic media", *Geophys.* 71(2), 17-30.

I. LIST OF PUBLICATIONS

I. List of publications

1. Singh, S.S. and Lianngenga, R. (2016). Plane waves in micropolar thermoelastic materials with voids, *Journal of Science and Technology*, **4(2)**: 141-151.
2. Singh, S.S., Lianngenga, R. (2017). Effect of micro-inertia in the propagation of waves in micropolar thermoelastic materials with voids, *Applied Mathematical Modelling*, **49(2017)**: 487-497.
3. Lianngenga, R. and Singh, S.S. (2017). Effect of micro-inertia on reflection/refraction of plane waves at the orthotropic and thermoelastic micropolar materials with voids, *Global Journal of Pure and Applied Mathematics*, **13(7)**: 2907-2921.
4. Lianngenga, R. and Singh, S.S. (2017). Effect of thermal and micro-inertia on the refraction of elastic waves in micropolar thermoelastic materials with voids, *Communicated to International Journal of Computational Method for Engineering Sciences and Mechanics*.

II. Conferences/Seminars/Workshops

1. Attended "National workshop on Dynamical Systems" organized by Department of Mathematics & Computer Science, Mizoram University, Aizawl - 796 004, Mizoram on 26th – 27th November, 2013.
2. Attended "One Day State Level Workshop on C⁺⁺ and Numerical Methods" organized by Department of Physics and Mathematics, Pachhunga University College, Aizawl - 796 001, Mizoram, on 16th – 20th March, 2015.
3. Presented a paper "Voids effect on the propagation of elastic waves in Micropolar medium" in the *Second Mizoram Mathematics Congresss - 2015* organized by Department of Mathematics and Computer Science, Mizoram Mathematics Society (M.M.S.)

in collaboration with Department of Mathematics, Pachhunga University College and Department of Mathematics & Computer Science, Mizoram University, Aizawl, Mizoram on 13th – 14th August, 2015.

4. Attend "Seminar on Science for National Building" organized by Mizo Academy of Sciences in collaboration with the Directorate of Science and Technology, Government of Mizoram, Pi Zaii Hall, Synod Conference Centre, Aizawl, Mizoram on 1st October, 2015.
5. Presented a paper "Elastic waves in the micropolar thermoelastic materials with voids" in the *International Conference on Emerging trends in Science and Engineering Research - 2015* organized by Department of Basic Sciences and Humanities, National Institute of Technology, Langol, Imphal, Manipur on 2th – 4th December, 2015.
6. Presented a paper "Harmonic waves in micropolar thermoelastic materials with voids" in the *National Conference on Application of Mathematics* organized by Department of Mathematics & Computer Science, Mizoram University, Aizawl- 796004, on 25th – 26th February, 2016.
7. Presented a paper "Incident wave at the interface of two micropolar thermoelastic materials with voids" in the *Mizoram Science Congress - 2016* organized by MAS & Co., Mizoram University, Aizawl, Mizoram on 13th – 14th October, 2016.

CURRICULUM VITAE

Personal Information:

Name : R. Lianggenga
Father's name : Ramthanhginga
Mother's name : Hmangaihzuali
Date of Birth : 30.09.1987
Nationality : Indian
Gender : Male
Marital Status : Single
Spoken Languages : English, Mizo (mother tongue)
Present Address : Y-24/2A, Mission Vengthlang, Aizawl-796 001, Mizoram.
E-mail : rengsi.9@gmail.com

Academic Records:

EXAMINATION	BOARD/UNIVERSITY	YEAR	DIVISION	PERCENTAGE
H.S.L.C	MBSE	2003	II	51
H.S.S.L.C	MBSE	2006	II	54
B.Sc. Mathematics	Mizoram University	2009	II	59
M.Sc.	Mizoram University	2012	I	71

Teaching Experience:

EXPERIENCE	DETAILS	YEAR
TEACHING	(i) Guest Lecturer at Dept. Maths. & Comp. Sc.	August, 2015
	Mizoram University	- July, 2016
	(ii) Substitute Lecturer at Mathematics Department	February, 2017
	PUC, Mizoram University	- Present

Award/Fellowship:

- (i) JRF under National Fellowship for Higher Education, UGC, New Delhi, 2016
- (ii) SLET, North East Region(SET), 2014.

(R. LIANGGENGA)